DEVELOPMENT AND ASSESSMENT OF ENVIRONMENTAL INDICATORS FOR MOBILE SOURCE IMPACTS ON EMISSIONS, AIR QUALITY, EXPOSURE AND HEALTH OUTCOMES

A Dissertation
Presented to
The Academic Faculty

By

Jorge Eduardo Pachon Quinche

In Partial Fulfillment
Of the Requirements for the Degree
Doctor of Philosophy in the
School of Civil and Environmental Engineering

Georgia Institute of Technology

December, 2011

DEVELOPMENT AND ASSESSMENT OF ENVIRONMENTAL INDICATORS FOR MOBILE SOURCE IMPACTS ON EMISSIONS, AIR QUALITY, EXPOSURE AND HEALTH OUTCOMES

Approved by:

Dr. Armistead G. Russell, Advisor
School of Civil and Environmental Engineering
Georgia Institute of Technology

Dr. James A. Mulholland
School of Civil and Environmental Engineering
Georgia Institute of Technology

Dr. Michael H. Bergin
School of Civil and Environmental Engineering
Georgia Institute of Technology

Dr. Rodney J. Weber
School of Earth and Atmospheric Sciences
Georgia Institute of Technology

Dr. Jeremy A. Sarnat
Rollins School of Public Health
Emory University

Date Approved: August 4, 2011

To my wife, daughter and family

ACKNOWLEDGEMENTS

I would like to show my gratitude to a number of people who were fundamental in the process to complete this dissertation. First of all, to my advisor Dr. Ted Russell for all his guidance and unconditional support. His wide knowledge and critical thinking have immensely contributed in my formation. I am deeply grateful to Dr. Jim Mulholland for all his thoughtful guidance and detailed looking at my work. I also want to thank Dr. Jeremy Sarnat for his insightful comments and Dr. Mike Bergin and Dr. Rodney Weber for their time and valuable suggestions to my thesis.

I take this opportunity to sincerely thank our peers at the Rollins School of Public Health at Emory University for providing the resources necessary to accomplish the health analysis of my research. I want to especially thank Dr. Lyndsey Darrow for her time and dedication running the epidemiologic models for this work. Also special thanks to Dr. Paige Tolbert, Dr. Stefanie Sarnat, Dr. Matt Strickland and Dr. Mitch Klein, for helpful comments.

The members of the Russell's group, Lambda, have contributed to my personal and professional life in many ways. My warmest thanks to my colleagues and friends: Yongtao Hu, Sivaraman Balachandran, Gretchen Goldman, Boris Galvis, Fernando Garcia, Aika Yano, Marcus Trail, Wenxian Zhang, Radhika Dhinga, Shannon Capps, Peng Liu, Marissa Maier, Neel Kotra, K.J. Liao, Burcak Kaynak, Jaemeen Baek, Soonchul Kwon, Emily Landtrip, Diane Ivy, Farhan Akhtar, Santosh Chandru, Efthimios Tagaris, Talat Odman.

I wish to thank officials at Universidad de La Salle in Colombia who supported me in my desire to earn my Doctoral degree. Thanks to Hno. Carlos Alberto Gomez, principal and Dr. Camilo Guaqueta Rodriguez, Dean of Engineering. Also thanks to the Colombian Institute for the Development of Science and Technology (COLCIENCAS) and the

Academic and Professional Programs for the Americas (LASPAU) for making possible my study in the United States.

Lastly, and most importantly, I wish to thank my wife Cristina for traveling in this journey with me and to my family for all their moral support.

This project was funded by the Environmental Protection Agency of the United States of America under grants Number R83362601, R83386601 R834797 and RD83479901, Georgia Power, the Southern Company, and the Colombian Institute for the Development of Science and Technology COLCIENCIAS. We thank Dr. Eric Edgerton at ARA, Inc for access to the SEARCH data. The content of this thesis is solely the responsibility of the grantee and do not necessarily represent the official views of the US-EPA. Further, US-EPA does not endorse the purchase of any commercial products or services mentioned in the publication.

TABLE OF CONTENTS

Page

LIST OF TABLES

LIST OF FIGURES

SUMMARY

Environmental indicators are developed and evaluated to assess the impact of mobile sources on emissions, air quality and health outcomes. Single species and multipollutant indicators are discussed. Among single pollutants, CO, NOx and elemental carbon (EC) were chosen as indicators of mobile sources because emissions of these pollutants are largely attributed to mobile sources and ambient concentrations have a close response to the change in mobile source emissions. CO, NOx and EC were used in the construction of the integrated mobile source indicators (IMSI), a metric that contributes in multipollutant air quality risk analyses.

The IMSI are simple to construct and calculate and demonstrate advantages over the use of single species. IMSI have stronger spatial representativeness, suggesting they are better indicators of the regional impact of mobile sources. They agree well with observed trends of traffic and they have stronger associations with emergency department visits for cardiovascular diseases (CVD), possibly due to their better spatial representativeness. The use of IMSI in epidemiologic modeling constitutes an alternative approach to assess the health impact of pollutant mixtures and can provide support for the setting of multipollutant air quality standards and other air quality management activities.

The changes in the incidence of adverse CVD impacts as result of the change in indicators of mobile source activity were examined. Single and multipollutant indicators were compared, finding that a multipollutant framework is more consistent to understanding health risk from mobiles source emissions than using single species.

The concept of indicator sets, which include a group of indicators and their relationships, along with associated attributes, facilitates a comprehensive analysis of the air quality chain, from emissions to ambient concentrations and to health outcomes. This proposed framework is of great utility for policy makers in the setting of cost-benefit analysis of air pollution reduction.

Uncertainties in estimates of emissions were found the lowest and uncertainties in source impacts from receptor models were found the highest. The estimation of health benefits were found also highly uncertain. While consideration of uncertainties is important, they do not obscure the choice of selecting multipollutant indicators versus singles species as surrogates of mobile source impact on air quality, exposure and cardiovascular health.

Four different methods were used to estimate long-term trends in secondary organic carbon (SOC) concentrations for use in epidemiologic studies and other applications. A regression method was found to be a simple and accurate approach to estimate SOC and primary OC (POC) from PM2.5 speciated data and gases concentrations. POC was found significantly associated with CVD in an epidemiologic model.

A method to estimate the fraction of potassium attributable to biomass burning (K_b) was developed and evaluated. This method demonstrated that K_b is a more robust indicator of the source than total potassium. The use of K_b in a receptor model results in a lower fraction of PM2.5 apportioned to biomass burning and a greater fraction to mobile sources. The use of K_b in health studies can help to distinguish the potential impacts of biomass burning and mobile sources on CVD.

CHAPTER 1 INTRODUCTION

The World Health Organization (WHO) estimates that two million people die prematurely per year as a result of air pollutants worldwide (WHO, 2006). In the United States (US), it is estimated that 160,000 cases of premature mortality in 2010 were prevented with reductions in particle matter (PM) and ozone (O_3) from the 1990 Clean Air Act amendments (US-EPA, 2011). Air pollution is particularly important in developing countries, where resources for measurement and control are scarce and legislation is more flexible.

The recognition that air pollutants have effects on health supported the establishment of the National Ambient Air Quality Standards (NAAQS) in the US in 1970 and similar legislation in other countries. Under the NAAQS, carbon monoxide (CO), nitrogen dioxide (NOx), sulfur dioxide (SO_2), particulate matter (PM10 and PM2.5), ozone (O_3) and lead (Pb) are recognized as criteria pollutants and their concentration limits are legislated.

In particular, PM2.5 has been recognized as one of the pollutants with more adverse health effects (Brook et al., 2010; Pope et al., 2002; Pope et al., 1995). PM2.5 is emitted by multiple sources and formed in the atmosphere from conversion of gas into particle phase (Seinfeld and Pandis, 2006) resulting in a diverse chemical composition. Though it is not clear what components of the PM2.5 are more responsible for particular health effects (Bell et al., 2009; Franklin et al., 2008; Ostro et al., 2009), the carbonaceous fraction of the PM2.5 has been associated with cardiovascular diseases and respiratory outcomes (Metzger et al., 2004; Mohr et al., 2008; Peel et al., 2005; Peng et al., 2009).

Elemental carbon (EC) is a primary pollutant directly emitted by the source and organic carbon (OC) is simultaneously emitted and formed in the atmosphere. Primary OC

(POC) is mainly emitted from fossil fuel combustion in mobile sources and biomass combustion (e.g., forest fires). Secondary OC (SOC) is formed in the atmosphere by photochemical reactions of volatile organic compounds (VOCs) of biogenic and anthropogenic origin followed by the condensation of reaction products onto particles (Kroll and Seinfeld, 2008). At present, there is no measurement approach that definitively differentiates between POC and SOC, and different methods have been used to estimate SOC. Methods that rely on the use of tracer species of primary activity and secondary photochemistry formation include the EC tracer (Turpin and Huntzicker, 1991) and regression (Blanchard et al., 2008) methods. Receptor models have also been used to estimate primary and secondary fractions in the PM2.5, notably Chemical Mass Balance (CMB) (Watson et al., 1984) and Positive Matrix Factorization (PMF) (Norris and Vedantham, 2008).

Source apportionment studies have associated PM2.5 elemental carbon (EC) and organic carbon (OC) with combustion sources, such as vehicles and biomass burning (Kim et al., 2003; Lee et al., 2008; Marmur et al., 2006). Furthermore, the application of epidemiologic models using source contributions from receptor models has permitted the association of health outcomes with specific emission sources (Laden et al., 2000; Mar et al., 2000). This approach has found that mobile sources, for example, are generally more closely associated with cardiovascular diseases than other primary sources (Sarnat et al., 2008).

The likely adverse impact of mobile sources on health is due in part to the magnitude of these sources in urban centers, in addition to their composition. In the Atlanta area, for example, traffic emissions are estimated to account for 30% of the PM2.5, 84% of the NOx and 97% of the CO emissions (US-EPA, 2007). Results from source apportionment indicate

that the contribution of tailpipe mobile source emissions to ambient PM2.5 varies from 17 to 26% and the total impact from mobile sources is likely larger considering that a significant amount of crustal material (i.e. Al, Si, Ca, Fe, K) originates from the re-suspension of dust due to vehicles (Kim et al., 2003, 2004; Lee et al., 2008; Liu et al., 2005). Formation of secondary species can contribute further (Docherty et al., 2008).

Biomass burning also emits carbonaceous material (EC and OC) that can be difficult to apportion in heavy traffic impacted areas without the use of accurate source profiles. In the Atlanta area, biomass burning is estimated to contribute between 1.7 and 3.7 $\mu g/m^3$ to PM2.5 (6-22% of total PM2.5 mass) (Kim et al., 2003, 2004; Lee et al., 2008; Liu et al., 2005). The upper limit is likely an overestimation of the real source impact due to the use of potassium (K) in the apportionment of PM2.5. Potassium has multiple emission sources (e.g., wood smoke, soil dust, sea salt, coal fire, industry and meat cooking) (Andreae, 1983; Watson and Chow, 2001; Watson et al., 2001) that can impact factor analysis receptor modeling.

Air quality management involves multiple tasks with different levels of complexity from the estimation of emissions from sources, analysis of ambient concentrations, assessment of exposure to air pollutants, and evaluation of health and ecosystem effects. A quantitative evaluation at every step is an important task for policy makers in order to show that specific policy decisions have produced the desired benefits, i.e. the accountability paradigm. However, the intended outcomes are not always quantifiable, or even observable. As a result of that limitation, surrogate measures of the environmental impacts are typically used as indicators of the range of outcomes experienced.

Environmental indicators, as defined by EPA, are numerical values whose time trends represent the condition of the environment on a particular geographic location (US-EPA, 2008). Bell et al. (2011) reviews environmental indicators related to human health at each step in the health system, from emissions through exposure and health endpoint. They conclude that indicators are useful for policy-makers and the general public to assess the state of the environment and the associated health and socio-economic impacts. They also comment on limitations of environmental indicators, such as the spatial and temporal representativeness of single pollutant indicators, and the lack of consideration to the simultaneous exposure to multiple pollutants.

Environmental indicators are often linked to health in the form of health outcome-based indicators. These indicators not only represent the state of the environment, but also describe their relationships to particular health outcomes (US-EPA, 2006), facilitating the evaluation of public health policy effectiveness as result of improvement in environmental conditions. In this thesis, emission and health outcome-based environmental indicators are developed and evaluated for use in air quality and health studies. Different indicators are explored, from single to multipollutant, with the idea that indicators should be easy to calculate from readily available data and should be able to represent a range of outcomes associated with source emissions and policies (Figure 1.1).

Indicators sets for single and multipollutant indicators are presented to facilitate their application in air quality management. Indicator sets include not only indicator values and uncertainties, but also relationships between indicators at different stages of the air quality chain, from emission to ambient concentrations to health outcomes. The attributes accompanied the indictor sets include type of information needed to estimate the indicator,

ease of use, range of validity or appropriate references. The indicator sets are expected to be useful for policy makers who are interested not only in the value of the indicators, but also in their associated uncertainties and their applicability at other times and other regions.

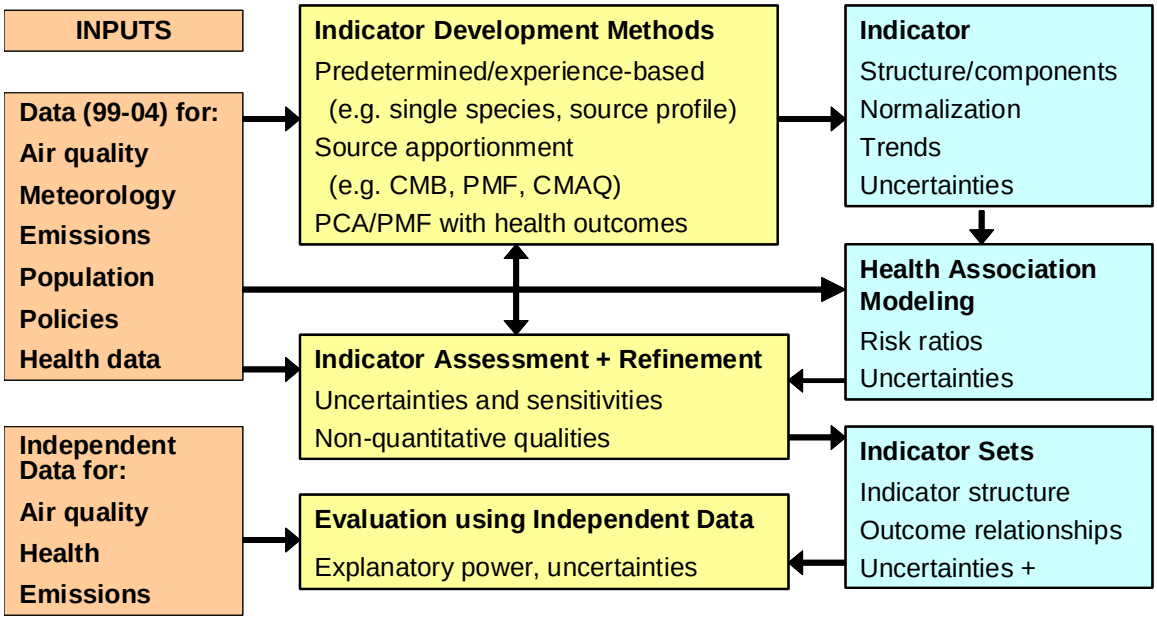

Figure 1.1 Proposed approach to developing and assessing outcome-based indicators and indicator sets.

The thesis is organized as follows.

Chapter 2: Comparison of SOC estimates and uncertainties from aerosol chemical composition and gas phase data in Atlanta. POC and SOC as indicators of combustion and photochemical activity are estimated and compared using four different methods: the EC tracer method, a regression method, PMF and CMB. Uncertainties for every method are calculated. SOC estimates are compared with the water soluble fraction of the OC, which has been suggested as a surrogate of SOC when biomass burning is negligible. Finally, total OC

and primary and secondary OC fractions are used in an epidemiologic model to assess differences in health outcomes.

Chapter 3: Revising the use of potassium (K) in the source apportionment of PM2.5. A method to estimate the fraction of potassium associated with biomass burning (K_b) is evaluated based on a linear regression with iron. Temporal and spatial variability of K_b is explored over a period of six years in the Atlanta area. K_b is implemented in a receptor model to assess the changes in PM2.5 apportionment with respect to the use of regular K. Finally, K and K_b and biomass burning source impacts are used in an epidemiologic model to assess differences in health outcomes.

Chapter 4: Development of outcome-based, multipollutant mobile source indicators. Multipollutant indicators of mobile source impacts are developed from readily available CO, NOx, and elemental carbon (EC) data for use in air quality and epidemiologic analysis. The development and assessment of Integrated Mobile Source Indicators (IMSI) are based on emission and health outcomes. The emission-based IMSI are derived from analysis of emissions such that pollutant concentrations are mixed and weighted based on emission ratios. EB-IMSI are developed and compared for Atlanta, GA and Dallas, TX. The health-based indicators (HB-IMSI) are weighted combinations of pollutants that have the strongest association with health outcomes in an epidemiologic model in Atlanta.

Chapter 5: Mobile source air quality impact indicator sets for policy utilization: evaluation and uncertainties. The analysis of long-term emission trends, pollutant concentrations, and concentration-response functions is used to develop a link between emissions and health outcomes for single and multipollutant indicators. The comparison of human health benefits (HHB) associated with CO versus NOx and EC suggests that emission

controls on gasoline vehicles have been more effective to improve public health than emission controls on diesel vehicles from 1999-2004. The evaluation of HHB using integrated indicators supports the previous finding. In addition, HHB estimated using IMSIs were found more consistent than using single indicators, possibly due to IMSIs being better surrogates of the source. Indicators sets for single and multipollutant indicators are presented to facilitate their application on air quality management.

Chapter 6: Conclusions and future research. Emission- and health-based multipollutant indicators for mobile sources were developed and evaluated using a novel approach. A framework to estimate human health benefits as a result of mobile source emission controls was proposed using indicators. Indicators sets were developed to assist with the application of indicators in other regions. Although this dissertation was focused on mobile sources, methods developed here can be extended to other sources.

1.1. References

Andreae, M. O., 1983. Soot carbon and excess fine potassium: long-range transport of combustion-derived aerosols. Science 220, 1148-1151.

Bell, M. L., Cifuentes, L. A., Davis, D. L., Cushing, E., Gusman Telles, A. and Gouveia, N., 2011. Environmental health indicators and a case study of air pollution in Latin American cities. Environmental Research 111, 57-66.

Bell, M. L., Ebisu, K., Peng, R. D., Samet, J. M. and Dominici, F., 2009. Hospital admissions and chemical composition of fine particle air pollution. American Journal of Respiratory and Critical Care Medicine 179, 1115-1120.

Blanchard, C. L., Hidy, G. M., Tanenbaum, S., Edgerton, E., Hartsell, B. and Jansen, J., 2008. Carbon in Southeastern US aerosol particles: empirical estimates of secondary organic aerosol formation. Atmospheric Environment 42, 6710-6720.

Brook, R. D., Rajagopalan, S., Pope, C. A., III, Brook, J. R., Bhatnagar, A., Diez-Roux, A. V., Holguin, F., Hong, Y., Luepker, R. V., Mittleman, M. A., Peters, A., Siscovick,

D., Smith, S. C., Jr, Whitsel, L. and Kaufman, J. D., 2010. Particulate matter air pollution and cardiovascular disease: an update to the scientific statement from the American Heart Association. Circulation 121, 2331-2378.

Docherty, K. S., Stone, E. A., Ulbrich, I. M., DeCarlo, P. F., Snyder, D. C., Schauer, J. J., Peltier, R. E., Weber, R. J., Murphy, S. M., Seinfeld, J. H., Grover, B. D., Eatough, D. J. and Jimenez, J. L., 2008. Apportionment of primary and secondary organic aerosols in Southern California during the 2005 study of organic aerosols in Riverside (SOAR-1). Environmental Science & Technology 42, 7655-7662.

Franklin, M., Koutrakis, P. and Schwartz, P., 2008. The role of particle composition on the association between PM2.5 and mortality. Epidemiology 19, 680-689.

Kim, E., Hopke, P. K. and Edgerton, E. S., 2003. Source identification of Atlanta aerosol by positive matrix factorization. Journal of the Air & Waste Management Association 53, 731-739.

Kim, E., Hopke, P. K. and Edgerton, E. S., 2004. Improving source identification of Atlanta aerosol using temperature resolved carbon fractions in positive matrix factorization. Atmospheric Environment 38, 3349-3362.

Kroll, J. H. and Seinfeld, J. H., 2008. Chemistry of secondary organic aerosol: formation and evolution of low-volatility organics in the atmosphere. Atmospheric Environment 42, 3593-3624.

Laden, F., Neas, L. M., Dockery, D. W. and Schwartz, J., 2000. Association of fine particulate matter from different sources with daily mortality in six U.S. cities. Environ. Health Perspect. 108, 941-947.

Lee, S., Liu, W., Wang, Y. H., Russell, A. G. and Edgerton, E. S., 2008. Source apportionment of PM2.5: comparing PMF and CMB results for four ambient monitoring sites in the Southeastern United States. Atmospheric Environment 42, 4126-4137.

Liu, W., Wang, Y. H., Russell, A. and Edgerton, E. S., 2005. Atmospheric aerosol over two urban-rural pairs in the southeastern United States: chemical composition and possible sources. Atmospheric Environment 39, 4453-4470.

Mar, T. F., Norris, G. A., Koenig, J. Q. and Larson, T. V., 2000. Associations between air pollution and mortality in Phoenix, 1995-1997. Environ. Health Perspect. 108, 347-353.

Marmur, A., Park, S. K., Mulholland, J. A., Tolbert, P. E. and Russell, A. G., 2006. Source apportionment of PM2.5 in the southeastern United States using receptor and emissions-based models: Conceptual differences and implications for time-series health studies. Atmospheric Environment 40, 2533-2551.

Metzger, K. B., Tolbert, P. E., Klein, M., Peel, J. L., Flanders, W. D., Todd, K., Mulholland, J. A., Ryan, P. B. and Frumkin, H., 2004. Ambient air pollution and cardiovascular emergency department visits. Epidemiology 15, 46-56.

Mohr, L. B., Luo, S., Mathias, E., Tobing, R., Homan, S. and Sterling, D., 2008. Influence of season and temperature on the relationship of elemental carbon air pollution to pediatric asthma emergency room visits. Journal of Asthma 45, 936 - 943.

Norris, G. and Vedantham, R., 2008. EPA Positive Matrix Factorization (PMF) 3.0. U.S. Environmental Protection Agency, Research Triangle Park, NC.

Ostro, B., Roth, L., Malig, B. and Marty, M., 2009. The effects of fine particle components on respiratory hospital admissions in children. Environ. Health Perspect. 117, 475-480.

Peel, J. L., Tolbert, P. E., Klein, M., Metzger, K. B., Flanders, W. D., Todd, K., Mulholland, J. A., Ryan, P. B. and Frumkin, H., 2005. Ambient air pollution and respiratory emergency department visits. Epidemiology 16, 164-174.

Peng, R. D., Bell, M. L., Geyh, A. S., McDermott, A., Zeger, S. L., Samet, J. M. and Dominici, F., 2009. Emergency admissions for cardiovascular and respiratory diseases and the chemical composition of fine particle air pollution. Environ. Health Perspect. 117, 957-963.

Pope, C. A., Burnett, R. T., Thun, M. J., Calle, E. E., Krewski, D., Ito, K. and Thurston, G. D., 2002. Lung cancer, cardiopulmonary mortality, and long-term exposure to fine particulate air pollution. JAMA 287, 1132-1141.

Pope, C. A., Dockery, D. W. and Schwartz, J., 1995. Review of epidemiological evidence of health-effects of particulate air-pollution. Inhalation Toxicology 7, 1-18.

Sarnat, J. A., Marmur, A., Klein, M., Kim, E., Russell, A. G., Sarnat, S. E., Mulholland, J. A., Hopke, P. K. and Tolbert, P. E., 2008. Fine particle sources and cardiorespiratory morbidity: An application of chemical mass balance and factor analytical source-apportionment methods. Environ. Health Perspect. 116, 459-466.

Seinfeld, J. H. and Pandis, S. N., 2006. Atmospheric Chemisty and Phyisics, 2 edition ed, Wiley-Interscience, Hoboken, NJ.

Turpin, B. J. and Huntzicker, J. J., 1991. Secondary formation of organic aerosols in the Los Angeles basin - A descriptive analysis of organic and elemental carbon concentrations. Atmospheric Environment 25, 207-215.

U.S. Environmental Protection Agency, 2006. Development of Environmental Health Outcome Indicators.Office of Research and Development, Washington, D.C. Available on the internet at: http://www.epa.gov/ncer/rfa/2006/2006_star_ephi.html

U.S. Environment Protection Agency, 2007. 2002 National Emissions Inventoriy Data & documentation.

U.S. Environmental Protection Agency, 2008. EPA's Report on the Environment.National Center for Environmental Assessment, Washington, D.C.

U.S. Environmental Protection Agency, 2011. The benefits and costs of the Clean Air Act from 1990 to 2020.Office of Air and Radiation, Washington, D.C.

Watson, J. G. and Chow, J. C., 2001. Source characterization of major emission sources in the Imperial and Mexicali Valleys along the US/Mexico border. Science of The Total Environment 276, 33-47.

Watson, J. G., Chow, J. C. and Houck, J. E., 2001. PM2.5 chemical source profiles for vehicle exhaust, vegetative burning, geological material, and coal burning in Northwestern Colorado during 1995. Chemosphere 43, 1141-1151.

Watson, J. G., Cooper, J. A. and Huntzicker, J. J., 1984. The effective variance weighting for least-squares calculations applied to the mass balance receptor model. Atmospheric Environment 18, 1347-1355.

World Health Organization, 2006. Air quality guidelines for particulate matter, ozone, nitrogen dioxide and sulfur dioxide.Geneva, Switzerland.

CHAPTER 2 COMPARISON OF SOC ESTIMATES AND UNCERTAINTIES FROM AEROSOL CHEMICAL COMPOSITION AND GAS PHASE DATA IN ATLANTA

(Pachon, J. E., Balachandran, S., Hu, Y., Weber, R. J., Mulholland, J. A. and Russell, A. G. *Atmospheric Environment* 44, 3907-3914, 2010).

2.1. Abstract

In the Southeastern US, organic carbon (OC) comprises about 30% of the $PM_{2.5}$ mass. A large fraction of OC is estimated to be of secondary origin. Long-term estimates of SOC and uncertainties are necessary in the evaluation of air quality policy effectiveness and epidemiologic studies. Four methods to estimate secondary organic carbon (SOC) and respective uncertainties are compared utilizing $PM_{2.5}$ chemical composition and gas phase data available in Atlanta from 1999 to 2007. The elemental carbon (EC) tracer and the regression methods, which rely on the use of tracer species of primary and secondary OC formation, provided intermediate estimates of SOC as 30% of OC. The other two methods, chemical mass balance (CMB) and positive matrix factorization (PMF) solve mass balance equations to estimate primary and secondary fractions based on source profiles and statistically-derived common factors, respectively. CMB had the highest estimate of SOC (46% of OC) while PMF led to the lowest (26% of OC). The comparison of SOC uncertainties, estimated based on propagation of errors, led to the regression method having the lowest uncertainty among the four methods. We compared the estimates with the water soluble fraction of the OC, which has been suggested as a surrogate of SOC when biomass burning is negligible, and found a similar trend with SOC estimates from the regression method. The regression method also showed the strongest correlation with daily SOC

estimates from CMB using molecular markers. The regression method shows advantages over the other methods in the calculation of a long-term series of SOC estimates.

2.2. Introduction

In the Southeastern US, OC comprises approximately 30% of the $PM_{2.5}$ mass. OC can be of both primary and secondary origin. Primary OC (POC) is mainly emitted from fossil fuel combustion in stationary, area and mobile sources, and biomass combustion (e.g., forest fires). In Atlanta, the major sources of POC are motor vehicles and biomass burning (Lee et al., 2007; Zheng et al., 2002). Secondary OC (SOC) is formed in the atmosphere by photochemical reactions of volatile organic compounds (VOCs) of biogenic and anthropogenic origin followed by the condensation of reaction products onto particles (Kroll and Seinfeld, 2008). At present, there is no measurement approach that definitively differentiates between POC and SOC, though detailed speciation can identify specific components that would be dominantly primary or secondary. Epidemiologic studies suggest differences in health outcomes associated with POC attributed to mobile and biomass burning sources, versus other OC, presumably SOC (Sarnat et al., 2008).

Typically, as part of the Speciation Trends Network for example, OC in $PM_{2.5}$ is measured on 24-hour filter-based samples, although greater resolution is possible using semi-continuous *in situ* instruments (Solomon et al., 2000). The amount of OC on the filters is quantified using thermal-optical techniques (Chow et al., 1993; Turpin et al., 2000). These techniques are designed to measure the total OC fraction, and do not distinguish between primary and secondary components. Since the formation of SOC leads to oxygenated, polar compounds, it has been suggested that the water soluble fraction of the OC (WSOC) is a surrogate for the SOC when biomass burning impact is negligible (Hennigan et al., 2008;

Weber et al., 2007). WSOC can be measured in the laboratory using $PM_{2.5}$ filters and posteriori separation of the water soluble fraction or *in-situ* using a Particle Into Liquid Sampler (PILS) that captures particles in water from where the carbonaceous fraction is quantified using a Total Organic Carbon (TOC) analyzer (Sullivan et al., 2006). Summertime measurements in Atlanta find that WSOC is about 55-65% of total OC.

Different methods have been used to estimate SOC. Methods that rely on the use of tracer species of primary activity and secondary photochemistry formation include the EC tracer and regression methods. Receptor models have also been used to estimate primary and secondary fractions in the $PM_{2.5}$, notably Chemical Mass Balance (CMB) and Positive Matrix Factorization (PMF). While estimates from chemical transport models (CTM) are available, simulated SOC values are viewed as highly uncertain, and likely biased (Eder and Yu, 2006; Tesche et al., 2006). Some studies have used organic molecular markers and specific compounds to separate the POC and SOC fractions (Zheng et al., 2006). Given that speciated organic compound concentrations are not widely available and that their measurement is resource intensive, methods that rely on typically available $PM_{2.5}$ speciation and gaseous data are preferable. Such methods are used in this study to construct multi-year time series of pollutants for epidemiologic analysis and air quality policy effectiveness studies.

Estimates of SOC in Atlanta vary between methods and have focused on different periods of time from one or two months during summer and winter to three years (Blanchard et al., 2008; Lee et al., 2008b; Lim and Turpin, 2002; Marmur et al., 2005; Zheng et al., 2007; Zheng et al., 2002). These studies have defined uncertainties in the SOC estimates as the standard deviation of the mean, with the exception of Blanchard et al., (2008) who

estimated uncertainties as one-half the range from alternative regressions. The standard deviation represents a good measure of the variation in SOC estimates but does not consider the different types of uncertainties involved in the SOC calculation (e.g. ambient measurements, source profiles, regression coefficients, primary ratios, fitting methods). Here, we assess and compare the uncertainty in the SOC estimates from four different methods, considering uncertainties in input datasets and methods.

2.3. Methods

Nine-year time series of SOC concentrations and respective uncertainties are estimated using four methods: EC tracer (Turpin et al., 2000), regression (Blanchard et al., 2008), CMB (Watson et al., 1984) and PMF (Paatero and Tapper, 1994). The results are then compared under the following metrics in order to choose the most accurate estimate: uncertainties (lowest uncertainty preferred) estimated by propagation of errors (Bevington and Robinson, 2003), seasonal estimates (summer SOC should exceed winter), day-to-day variability (smooth for a secondary pollutant), comparison with related work (i.e. molecular marker-based CMB) and comparison with WSOC measurements (as a surrogate of SOC).

2.3.1. EC tracer method

The EC tracer method consists of estimating a primary OC/EC ratio during periods when SOC is expected to be negligible (e.g. night, winter, overcast, clean background, minimal long range transport).

$$POC = (OC/EC)_p * EC + (OC)_{nc} \quad (2.1)$$

$$SOC = OC - POC \quad (2.2)$$

Here $(OC)_{nc}$ is the non-combustion contribution to the OC, from sources such as vegetative detritus, tire wear and industrial processes. Equation 2.2 can result in negative values of SOC, in which case SOC is set to zero.

Typically, $(OC/EC)_p$ in Equation 2.1 is determined from the linear regression between OC and EC (e.g. Demming regression, (Saylor et al., 2006) over a long period of time, with the intercept determining $(OC)_{nc.}$ Alternatively, $(OC/EC)_p$ can be estimated from days when primary or secondary activity is more pronounced (such as in (Cabada et al., 2004). For this study, the $(OC/EC)_p$ ratio was estimated in three steps: i) we selected days from 1999-2007 with low photochemical activity, defined as days with O_3 (max 8hr average) concentration below the 25^{th} percentile, O_3<41ppb in summer and O_3<20ppb in winter ii) we plotted time series of OC, EC, OC/EC, CO and O_3 and identified days when primary activity was more pronounced (an example of this selection is shown in Figure 2.1) and iii) we computed averaged OC/EC ratios on those days, obtaining 1.7 for summer and 2.4 for winter. The application of a unique $(OC/EC)_p$ ratio for year-round estimates may not account for seasonal variation (Snyder et al., 2009). The larger winter value suggests an increased influence of biomass burning which has a higher OC/EC primary emissions ratio. Other studies in the area have found similar values for these ratios. Using time-resolved OC fractions in summer time for the estimation of SOC, Lim and Turpin (2002) found a ratio $(OC/EC)_P$ of 1.8 as reasonable and 2.1 as the upper limit. Using a multiscale air quality model over the United States, Yu et al (2007) found $(OC/EC)_p$ ratios for Atlanta of 1.76 in summer and 2.76 in winter. For this study, the EC tracer refers exclusively to the application of the method using summer/winter ratios. Variation of the $(OC/EC)_p$ ratio on time scales less than half a year is beyond the scope of this study.

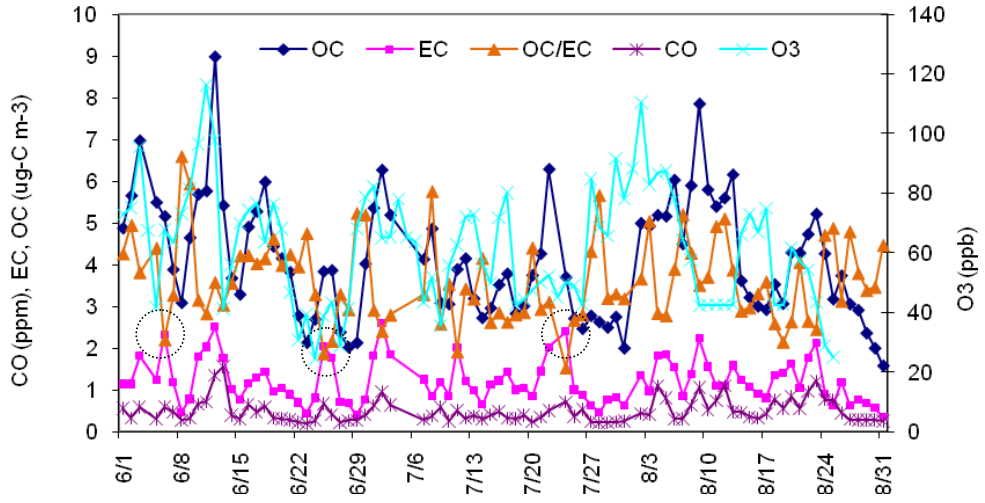

(a)

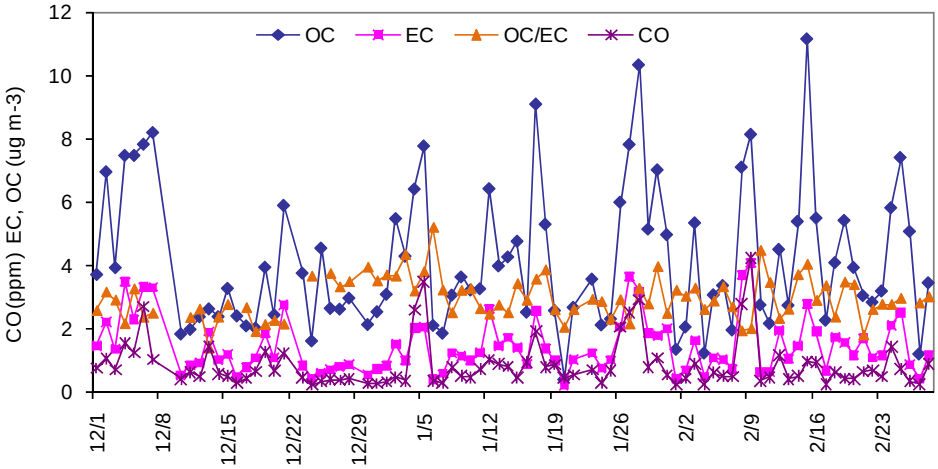

(b)

Figure 2.1 Time series of primary and secondary species and OC/EC ratio during (a) summer 2002 (b) and winter 2002. During summer, the circled days have a decrease in O_3 concentrations, and high levels of OC, EC and CO, denoting a predominance of primary activity. For those days the average (OC/EC) ratio was 1.7. During winter, days with ozone concentrations below the 25th percentile had an average (OC/EC) ratio of 2.4.

The initial estimate of the uncertainty (σ) is calculated using propagation of relative errors.

$$\sigma_{POC}{}^2 = \sigma_{EC}{}^2 \left(\frac{OC}{EC}\right)_P^2 + \sigma^2_{\left(\frac{OC}{EC}\right)_P} EC^2 + \sigma_{OC_{nc}}{}^2 \quad (2.3)$$

Here, the uncertainty in the EC and OC components was calculated using the procedure of Polissar et al (1998). Briefly, the uncertainty in the observed concentrations was set as the sum of the analytical uncertainty times the concentration plus one-third of the detection limit (DL) value. The uncertainty in the primary (OC/EC) ratio was defined as one standard deviation of the estimated ratios. The uncertainty in the secondary organic fraction was calculated by propagating the uncertainties in the POC fraction and the measured OC.

$$\sigma_{SOC}{}^2 = \sigma_{OC}{}^2 + \sigma_{POC}{}^2 \quad (2.4)$$

The root mean square average of the uncertainty for the POC and SOC estimates over the nine-year period of time is calculated as

$$\overline{\sigma_i} = \sqrt{\frac{1}{N}\sum_{j=1}^{N}\sigma_{ij}^2} \quad (2.5)$$

where σ_{ij} is the uncertainty in the i^{th} parameter on the j^{th} day, with a total of N days.

2.3.2. Regression method

The regression method uses tracers of primary emissions (EC, 8-h average CO) as well as photochemical activity (8-h average O_3, sulfate SO_4, nitrate NO_3) to determine POC and SOC. We modified this approach by adding potassium (XRF K from the SEARCH data) to identify POC from biomass burning which accounts for a large part of the POC in the southeastern US (Kim et al., 2003, 2004):

$$OC = a + b*EC + c*CO + d*O_3 + e*lag(O_3) + f*SO_4 + g*NO_3 + h*K \quad (2.6)$$

$$POC_o = b*EC + c*CO + h*K \quad (2.7)$$

$$SOC_o = d*O_3 + e*lag(O_3) + f*SO_4 + g*NO_3 \quad (2.8)$$

The regression coefficients (a-h) are determined using least square fitting (LSF), and each coefficient is evaluated for its statistical significance. Here POC_o and SOC_o are initial estimates for each day. To guarantee that the sum of POC and SOC is equal to the observed OC, we distributed the initial estimates based on the mass fraction ratios.

$$POC = \left(\frac{POC_O}{POC_O + SOC_O} \right) OC \quad (2.9)$$

$$SOC = \left(\frac{SOC_O}{POC_O + SOC_O} \right) OC \quad (2.10)$$

On a year-round basis, multivariate regression of OC with EC, CO, K, SO_4, NO_3 and O_3 led to an R^2=0.65 (n=2921), suggesting common sources between OC and primary and secondary pollutants. In summer, regression of OC with EC, K, SO_4, NO_3 and O_3 results in a slightly stronger statistical fit (R^2=0.68, n=1476). The regression coefficient for NO_3 was not statistically significant ($p>0.05$) and the independent term 'a' (in Equation 2.6) had the lowest significance; therefore, the regression was performed with an intercept of zero. In this case, the significance of secondary tracers, such as O_3 (t-Stat=22.7, $p<0.01$), is comparable with primary tracers, such as EC (t-Stat=21.4, $p<0.01$). In winter, regression of OC with EC, CO, K, NO_3 and O_3 results in a stronger statistical fit (R^2=0.78, n=1427) than the summer regression. The independent term 'a' and the SO_4 regression coefficient were not statistically significant ($p>0.05$); EC (t-Stat=26.8, $p<0.01$) and K (t-Sat=13.6, $p<0.01$) were the most

significant coefficients, suggesting a strong impact of mobile sources and biomass burning on OC. Hereafter the regression method will refer to the application of the method using separate summer/winter regression results.

We calculate the uncertainty by propagating errors for every term in the regression method. The uncertainty in each regression coefficient (i.e. σ_b) was obtained from the standard error in the regression analysis and the uncertainty in the species concentration (i.e. σ_{EC}) was estimated using the procedure of Polissar et al (1998). The uncertainties were propagated to find daily uncertainties in POC and SOC:

$$(\sigma_{POC})^2 = (\sigma_{EC})^2 * b^2 + (\sigma_{CO})^2 * c^2 + (\sigma_K)^2 * h^2 + (\sigma_b)^2 * EC^2 + (\sigma_c)^2 * CO^2 + (\sigma_h)^2 * K^2 \quad (2.11)$$

$$(\sigma_{SOC})^2 = (\sigma_{O3})^2 * d^2 + (\sigma_{SO4})^2 * f^2 + (\sigma_{NO3})^2 * g^2 + (\sigma_d)^2 * O_3^2 + (\sigma_f)^2 * SO_4^2 + (\sigma_g)^2 * NO_3^2 \quad (2.12)$$

The average uncertainties for the POC and SOC estimates, over the nine-year period, are calculated using the root mean square average (Equation 2.5).

2.3.3. Chemical Mass Balance (CMB)

To estimate the SOC fraction in the CMB model, we include six primary source profiles and four profiles that represent secondary species formation (Marmur et al., 2005). $PM_{2.5}$ components NO_3, SO_4, NH_4, EC, OC, and metals Br, Al, Si, Ca, Fe, K, Mn, Pb, Cu, Se, Zn and Cr were used as fitting species. Primary source profiles used include gasoline vehicles (LDGV), diesel vehicles (HDDV), soil dust (SDUST), biomass burning (BURN), coal-fired power plants (CFPP) and cement production (CEM). Both BURN and LDGV have high fractions of OC in their source profiles (0.64 and 0.55 respectively). Profiles for components formed from atmospheric reactions are secondary ammonium sulfate (AMSULF), secondary

ammonium bisulfate (AMBSLFT), secondary ammonium nitrate (AMNITR) and other OC (OTHROC). CMB reproduces 91% of $PM_{2.5}$ mass (R^2 =0.90, n=2698, χ^2 =3.39), apportioning 15% of the $PM_{2.5}$ mass as 'other OC' which we take as the SOC fraction. It is recognized that there are potential non-secondary sources of OTHROC, including vegetative detritus, and unapportioned primary organic carbon in this source (e.g., (Zheng et al., 2002) and therefore OTHROC may not include only SOC (Ding et al., 2008).

Uncertainties in CMB source contributions are given by the model and were calculated using a weighted variance approach:

$$\sigma_{g_{ik}} = \sum_{i=1}^{n} \left[\frac{f_{kj}^2}{\sigma_{C_{ij}}^2 + \sum_{k=1}^{N} \sigma_{f_{jk}}^2 g_k^2} \right]^{-1/2} \tag{2.13}$$

where f_{kj} is the source profile of species j in source k, $\sigma_{f_{jk}}$ is the uncertainty in the profile, g_k is the source contribution of source k, $\sigma_{g_{ik}}$ is the uncertainty in the contribution, and $\sigma_{c_{ij}}$ is the uncertainty in the measured concentration c_{ij}. The uncertainty in the POC fraction was estimated by propagating the uncertainties in the organic carbon fraction of the primary sources (SDUST, BURN, HDDV, LDGV, CFPP, CEM) and the uncertainty in the SOC fraction was estimated propagating the uncertainties in the POC and the measured OC (such as in Equation 2.4). The average uncertainties for the POC and SOC estimates, over the nine-year period, are calculated using the root mean square average (Equation 2.5).

2.3.4. Positive Matrix Factorization (PMF)

We used EPA-PMF 3.0 (Norris and Vedantham, 2008) for our simulations and classified species in the input model based on the signal/noise ratio. Strong species for this study were NO_3, SO_4, NH_4, EC, OC, Br, Al, Si, Ca, Fe, and K. Weak species were Mn, Pb, Cu, Se, Zn

and Cr. Since $PM_{2.5}$ was included and classified as a total variable, the model assigns it as a weak species in order to not double count its importance (Reff et al., 2007). We used 10 convergent runs and chose the run with the lowest error in the minimization of the mass balance equation. PMF reproduces 87% of the $PM_{2.5}$ (R^2=0.91, n=2931). To identify the optimum number of factors, we ran PMF with five, six and seven factors and obtained the best fit with six factors (soil dust, biomass burning, secondary sulfate, secondary nitrate, cement and mobile sources). The SOC fraction in PMF is calculated by adding the OC fractions in the secondary factors and the unidentified OC fraction, defined as the difference between measured and fit OC (Lee et al., 2008b). The procedure of Polissar et al. (1998) was used in this study to calculate uncertainties in the species concentrations. Briefly, for data below DL, the concentrations were replaced with the value DL/2 and the uncertainty was set as (5/6)*DL. For missing data, concentrations were replaced by the geometric mean and the respective uncertainty was set at four times that of this mean concentrations. PMF provides uncertainties in factor profiles ($\sigma_{f_{jk}}$), defined as the standard deviation of 100 bootstrapping runs. The uncertainty in factor contribution of species j (σ_{ij}) is calculated as the product of the factor contribution (g_{ik}) times the uncertainty in the factor profiles.

$$\sigma_{ji}^2 = \sum_k \sigma_{f_{jk}}^2 g_{ki}^2 \qquad (2.14)$$

Similar to CMB, POC uncertainty was propagated from the uncertainty in the OC fraction of primary factors (soil dust, biomass burning, cement and mobile sources). The uncertainty in the SOC estimate was propagated from the uncertainty in OC in the secondary factors (sulfate, nitrate) and the unidentified OC fraction. The average uncertainties for the POC and

SOC estimates, over the nine-year period, are calculated using the root mean square average (Equation 2.5).

2.3.5. Air Quality Data

Aerosol chemical composition and gas phase data for this project were obtained for the Jefferson Street (JST) monitoring site, a mixed industrial-residential area near downtown Atlanta, GA (coordinates 33.7 N, 84.4 W and at an elevation of 275m above sea level) during the period 1/2/1999-12/31/2007. Sampling at JST is part of a larger study called the Southeastern Aerosol Research and Characterization (SEARCH) network. Further information on this study and characteristics of the network are found elsewhere (Edgerton et al., 2005, 2006; Hansen et al., 2003). $PM_{2.5}$ monitoring includes daily 24-hour average measurements of ionic, carbonaceous and metal species concentrations. For the period, a total of 2937 days had valid data available. Data treatment of missing data and values below detection limits was performed as suggested by the network to ensure data quality (Hansen et al., 2003). A sample in which one or more major components were missing after the data treatment was discarded. Samples from the 4th of July, New Years (12/31) and adjacent days were removed from the analysis to avoid unusual noise in the concentrations due to fireworks (e.g. unusually high K concentrations). Measurements of WSOC in Atlanta were available for 120 days in the summer of 2007 (5/17-9/20). The WSOC fraction was measured semi-continuously using a PILS-TOC instrument at the roof of the Ford Environmental Science & Technology building at the Georgia Institute of Technology (GT). This site is approximately two miles away from the JST site. More information on the WSOC measurements can be found elsewhere (Hennigan et al., 2008; Sullivan and Weber, 2006). We found that OC measured with the continuous instruments at GT was higher than the OC measured at JST

(5.76 vs 3.97 ug-C m^{-3}). Explanation for this bias includes the loss of semi-volatile compounds from the filters (Edgerton et al., 2005; Turpin et al., 2000) and the positive artifact in the use of semi-continuous analyzers associated with the low air volume sampled and instrumental blanks (Offenberg et al., 2007; Peltier et al., 2007). To estimate the amount of WSOC at JST, we adjusted the WSOC at GT using the OC ratio between both sites.

$$WSOC_{JST} = WSOC_{GT} * \left(\frac{OC_{JST}}{OC_{GT}} \right)_{avg} \quad (2.15)$$

For the summer of 2007, the (OC_{JST}/OC_{GT}) ratio was 0.69, giving an estimated averaged WSOC value of 2.29 μg-C/m^3 at JST (vs. 3.31 μg-C/m^3 at GT).

2.3.6. Associations of SOC estimates with health outcomes

Estimates of POC and SOC from the regression method were implemented in an epidemiologic model to evaluate the health impacts of different OC fractions. Cardiovascular diseases were chosen as the health endpoint for evaluation given that they have shown a significant association with OC in previous studies (Sarnat et al., 2008). The epidemiologic model is described in detail elsewhere (Metzger et al., 2004; Peel et al., 2005) and later in this dissertation (see Section 4.6).

2.4. Results

During the nine-year period, the average OC concentration in Atlanta was 4.09±2.25 μg-C/m^3 (± one standard deviation), with a summer (April-September) mean of 3.90±1.80 μg-C/m^3 and a winter (October-March) mean of 4.25±2.63 μg-C/m^3. The higher OC value in winter in Atlanta is explained by an increase in mobile emissions and biomass burning activity (Lee et al., 2009; Zheng et al., 2002) accompanied by a decrease in the mixing layer.

2.4.1. EC tracer method

The EC tracer method estimates 1.51±1.36 μg-C/m^3 (± root mean square of the uncertainty as defined in Equation 2.5) of SOC in summer (39% of OC) and 0.77±1.96 μg-C/m^3 in winter (18% of OC). The lower amount of SOC in winter is consistent with the SOC formation mechanisms and fewer emissions of biogenic VOCs, which are responsible for a large portion of SOC in Atlanta (Weber et al., 2007). The greater SOC uncertainty in winter (> 100% of the SOC) vs. summer (90% of the SOC) is explained by the higher uncertainties in the OC and EC species and the uncertainty in the primary (OC/EC) ratio during winter. The average of summer and winter estimates gives a SOC fraction of 1.19±1.71 μg-C/m^3 (29% of OC).

2.4.2. Regression Method

The regression method estimates 1.70±0.80 μg-C/m^3 of SOC (44% of OC) in summer and 0.76±0.60 μg-C/m^3 of SOC (18% of OC) in winter. The SOC uncertainty is higher in summer given the larger concentrations and uncertainties in O_3 and SO_4 and the larger values of the regression coefficients. However, the amount of SOC is significantly lower in winter and the uncertainty represents 80% of the SOC value vs. 47% in the summer. The overall SOC uncertainty is driven by the estimate in winter, similar to the EC tracer method. The average of summer and winter estimates gives a SOC fraction of 1.25±0.71 μg-C/m^3 (30% of OC).

2.4.3. Chemical Mass Balance and Positive Matrix Factorization

We applied CMB and PMF with data from 1/2/1999 to 12/31/2007. The fit between measured and predicted OC was better in CMB (R^2=0.99, n=2698) than PMF (R^2=0.77, n=2931). The SOC estimates are 1.92±0.98 μg-C/m^3 (46% of OC) in CMB and 1.12±0.87

ug-C m^{-3} (26% of OC) in PMF. Summer SOC estimates are higher in both methods (2.00±0.93 μg-C/m^3 in CMB and 1.37±0.81 μg-C/m^3 in PMF) with lower uncertainties. In winter, the uncertainty in the SOC estimate is a significant fraction of the SOC concentration (56% in CMB & >100% in PMF). In CMB, it is known that uncertainties in source contributions are more influenced by uncertainties in the source profiles than ambient measurement data (Lee and Russell, 2007). Uncertainties in PMF are driven by the uncertainty in the measured OC species.

2.5. Comparison of SOC estimates and uncertainties

The four methods estimate SOC fractions between 1.12±0.87 and 1.92±0.98 μg-C/m^3 representing 26-46% of the OC respectively (Figure 2.2). CMB led to the highest estimate of SOC while the PMF led to the lowest. The EC tracer and the regression methods provided intermediate estimates of SOC. The higher SOC estimate in CMB is explained by the inclusion of all unapportioned OC into one secondary source. The other-OC source in CMB is correlated with both biomass burning (R^2=0.57) and mobile (R^2=0.55) factors in PMF. This correlation can be explained in part by: i) the other-OC includes primary OC from unidentified sources (such as meat cooking and natural gas combustion) that may correlate with biomass burning and mobile factors in PMF, ii) SOC may be included in the biomass burning factor in PMF since carbon emitted during biomass burning is in some cases oxygenated and water soluble (Lee et al., 2008a), or in the mobile factor since OC emissions from traffic can potentially evolve into SOC (Robinson et al., 2007). The low estimate of SOC by PMF has been found in previous studies in the southeastern US (Lee et al., 2008b). Without use of detailed oxygenated species, PMF is not able to provide further information on SOC because of the colinearity of OC sources.

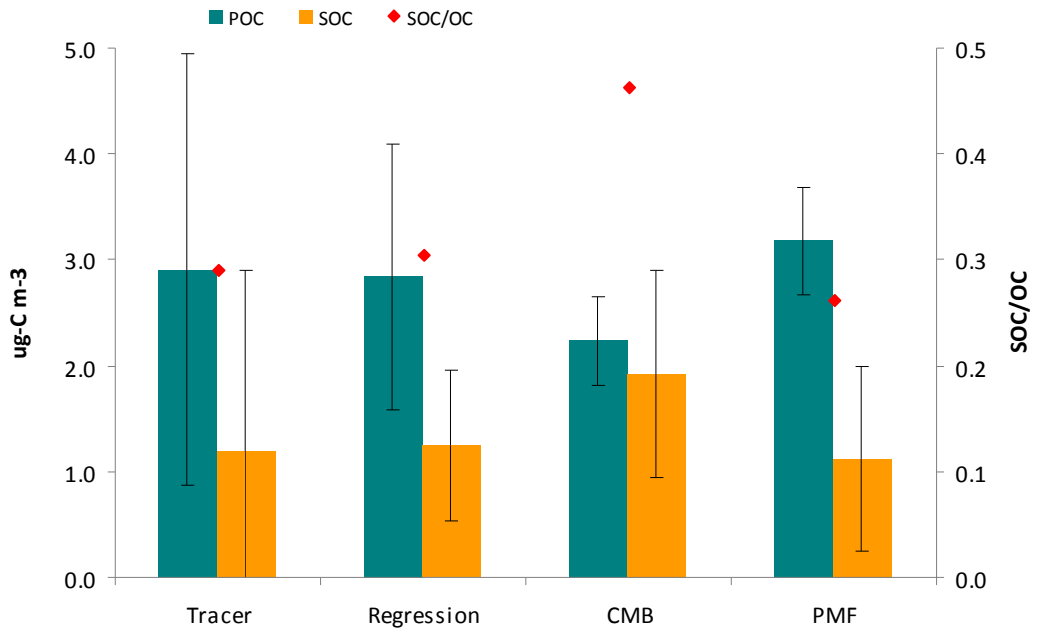

Figure 2.2 Comparison of the four estimates from 1999-2007. The EC tracer (n= 2932) and regression (n=2932) estimates include the use of summer/winter datasets with respective $(OC/EC)_p$ ratios and regression coefficients. For CMB (n= 2698) and PMF (n=2932) the data was not separated by season. Error bars denote the root mean square of the uncertainty in POC and SOC fractions estimated by a propagation of errors.

2.5.1. Uncertainties

The lowest uncertainty in the SOC estimate is found in the regression method and the highest is the EC tracer method (Table 2.1). The CMB uncertainties are comparable to the regression method, and if expressed as a fraction of the SOC concentrations they are even lower. The PMF uncertainties are significantly higher than the uncertainties in the CMB method.

Table 2.1 Comparison of SOC Estimates using four methods

	EC Tracer	**Regression**	**CMB**	**PMF**
n (days)	2931	2931	2698	2931
POC (μg-C/m^3)	2.90 (2.04)[a]	2.84 (1.25)[b]	2.24 (0.41)[c]	3.18 (0.51)[d]
SOC (μg-C/m^3)	1.19 (1.71)	1.25 (0.71)	1.92 (0.98)	1.12 (0.87)
SOC/OC	0.29	0.30	0.46	0.26
σSOC/SOC	1.44	0.57	0.51	0.78
CV	1.06	0.60	0.87	0.92
Zero days of SOC	478	0	114	0
Summer SOC (μg-C/m^3)	1.51 (1.36)	1.70 (0.80)	2.00 (0.93)	1.37 (0.81)
Summer SOC/OC	0.39	0.44	0.51	0.34
σSOC/SOC	0.90	0.47	0.46	0.60
Winter SOC (μg-C/m^3)	0.77 (1.96)	0.76 (0.60)	1.84 (1.03)	0.86 (0.89)
Winter SOC/OC	0.18	0.18	0.45	0.19
σSOC/SOC	2.56	0.80	0.56	1.03

[a] uncertainties in EC tracer method calculated with Equation 2.3-2.5; [b] uncertainties in the regression method calculated with Equation 2.5, 2.11-2.12; [c] uncertainties in CMB calculated with Equation 2.5,2.13; [d] uncertainties in PMF calculated with Equation 2.5,2.14.

2.5.2. Seasonal estimates

In summer, the proportion of SOC estimated by the four methods is similar, with CMB having the highest and PMF the lowest fractions (Figure 2.3). In winter, CMB estimates are much higher than the other methods, indicating the likely inclusion of primary OC in this fraction and therefore, an overestimate of the SOC fraction.

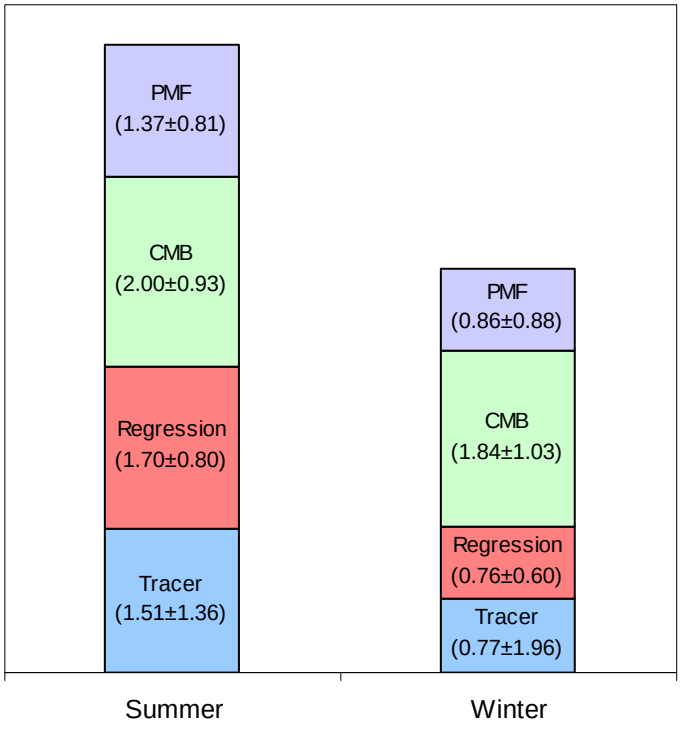

Figure 2.3 Seasonal Estimates of SOC from 1999-2007. Units are μg-C/m^3, for concentrations and uncertainties (defined as the root mean square average).

2.5.3. Day-to-day variability

During the summer 2002, the four estimates exhibit similar day to day variability (Figure 2.4). In winter 2002/2003, regression is the only method that yields smooth pattern, which would be expected for a secondary pollutant. The other estimates have significant variability typically more associated with primary pollutants. The lowest coefficient of variance, associated with this temporal trend, was for the regression method (Table 2.1). The EC tracer and the CMB methods had 478 and 114 days of zero estimated SOC, respectively, occurring when estimated POC is greater than measured OC.

a)

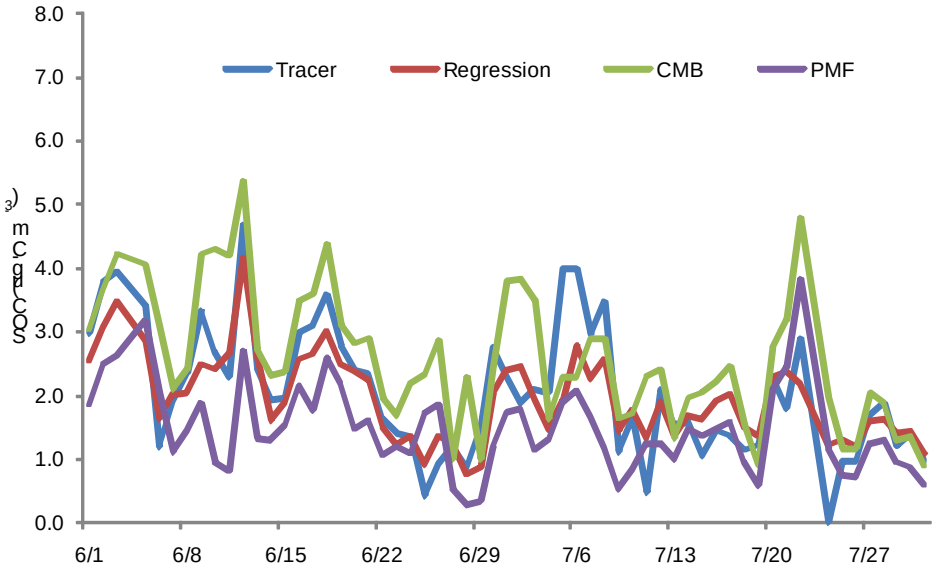

b)

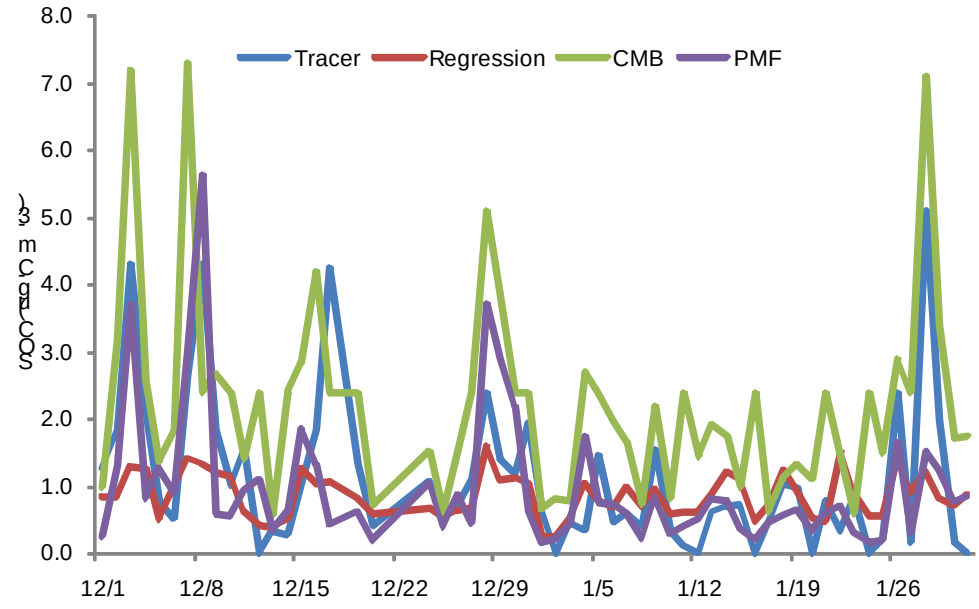

Figure 2.4 Day to day variability of SOC estimates for (a) June-July 2002 and (b) Dec. 2002-January 2003

2.6. Comparison with related work

The range of SOC estimates in this study was 26-47% which is comparable with findings of other studies at Jefferson St in Atlanta (Table 2.2). The lowest SOC estimate (19% of OC) was obtained using PMF (Lee et al., 2008b) and the highest (58% of OC) using CMB-LGO (Marmur et al., 2005). For summer, our estimates vary from 34 to 51% as compared to results of other studies in Atlanta ranging from estimated SOC of 34% using the EC tracer method (Blanchard et al., 2008) to 75% using CMB-MM (Zheng et al., 2007). Since the time periods differ between studies, different SOC estimates are expected. Some studies (De Gouw and Jimenez, 2009; Robinson et al., 2007) suggest an underestimation of SOA in urban centers due to the rapid formation of SOA from semi-volatile and intermediate-volatile organic compounds emitted by traffic. Docherty et al. (2008) found ratios of SOA/OA between 70-90% on aged aerosols downwind of Los Angeles in a summer period with an ozone concentration of 86ppb. Our SOC estimate is equivalent to 35-57% being SOA using ratios of SOC/SOA=1.8 and POC/POA=1.2 (similar to Docherty et al., 2008) and for Atlanta the average 8h-maximum O_3 concentration was 60ppb, lower than the observed in the L.A. basin. While estimates of SOA formation using aerosol mass spectrometry have also being conducted (Jimenez et al., 2009), such data were unavailable in Atlanta for comparison here.

Table 2.2 Comparison of SOC Estimates with related work, SOC (ug-C m^{-3}) or (%)

	Year-round μg-C/m^3 (%)	Summer time μg-C/m^3 (%)
This study, EC tracer	1.19 (30%)	1.52 (40%)
This study, regression	1.25 (33%)	1.70 (44%)
This study, CMB	1.92 (46%)	2.00 (51%)
This study, PMF	1.12 (26%)	1.37 (34%)
EC tracer[a]	34%	34%
CO tracer[a]	45%	57%
Multiple regression[a]	27%	35%
Regular CMB[b]	1.59 (39%)	-
CMB-LGO[c]	2.59 (58%)	-
CMB-MM[d]	-	2.43 (57%)
CMB-MM[e]	-	3.18 (75%)
PMF[b]	0.77 (19%)	-
Time resolved[f]	-	3.9±2.2 (46%)

[a]EC tracer, CO tracer and Multiple regression from (Blanchard et al., 2008), [b]Regular CMB and PMF from (Lee et al., 2008a), cCMB-LGO from (Marmur et al. 2005), [d]CMB-MM in 1999 from (Zheng, 2002), [e]CMB-MM in summer 2001 and winter 2002 from (Zheng et al, 2007) [f]Time resolved from (Lim and Turpin, 2002).

We compare our estimates with results from CMB using molecular markers during summer of 2001 (Zheng et al., 2007). Data were not available to conduct a long-term analysis of SOC estimated by CMB-MM. Here SOC is estimated the same way using regular CMB, as the difference between measured OC and the identified primary fraction, but using a greater number of fitting species from $PM_{2.5}$ organic speciation. The correlation was strongest with estimates from the regression method (Table 2.3a).

Table 2.3 Comparison of SOC Estimates to SOC from CMB-MM and WSOC

	a. CMB-MM			**b. WSOC**		
	R^2	**Bias[*]**	**Error[&]**	**R^2**	**Bias**	**Error**
Regression	0.87	-1.05	1.86	0.50	-0.48	0.93
EC tracer	0.58	-1.45	2.20	0.41	-0.49	1.10
CMB	0.75	-1.53	2.42	0.48	-0.10	0.98
PMF	0.80	-1.30	1.90	0.45	-0.68	1.14

a. CMB-MM from Zheng et al., 2007, b. WSOC from Hennigan et al., 2008
[*,&] expressed in μg-C/m^3, Bias expressed as $1/N\ \Sigma(SOC_i\text{-}WSOC)$ and Error expressed as $1/N\ \Sigma(SOC_i\text{-}WSOC)^2$, where i denotes the method and N the number of samples.

2.7. Comparison with WSOC measurements

In an effort to compare our estimates with new methods to quantify organic aerosols, we compared the four estimates with the WSOC fraction in Atlanta during the summer of 2007, when biomass burning contribution was negligible (Zhang et al., 2010) and therefore, we expect WSOC to be a good surrogate of SOC. The ratio of WSOC/OC observed was 0.52, slightly higher than our summer SOC/OC estimates (0.34-0.51). The strongest correlation and the lowest error were between WSOC and estimates from the regression method (Table 2.3b). The regression estimate had a slope close to 1.0 when plotted against WSOC (Figure 2.5) indicating a good estimation of this secondary fraction.

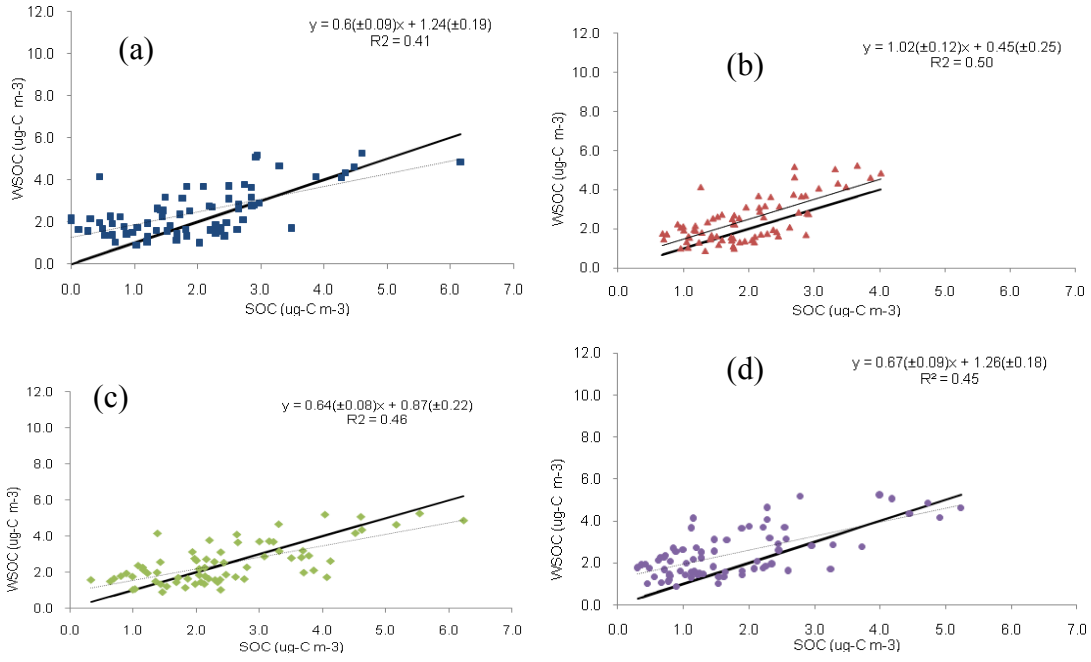

Figure 2.5 Comparison of WSOC measurements with SOC estimates in 2007 by the (a) EC-tracer, (b) regression method, (c) CMB and (d) PMF. Solid line is the 1:1.

2.8. Association of SOC estimates with health outcomes

Results from the inclusion of OC fractions in an epidemiologic model show a significant association of POC and CVD in the same day (lag0), while associations of OC and SOC with CVD were not significant (Figure 2.6). This finding suggests that combustion-emitted OC, and not photochemistry-formed OC, is responsible for associations of OC with CVD.

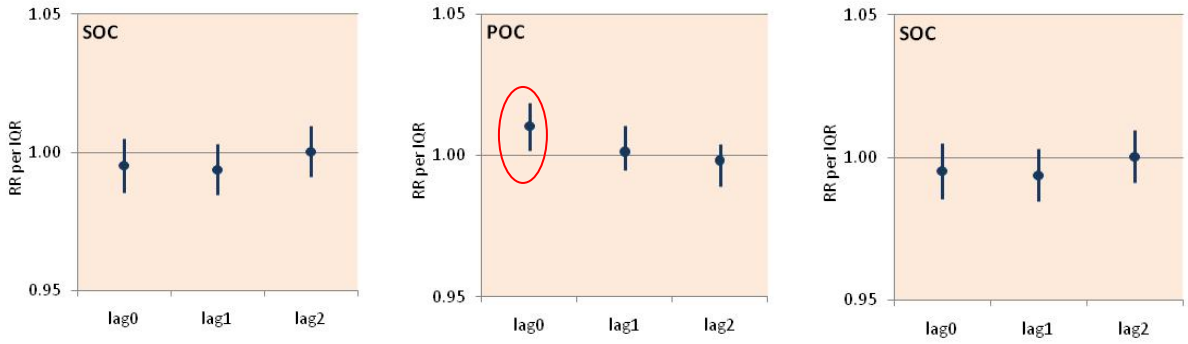

Figure 2.6 Association of OC, POC and SOC with CVD outcomes in Atlanta

2.9. References

Bevington, P. and Robinson, K., 2003. Data reduction and error analysis for the physical sciences, Third ed, McGraw Hill, New York.

Blanchard, C. L., Hidy, G. M., Tanenbaum, S., Edgerton, E., Hartsell, B. and Jansen, J., 2008. Carbon in Southeastern US aerosol particles: empirical estimates of secondary organic aerosol formation. Atmospheric Environment 42, 6710-6720.

Cabada, J. C., Pandis, S. N., Subramanian, R., Robinson, A. L., Polidori, A. and Turpin, B., 2004. Estimating the secondary organic aerosol contribution to PM2.5 using the EC tracer method. Aerosol Science and Technology 38, 140-155.

Chow, J. C., Watson, J. G., Pritchett, L. C., Pierson, W. R., Frazier, C. A. and Purcell, R. G., 1993. The DRI thermal optical reflectance carbon analysis system - description, evaluation and applications in United-States air quality studies. Atmospheric Environment Part a-General Topics 27, 1185-1201.

De Gouw, J. and Jimenez, J. L., 2009. Organic aerosols in the Earth's atmosphere. Environmental Science & Technology 43, 7614-7618.

Ding, X., Zheng, M., Edgerton, E. S., Jansen, J. J. and Wang, X. M., 2008. Contemporary or fossil origin: split of estimated secondary organic carbon in the Southeastern United States. Environmental Science & Technology 42, 9122-9128.

Docherty, K. S., Stone, E. A., Ulbrich, I. M., DeCarlo, P. F., Snyder, D. C., Schauer, J. J., Peltier, R. E., Weber, R. J., Murphy, S. M., Seinfeld, J. H., Grover, B. D., Eatough, D. J. and Jimenez, J. L., 2008. Apportionment of primary and secondary organic aerosols in Southern California during the 2005 study of organic aerosols in Riverside (SOAR-1). Environmental Science & Technology 42, 7655-7662.

Eder, B. and Yu, S., 2006. A performance evaluation of the 2004 release of Models-3 CMAQ. Atmospheric Environment 40, 4811-4824.

Edgerton, E. S., Hartsell, B. E., Saylor, R. D., Jansen, J. J., Hansen, D. A. and Hidy, G. M., 2005. The Southeastern aerosol research and characterization study: Part II. Filter-based measurements of fine and coarse particulate matter mass and composition. Journal of the Air & Waste Management Association 55, 1527-1542.

Edgerton, E. S., Hartsell, B. E., Saylor, R. D., Jansen, J. J., Hansen, D. A. and Hidy, G. M., 2006. The Southeastern aerosol research and characterization study, Part 3: continuous measurements of fine particulate matter mass and composition. Journal of the Air & Waste Management Association 56, 1325-1341.

Hansen, D. A., Edgerton, E. S., Hartsell, B. E., Jansen, J. J., Kandasamy, N., Hidy, G. M. and Blanchard, C. L., 2003. The Southeastern aerosol research and characterization study: Part 1-overview. Journal of the Air & Waste Management Association 53, 1460-1471.

Hennigan, C. J., Bergin, M. H., Dibb, J. E. and Weber, R. J., 2008. Enhanced secondary organic aerosol formation due to water uptake by fine particles. Geophys. Res. Lett. 35, L18801.

Jimenez, J. L., Canagaratna, M. R., Donahue, N. M., Prevot, A. S. H., Zhang, Q., Kroll, J. H., DeCarlo, P. F., Allan, J. D., Coe, H., Ng, N. L., Aiken, A. C., Docherty, K. S., Ulbrich, I. M., Grieshop, A. P., Robinson, A. L., Duplissy, J., Smith, J. D., Wilson, K. R., Lanz, V. A., Hueglin, C., Sun, Y. L., Tian, J., Laaksonen, A., Raatikainen, T., Rautiainen, J., Vaattovaara, P., Ehn, M., Kulmala, M., Tomlinson, J. M., Collins, D. R., Cubison, M. J., E., Dunlea, J., Huffman, J. A., Onasch, T. B., Alfarra, M. R., Williams, P. I., Bower, K., Kondo, Y., Schneider, J., Drewnick, F., Borrmann, S., Weimer, S., Demerjian, K., Salcedo, D., Cottrell, L., Griffin, R., Takami, A., Miyoshi, T., Hatakeyama, S., Shimono, A., Sun, J. Y., Zhang, Y. M., Dzepina, K., Kimmel, J. R., Sueper, D., Jayne, J. T., Herndon, S. C., Trimborn, A. M., Williams, L. R., Wood, E. C., Middlebrook, A. M., Kolb, C. E., Baltensperger, U. and Worsnop, D. R., 2009. Evolution of organic aerosols in the atmosphere. Science 326, 1525-1529.

Kim, E., Hopke, P. K. and Edgerton, E. S., 2003. Source identification of Atlanta aerosol by positive matrix factorization. Journal of the Air & Waste Management Association 53, 731-739.

Kim, E., Hopke, P. K. and Edgerton, E. S., 2004. Improving source identification of Atlanta aerosol using temperature resolved carbon fractions in positive matrix factorization. Atmospheric Environment 38, 3349-3362.

Kroll, J. H. and Seinfeld, J. H., 2008. Chemistry of secondary organic aerosol: formation and evolution of low-volatility organics in the atmosphere. Atmospheric Environment 42, 3593-3624.

Lee, D., Balachandran, S., Pachon, J., Shankaran, R., Lee, S., Mulholland, J. A. and Russell, A. G., 2009. Ensemble-trained PM2.5 source apportionment approach for health studies. Environmental Science & Technology 43, 7023-7031.

Lee, S., Kim, H. K., Yan, B., Cobb, C. E., Hennigan, C., Nichols, S., Chamber, M., Edgerton, E. S., Jansen, J. J., Hu, Y., Zheng, M., Weber, R. J. and Russell, A. G., 2008a. Diagnosis of aged prescribed burning plumes impacting an urban area. Environmental Science & Technology 42, 1438-1444.

Lee, S., Liu, W., Wang, Y. H., Russell, A. G. and Edgerton, E. S., 2008b. Source apportionment of PM2.5: comparing PMF and CMB results for four ambient monitoring sites in the Southeastern United States. Atmospheric Environment 42, 4126-4137.

Lee, S. and Russell, A. G., 2007. Estimating uncertainties and uncertainty contributors of CMB PM2.5 source apportionment results. Atmospheric Environment 41, 9616-9624.

Lee, S., Russell, A. G. and Baumann, K., 2007. Source apportionment of fine particulate matter in the Southeastern United States. Journal of the Air & Waste Management Association 57, 1123-1135.

Lim, H.-J. and Turpin, B. J., 2002. Origins of primary and secondary organic aerosol in Atlanta: results of time-resolved measurements during the Atlanta supersite experiment. Environmental Science & Technology 36, 4489-4496.

Marmur, A., Unal, A., Mulholland, J. A. and Russell, A. G., 2005. Optimization-based source apportionment of PM2.5 incorporating gas-to-particle ratios. Environmental Science & Technology 39, 3245-3254.

Metzger, K. B., Tolbert, P. E., Klein, M., Peel, J. L., Flanders, W. D., Todd, K., Mulholland, J. A., Ryan, P. B. and Frumkin, H., 2004. Ambient air pollution and cardiovascular emergency department visits. Epidemiology 15, 46-56.

Norris, G. and Vedantham, R., 2008. EPA Positive Matrix Factorization (PMF) 3.0. U.S. Environmental Protection Agency, Research Triangle Park, NC.

Offenberg, J. H., Lewandowski, M., Edney, E. O. and Kleindienst, T. E., 2007. Investigation of a systematic offset in the measurement of organic carbon with a semicontinuous analyzer. Journal of the Air & Waste Management Association 57, 596-599.

Paatero, P. and Tapper, U., 1994. Positive matrix factorization: a non-negative factor model with optimal utilization of error estimates of data values. Environmetrics 5, 111-126.

Peel, J. L., Tolbert, P. E., Klein, M., Metzger, K. B., Flanders, W. D., Todd, K., Mulholland, J. A., Ryan, P. B. and Frumkin, H., 2005. Ambient air pollution and respiratory emergency department visits. Epidemiology 16, 164-174.

Peltier, R. E., Weber, R. J. and Sullivan, A. P., 2007. Investigating a liquid-based method for online organic carbon detection in atmospheric particles. Aerosol Science and Technology 41, 1117-1127.

Polissar, A. V., Hopke, P. K. and Paatero, P., 1998. Atmospheric aerosol over Alaska - 2. Elemental composition and sources. J. Geophys. Res.-Atmos. 103, 19045-19057.

Reff, A., Eberly, S. I. and Bhave, P. V., 2007. Receptor modeling of ambient particulate matter data using Positive Matrix Factorization: review of existing methods. Journal of the Air & Waste Management Association 57, 146-154.

Robinson, A. L., Donahue, N. M., Shrivastava, M. K., Weitkamp, E. A., Sage, A. M., Grieshop, A. P., Lane, T. E., Pierce, J. R. and Pandis, S. N., 2007. Rethinking organic aerosols: semivolatile emissions and photochemical aging. Science 315, 1259-1262.

Sarnat, J. A., Marmur, A., Klein, M., Kim, E., Russell, A. G., Sarnat, S. E., Mulholland, J. A., Hopke, P. K. and Tolbert, P. E., 2008. Fine particle sources and cardiorespiratory morbidity: An application of chemical mass balance and factor analytical source-apportionment methods. Environ. Health Perspect. 116, 459-466.

Saylor, R. D., Edgerton, E. S. and Hartsell, B. E., 2006. Linear regression techniques for use in the EC tracer method of secondary organic aerosol estimation. Atmospheric Environment 40, 7546-7556.

Snyder, D. C., Rutter, A. P., Collins, R., Worley, C. and Schauer, J. J., 2009. Insights into the origin of water soluble organic carbon in atmospheric fine particulate matter. Aerosol Science and Technology 43, 1099 - 1107.

Solomon, P. A., Mitchell, W., Tolocka, M., Norris, G., Gemmill, D., Wiener, R., Vanderpool, R., Murdoch, R., Natarajan, S. and Hardison, E., 2000. Evaluation of PM2.5 chemical speciation samplers for use in the EPA National PM2.5 Chemical Speciation Network. US Environmental Protection Agency, Research Triangle Park, NC.

Sullivan, A. P., Peltier, R. E., Brock, C. A., de Gouw, J. A., Holloway, J. S., Warneke, C., Wollny, A. G. and Weber, R. J., 2006. Airborne measurements of carbonaceous aerosol soluble in water over northeastern United States: Method development and an investigation into water-soluble organic carbon sources. J. Geophys. Res.-Atmos. 111, D23.

Sullivan, A. P. and Weber, R. J., 2006. Chemical characterization of the ambient organic aerosol soluble in water: 1. Isolation of hydrophobic and hydrophilic fractions with a XAD-8 resin. J. Geophys. Res. 111, D05314.

Tesche, T. W., Morris, R., Tonnesen, G., McNally, D., Boylan, J. and Brewer, P., 2006. CMAQ/CAMx annual 2002 performance evaluation over the eastern US. Atmospheric Environment 40, 4906-4919.

Turpin, B. J., Saxena, P. and Andrews, E., 2000. Measuring and simulating particulate organics in the atmosphere: problems and prospects. Atmospheric Environment 34, 2983-3013.

Watson, J. G., Cooper, J. A. and Huntzicker, J. J., 1984. The effective variance weighting for least-squares calculations applied to the mass balance receptor model. Atmospheric Environment 18, 1347-1355.

Weber, R. J., Sullivan, A. P., Peltier, R. E., Russell, A., Yan, B., Zheng, M., de Gouw, J., Warneke, C., Brock, C., Holloway, J. S., Atlas, E. L. and Edgerton, E., 2007. A study of secondary organic aerosol formation in the anthropogenic-influenced southeastern United States. J. Geophys. Res.-Atmos. 112, D13302.

Yu, S., Bhave, P. V., Dennis, R. L. and Mathur, R., 2007. Seasonal and regional variations of primary and secondary organic aerosols over the continental United States: semi-empirical estimates and model evaluation. Environmental Science & Technology 41, 4690-4697.

Zhang, X., Hecobian, A., Zheng, M., Frank, N. H. and Weber, R. J., 2010. Biomass burning impact on PM2.5 over the Southeastern US during 2007: integrating chemically speciated FRM filter measurements, MODIS fire counts and PMF analysis. Atmos. Chem. Phys. 10, 6839-6853.

Zheng, M., Cass, G. R., Ke, L., Wang, F., Schauer, J. J., Edgerton, E. S. and Russell, A. G., 2007. Source apportionment of daily fine particulate matter at Jefferson street, Atlanta, GA, during summer and winter. Journal of the Air & Waste Management Association 57, 228-242.

Zheng, M., Cass, G. R., Schauer, J. J. and Edgerton, E. S., 2002. Source apportionment of PM2.5 in the Southeastern United States using solvent-extractable organic compounds as tracers. Environmental Science & Technology 36, 2361-2371.

Zheng, M., Ke, L., Edgerton, E. S., Schauer, J. J., Dong, M. and Russell, A. G., 2006. Spatial distribution of carbonaceous aerosol in the southeastern United States using molecular markers and carbon isotope data. J. Geophys. Res. 111, D10S06.

CHAPTER 3 REVISING THE USE OF POTASSIUM (K) IN THE SOURCE APPORTIONMENT OF PM2.5

(Pachon, J. E., Weber, R. J., Zhang, X., Mulholland, J. A. and Russell, A. G. *Atmospheric Environment*. Submitted)

3.1. Abstract

Elemental potassium has been extensively used as an indicator of biomass burning in the source apportionment of PM2.5. However, soil dust and sea-salt are also significant sources of atmospheric potassium. We present a method to estimate the fraction of potassium associated with biomass burning (K_b) based on a linear regression with iron. The estimated fraction has a significantly greater correlation with levoglucosan (R^2=0.63), an organic tracer of biomass burning, than total potassium (R^2=0.39). We explore temporal and spatial variability of K_b over a period of six years in the Atlanta area. K_b is larger in spring when biomass burning activity is more prevalent and during weekends due to the use of fireplaces in winter and outdoor charcoal cooking in summer. K_b is the predominate form of potassium in rural areas. The use of K_b in a receptor model results in a lower fraction of PM2.5 apportioned to biomass burning and a greater fraction to mobile sources. Results suggest that K_b is a good indicator of biomass burning as opposed to total K in source apportionment studies when source profiles are not available. The use of K_b in health studies can help to distinguish the potential impacts of biomass burning and mobile sources on cardiovascular diseases.

3.2. Introduction

Source apportionment is an important tool to identify emission sources contributing to ambient PM2.5. Receptor models solve the mass balance equation with or without the use of source profiles to estimate source impacts at a receptor site. When source profiles are available, specific species are often identified as indicator of sources, alone or in concert with other species. For example, the elemental carbon (EC) to organic carbon (OC) ratio is used to differentiate combustion sources (e.g. gasoline and diesel vehicles, biomass burning) and potassium (K) has been used to further differentiate the impact of biomass burning (Lee et al., 2008; Pio et al., 2008; Watson et al., 2008). When sources profiles are not available, the same species can be used to associate factors with emissions sources. Potassium, for example, has been extensively used to apportion PM2.5 to biomass burning in Positive Matrix Factorization EPA-PMF model applications (Kim et al., 2003, 2004; Lee et al., 2009; Liu et al., 2005, 2006; Marmur et al., 2006; Marmur et al., 2005).

One disadvantage of using potassium in source apportionment modeling by factor analysis is that this element has multiple emission sources (e.g., wood smoke, soil dust, sea salt, coal fire, industry and meat cooking) (Andreae, 1983; Watson and Chow, 2001; Watson et al., 2001) and can result in an overestimation of biomass burning contributions to total PM2.5 mass. Furthermore, recent studies indicate that soluble potassium (K^+) concentrations do not exhibit seasonal trends expected if it is dominantly from biomass burning and have a low correlation with fire counts from satellite data (Zhang et al., 2010). Several studies have proposed that organic tracers, such as levoglucosan and retene, can be used as a biomass tracer instead of K (Jordan et al., 2006; Lewis et al., 1988; Puxbaum et al., 2007; Simoneit et al., 1999). Zhang et al. (2010) have found levoglucosan to be more correlated with satellite

fire counts when biomass burning emissions are expected to be mainly from outdoor burning (e.g., not winter), while Li et al. (2009) found retene more concentrated in March and December when prescribed fires and residential wood burning are more intense. Unfortunately, measurements of these organic compounds are not as widely available as potassium.

Attempts to estimate the fraction of potassium from biomass burning have used relationships between K and other metals. Andreae (1983) defined excess potassium as the portion not attributable to sea salt or soil dust in aerosol samples collected on a cruise in the Atlantic Ocean. The excess potassium was estimated as K'=K-0.75*Ca. The K/Ca ratio of 0.75 was the best fit in the coarse fraction ($D_p > 2\mu m$). In that study Ca was selected for its abundance in sea salt. The K' fraction showed a similar temporal trend to soot and was attributed to biomass burning emissions from land (fire wood, waste incineration, agricultural burning). Lewis et al. (1988) estimated a soil-corrected potassium as K'=K–0.45*Fe. The K/Fe ratio of 0.45 was the average of samples in the coarse fraction taken in Albuquerque, NM. The K' fraction had a maximum value at night because of residential wood burning. Miranda et al. (1994) used a similar approach defining non-soil K (NSK)=K–0.52*Fe, then applying K/Fe ratio of coarse soil. Using ratios of K/Ca and K/Na, Pio et al. (2008) estimated potassium not associated with sea salt and soil particles as K_{bb}=K-0.036*Na-0.12(Ca_{ns}-Ca_{bb}) and is proposed to be related with biomass combustion.

Though these methods have been successfully employed to estimate K in biomass burning emissions in these studies, they have not been applied in the source apportionment of PM2.5 in urban regions where potassium is emitted by multiple sources and biomass burning can greatly impact air quality. In the Atlanta area, for example, biomass burning was

estimated to contribute between 1.72 and 3.68 μg/m^3 to PM2.5 (6-22% of total PM2.5 mass) (Kim et al., 2003, 2004; Lee et al., 2008; Liu et al., 2005, 2006). Biomass burning also emits carbonaceous material (EC and OC) that can be difficult to apportion in heavily traffic impacted areas without the use of accurate source profiles. The OC/EC ratio has been used to confirm the profiles of biomass burning and mobile sources, since biomass burning usually has higher OC/EC ratios (Lee et al., 2005; Pio et al., 2008) than gasoline (3.0-4.0) or diesel vehicles (<1.0) (Lee and Russell, 2007; Zheng et al., 2007).

The objective of this study is to estimate the fraction of potassium associated with biomass burning (here called K_b) in the PM2.5, using a relationship between K and a species (M) that shares similar sources with K but is not emitted by biomass burning. From previous studies, it is expected that either Fe or Ca can be used for M. We examine temporal and spatial variability of K_b and compare K_b concentrations with levoglucosan concentrations. Finally, we assess the changes in source apportionment of PM2.5 when PMF is implemented with K_b instead of total K and compare factor impacts with other studies.

3.3. Methods

This work follows five steps to estimate the K_b fraction and assess its performance as an indicator of biomass burning activity: i) estimation of the K_b fraction, ii) assessment of temporal and spatial variability of K_b, iii) evaluation of the relationship between K_b and organic tracers, iv) assessment of changes in source apportionment using K_b and v) comparison with similar studies.

3.3.1. Estimation of the K_b fraction

Factor analysis is used to examine the variability in PM2.5 data and identify species (M) that share similar sources with K but are not emitted by biomass burning. The statistical package

R (R Development Core Team, 2011) is used to conduct traditional factor analysis. The number of factors are selected based on the number of eigenvalues greater than one and the overall statistical fit of the analysis. The association of factors with PM2.5 emissions sources is conducted based on the analysis of factor loadings (i.e., correlations between factor scores and the original species). PM2.5 speciation data was obtained at the Jefferson Street site in downtown Atlanta from 1999-2007. A total of 2,586 samples were available with concentrations of the needed species above their detection limits. JST is part of the SEARCH project and description of the network is found elsewhere (Edgerton et al., 2005; Hansen et al., 2003). The PM2.5 species considered in the analysis are NO_3, SO_4, EC, OC, Al, Si, K, Fe, Ca, Br, Se and Zn. Total K, measured by X-ray fluorescence, is reported in its oxidized form (K_2O) by SEARCH.

After an associated species (M) is identified, linear regression between total K and M, based on the 2,586 samples, is used to estimate the fraction of potassium from common sources and excess potassium (intercept in Equation 3.1). Daily estimates of K_b can then be obtained using the regression results and total potassium (Equation 3.2).

$$K = a + b*M \quad (3.1)$$

$$K_b = K - b*M \quad (3.2)$$

One condition that this estimate should satisfy is that $K_b>0$ in all cases. If $K_b<0$ for a particular day, K_b is set to zero.

3.3.2. Assessment of temporal and spatial variability of K_b

Daily and seasonal trends of K and K_b are examined at the JST site. Two additional monitoring sites in the area are considered for the assessment of spatial variability: South

DeKalb (SD) and Yorkville (YKV) (Figure 3.1). SD is part of the Speciation Trends Network (EPA-STN) and is located 15 km southeast from JST. SD is 200 m away from a major interstate with significant heavy-duty traffic. YKV is a rural site operated by the SEARCH project located 60 km west of JST. JST and SD are classified as urban and suburban sites predominately influenced by traffic. In contrast, YKV is a rural site influenced predominantly by area sources, such as biomass burning.

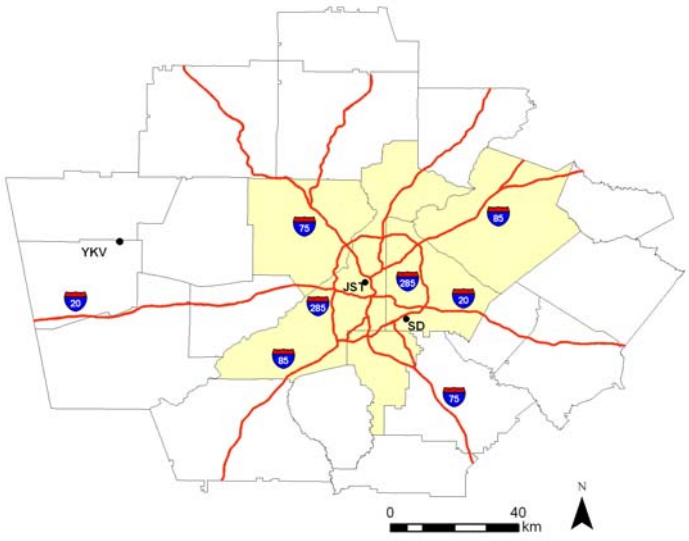

Figure 3.1 Monitoring station location (area in yellow is the 5-county Atlanta metro area).

To explore the variability in combustion source impacts between sites, we apply factor analysis again, but this time including only the following species: EC, OC, K and Fe, measured at JST, YKV and SD. K_b at YKV and SD was also estimated similarly to K_b at JST (Equations. 3.1-3.2) and included in the inter-site variability analysis. In addition, correlation between K and K_b for each pair of sites (JST-SD, JST-YKV, YKV-SD) is also assessed as part of the spatial variability analysis.

3.3.3. Evaluation of the relationship between K_b with organic tracers

Levoglucosan concentrations were available during 2007 from PM2.5 filters collected from the EPA-STN monitoring sites in the Southeastern US. PM2.5 is determined using the Federal Reference Method on a six-day basis (e.g. 1 filter/6 days) and levoglucosan was quantified using ion chromatography with pulsed amperometric detection (IC-PAD) (Zhang et al., 2010). Because JST is not an EPA-STN site, surrogate data from the SD site was used. Similar emissions sources at JST and SD and the relatively short distance between sites supports the use of SD levoglucosan as a surrogate for JST levoglucosan. These concentrations were compared with the estimated K_b fraction at JST. Ratios between levoglucosan and potassium (K and K_b) are estimated and compared with ratios from biomass burning samples.

3.3.4. Assessment of changes in source apportionment using K_b

Changes in source apportionment of PM2.5 are assessed when K_b is used instead of K in EPA-PMF v.3.0 (Norris and Vedantham, 2008). SO_4, NO_3, NH_4, EC, temperature-resolved OC1 through OC4, Al, Si, Ca, Br, Mn, and Zn were selected as strong species, while Cu, Pb, and Se were selected as weak species. Two cases were compared: the first included K as a strong species, while the second considered K_b as strong species. Since K constitutes less than 1% of the PM2.5 mass, it is expected that changes in the PM2.5 are a result of the redistribution of major species associated with combustion.

3.3.5. Comparison with similar studies

Comparing source apportionment results from PMF with previous studies is challenging. First, differences in source impacts from different time periods may be influenced by the implementation of controls or economic considerations. Secondly, data treatment (e.g.

methods by which missing days and samples below the detection limit are treated and uncertainty is estimated) vary considerably, resulting in different factor impacts in PMF. Third, the association of factors in PMF with emission sources is subjective; thus, species used as indicators of a particular source may change with time. Reff et al. (2007) offers a more complete review of methodological details in PMF. Here, local studies with similar conditions were compared to our PMF results using K (PMF-K) and K_b (PMF-K_b) to examine how using K_b can improve source apportionment results.

3.3.6. Association of K and Kb with health outcomes

Biomass burning source impacts from PMF-K and PMF-K_b were implemented in an epidemiologic model to assess the health impact of these fractions. Cardiovascular diseases were chosen as the health endpoint for evaluation given that they have shown a significant association with PMF wood smoke in previous studies (Sarnat et al., 2008). The epidemiologic model is described in detail elsewhere (Metzger et al., 2004; Peel et al., 2005) and later in this dissertation (see Section 4.6).

3.4. Results

3.4.1. Development of a method to estimate K from biomass burning

The application of factor analysis to the JST data resolved four factors with eigenvalues greater than one leading to a good statistical fit (p-value<0.01), explaining 67% of the total variance. The interpretation of the factors was conducted based on the most significant species in each factor (highlighted in bold in Table 3.1a, base case): soil dust factor (F1) has high correlations with Al and Si, traffic factor (F2) with EC and OC, biomass burning factor (F3) with K and Br, and secondary sulfate factor (F4) with SO_4. K has the strongest

correlation with F3, but significant correlations with F1 and F2, suggesting multiple sources of this species.

Table 3.1 Factor loadings using K and K_b (factors denoted with prime) for the 4-factor solution.

	a. Factors using regular K (Base Case)				b. Factors using K_b			
Species	F1	F2	F3	F4	F1'	F2'	F3'	F4'
NO3	-0.16	0.08	0.45	-0.09	-0.16	0.18	0.36	-0.11
SO4	0.08	0.08	-0.08	**0.99**	0.08	0.08	-0.05	**0.99**
EC	0.10	**0.88**	0.26	0.17	0.10	**0.90**	0.13	0.16
OC	0.12	**0.71**	**0.46**	0.24	0.12	**0.78**	0.35	0.22
Al	**0.95**	-0.03	-0.05	0.04	**0.95**	-0.03	-0.04	0.04
Si	**0.99**	0.09	-0.02	0.01	**0.99**	0.08	-0.02	0.01
Fe	0.67	0.65	0.11	0.13	0.66	**0.69**	-0.05	0.11
Ca	0.58	0.43	0.01	0.09	0.58	0.43	-0.07	0.09
K	0.41	0.35	**0.67**	0.13	-	-	-	-
K_b	-	-	-	-	0.02	0.07	**0.87**	0.05
Br	0.01	0.27	**0.60**	0.14	0.00	0.40	0.46	0.11
Se	0.02	0.16	0.10	0.39	0.01	0.19	0.04	0.38
Zn	0.07	0.54	0.30	0.11	0.06	0.59	0.19	0.10
Variance	0.24	0.20	0.12	0.11	0.23	0.22	0.11	0.10
Cumulative	0.24	0.44	0.56	0.67	0.23	0.45	0.56	0.66

Fe and Ca have significant loadings on F1, since they are crustal elements. In addition, these elements are also observed in F2, likely due to the presence of Fe and Ca in mobile source emissions (e.g. from brake dust, tire wear, road dust and oil) (Majestic et al., 2009). The correlations between Fe and Ca with F3, however, are poor, suggesting that Fe and Ca are not significant constituents of biomass burning emissions. This result is consistent with the chemical composition of PM2.5 from prescribed burning emissions, where Ca and Fe are typically found in low percentages of the PM2.5 mass (<0.1%) compared to K (0.57%) (Lee et al., 2005). Based on this result, Fe or Ca can be used to identify the fraction of potassium largely associated with traffic and soil dust rather than biomass burning (i.e., Fe or Ca serves as the M species in the linear regression in Equation 3.1). These results support the use of Fe

and Ca in PM2.5 for source attribution to improve the use of K as biomass burning tracer as previously proposed in the coarse fraction by several studies (Andreae, 1983; Lewis et al., 1988). However, in coastal areas, Ca should be included to subtract the influence of sea-salt as shown by Pio et al.(2008).

The linear regression of K with Fe and Ca for all data (1999-2007) gives the following results:

$$K = 30.1\ (\pm 0.93) + 0.38\ (\pm 0.02)*Fe,\ R^2=0.35 \quad (3.3)$$

$$K = 40.6\ (\pm 0.99) + 0.41\ (\pm 0.02)*Ca,\ R^2=0.16 \quad (3.4)$$

where K, Fe and Ca are expressed in ng/m^3. A more significant correlation (R^2) with K is observed for Fe rather than Ca. Furthermore, the use of Ca to estimate K_b resulted in more cases of $K_b < 0$ (23% of the days vs. 4% for Fe). For this reason, our analysis was based on the separation of K with Fe as $K_b = K - 0.38*Fe$. The intercept of Equation 3.3 (30.1±0.93 ng/m^3) represents the average amount of potassium from sources other than traffic and soil dust, e.g. biomass burning. The slope (K/Fe) of 0.38 is slightly lower than those reported in previous studies (0.45-0.52) in the coarse fraction (Lewis et al., 1988; Miranda et al., 1994) which is explained by lower potassium concentrations in the PM2.5 fraction or differences in soil composition.

The estimated K_b is used instead of K in a new application of factor analysis. The number of factors and their association with emissions sources is similar to the base case (F1'-soil dust, F2'-traffic, F3'-biomass burning, F4'-secondary sulfate in Table 3.1b), but some important changes are highlighted. The correlation of K_b with F3' (R^2=0.87) is larger

than the corresponding correlation of K with F3 (R^2=0.67), denoting a better separation of the biomass burning factor. K_b is not correlated with F1' or F2' which suggests little to no influence of soil and traffic dust on K_b. The total variance (67%) explained by the four factors is maintained in both cases

3.4.2. Assessment of temporal variability of K and K_b

Daily estimates of K_b were obtained from 1999 through 2007. Approximately half of the PM2.5 potassium loading is from biomass burning (Table 3.2) which implies that the other half is associated with soil and traffic dust. These results are in agreement with local source profiles where potassium is associated with multiple sources (Marmur et al., 2007).

Table 3.2 Temporal trends of K and K_b

		K	K_b
Average 1999-2007 (ng/m^3)		57.6	30.4
Standard deviation (ng/m^3)		33.2	26.7
Weekend/weekday ratio		0.97	1.23
Seasonal averages (ng/m^3)	Winter (Dec-Feb)	62.4	35.8
	Spring (Mar-May)	58.6	32.3
	Summer (Jul-Sep)	45.5	18.4
	Fall (Oct-Dec)	64.0	29.9
Spring/Summer ratio		1.3	1.8

K concentrations are similar during weekdays and weekends, whereas K_b concentrations are larger during weekends, possibly due to the use of fireplaces during winter and more intense yard waste and charcoal cooking during summer. K is largest in fall and winter, while K_b is largest in winter and spring. During spring, and particularly in March and April, prescribed burning activities around Georgia is more intense (Li et al., 2009). In summer, biomass burning is expected to be less pronounced (Tian et al., 2008; Zhang et al.,

2010) and K_b is lowest during this season. The spring/summer ratio is higher for K_b than K, which is more consistent with observed biomass burning activity.

3.4.3. Evaluation of the correlation with levoglucosan

Levoglucosan was more strongly correlated with the estimated K_b fraction than the total potassium during winter of 2007 (Figure 3.2). The intercept of the regression between levoglucosan and K_b (18.5 ng/m^3) is half of the value of the intercept with K (41.5 ng/m^3) denoting a closer relationship between K_b and levoglucosan. The regression slopes of K and K_b with levoglucosan were both about 0.15. These slopes are similar to the K/levoglucosan ratio of 0.1 found in samples taken during biomass burning campaigns in Georgia (Lee et al., 2005). Puxbaum et al. (2007) report that K/levoglucosan ratios < 0.2 are associated with domestic heating with wood in the US. It is expected then that both prescribed fires and wood smoke from fireplaces impact the receptor at JST, supporting the greater weekend/weekday ratio for K_b due to the use of fireplaces observed during the winter.

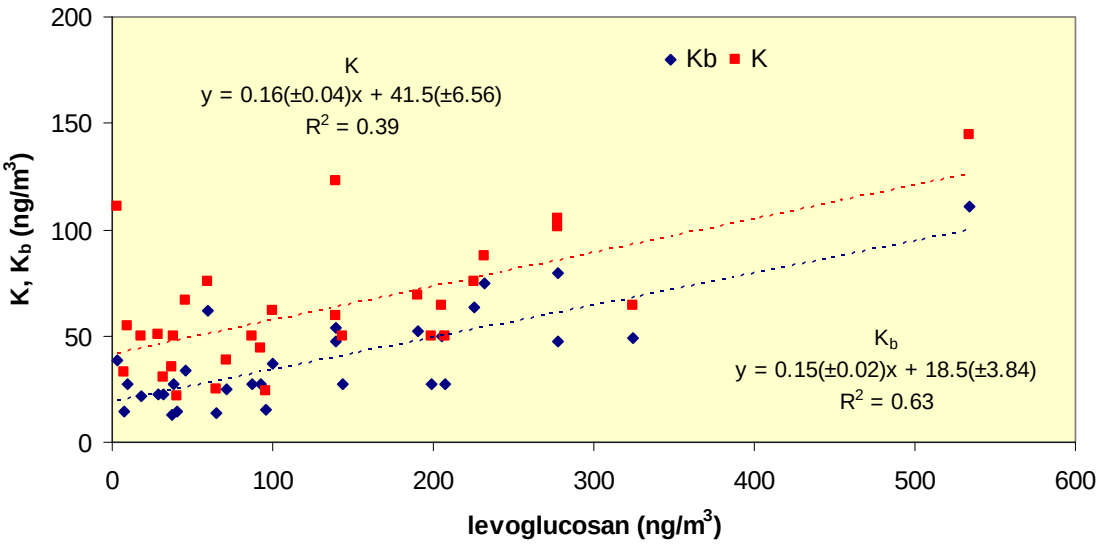

Figure 3.2 Correlation between K & K_b with levoglucosan during winter 2007

3.4.4. Assessment of spatial variability of K and K_b

The regression of K with Fe for the JST site is compared to results for the SD and YKV sites (Table 3.3). The correlation between K and Fe is significantly lower at YKV (R^2=0.18) compared to JST and SD, and suggests that only 18% of the variability of K is explained by common sources with Fe. The K/Fe ratio (slope) is approximately the same for JST and SD and larger for YKV due to relatively large concentrations of K with respect to Fe at this rural site.

Table 3.3 Results of regression of K into Fe for the three sites

	Slope ± std error	Intercept ± std error (ng/m^3)	R^2	K (ng/m^3)	K_b/K (summer - winter)
JST	0.38 ± 0.02	30.1 ± 0.93	0.35	57.6	0.46 – 0.58
YKV	0.45 ± 0.03	33.3 ± 0.98	0.18	45.0	0.64 – 0.82
SD	0.32 ± 0.02	31.8 ± 1.70	0.32	59.0	0.34 – 0.49

The fraction of K_b to K is the largest at YKV, confirming that a significant amount of potassium is associated with biomass burning at this rural site. This fraction explains the low correlation coefficient between K and Fe, the latter species more associated with soil and traffic dust. At the three sites, K_b/K ratios are greater in winter than summer in concordance with more intense biomass burning in winter. The fact that 82% of the K is estimated as K_b for YKV suggests that separation of potassium at rural sites is not as critical as in urban sites.

A new application of factor analysis, this time using only EC, OC, Fe and K species at the three sites, resulted in four factors explaining a variance between 75% and 78% when K_b or K were considered respectively (Table 3.4). Analyses of inter-site variability suggest that carbonaceous species (EC, OC) are more similar between JST and SD (higher loadings in F1) than YKV and is explained by a significant influence of traffic at the urban sites, while EC and OC at YKV have an independent source (higher loadings in F3) attributed to biomass

burning. F2 explains the shared variability between K at the three sites with similar correlations that denotes a low spatial variability of total potassium.

When K_b is included in the analysis instead of K, a similar interpretation of F1' and F3'factors is observed, this is, F1' explains the variability of traffic impacts at JST and SD, whereas F2' explains the influence of biomass burning impacts at YKV. However, K_b has a higher correlation with F2' at JST than YKV and SD, denoting a greater spatial variability of K_b compared to K. In fact, correlations between K and K_b among the three sites shows that K_b has a stronger association between JST and YKV (R^2=0.6) while correlations of K_b between JST-SD (R^2=0.45) and YKV-SD (R^2=0.36) are lower. The high impact of traffic on SD may explain the low correlations of K_b to other sites.

Table 3.4 Factor loadings using K and K_b (factors denoted with prime) for three sites in the Atlanta area. Most influential species are highlighted in bold.

		a. Factors using regular K				b. Factors using K_b			
		F1	F2	F3	F4	F1'	F2'	F3'	F4'
JST	EC	**0.89**	0.14	0.21	0.00	**0.95**	0.03	0.22	-0.04
	OC	**0.75**	0.32	0.37	-0.02	**0.77**	0.24	0.35	0.09
	Fe	0.71	0.17	0.08	**0.56**	0.72	-0.12	0.12	0.49
	K	0.45	**0.78**	0.19	0.18	-	-	-	-
	K_b	-	-	-	-	0.14	**0.91**	0.11	0.09
YKV	EC	0.19	0.14	**0.62**	-0.02	0.23	0.14	**0.63**	-0.03
	OC	0.21	0.22	**0.93**	0.18	0.23	0.19	**0.92**	0.24
	Fe	-0.01	0.27	0.05	**0.81**	0.06	-0.03	0.08	**0.69**
	K	0.12	**0.79**	0.28	0.31	-	-	-	-
	K_b	-	-	-	-	0.26	**0.77**	0.25	0.03
SD	EC	**0.74**	0.24	0.16	0.16	**0.76**	0.12	0.14	0.25
	OC	0.59	0.41	0.45	0.03	0.60	0.34	0.42	0.22
	Fe	0.60	0.29	0.10	**0.62**	0.62	0.01	0.07	**0.78**
	K	0.29	**0.79**	0.16	0.22	-	-	-	-
	K_b	-	-	-	-	-0.09	**0.76**	0.09	-0.17
Variance		0.29	0.21	0.15	0.13	0.29	0.19	0.14	0.13
Cumulative		0.29	0.50	0.65	0.78	0.29	0.48	0.62	0.75

3.4.5. Inclusion of K into source apportionment using PMF

PMF-K and PMF-K_b were run independently at JST solving for eight factors in each case. Resolved factor profiles are included in the Appendix A (Figure A.1-A.2). In both cases, the correlation between PM2.5 estimated and predicted was R^2=0.88. Factors were associated with secondary sulfate (SULF), secondary ammonium (add it to the secondary sulfate), secondary nitrate (NITR), soil dust (SOIL), gasoline vehicles (GV), diesel vehicles (DV), biomass burning (BURN) and industrial source (IND). Gasoline and diesel vehicles were grouped into a mobile factor (MOB) since major species (EC, OC) are present in both GV and DV factor profiles and we found that separation of factor impacts using the thermal fractions of OC is problematic. The lumped mobile factor also facilitates comparison with other studies. K_b is almost exclusively apportioned to the biomass burning factor, compared to K which is apportioned to multiple sources (Figure 3.3), supporting the use of K_b as a better indicator of biomass burning impacts.

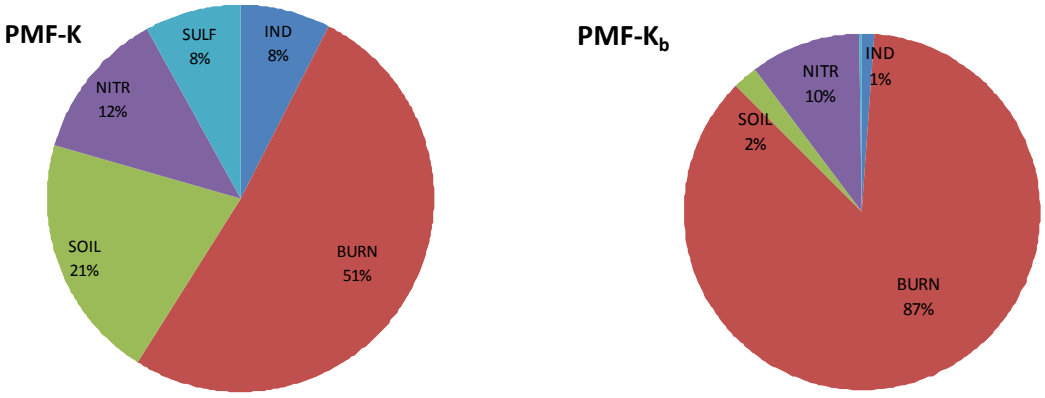

Figure 3.3 Distribution of potassium (K) and estimated potassium from biomass burning (K_b) among emission sources at JST

The major difference between PMF-K and PMF-K_b is in the apportionment of PM2.5 to biomass burning and mobile factors (Figure 3.4). The biomass burning impact decreases from 2.67 μg/m^3 in PMF-K to 1.40 μg/m^3 in PMF-K_b (reduction of 47%) while the mobile source impact increases from 3.23 μg/m^3 in PMF-K to 4.55 μg/m^3 in PMF-K_b (increase of 41%).

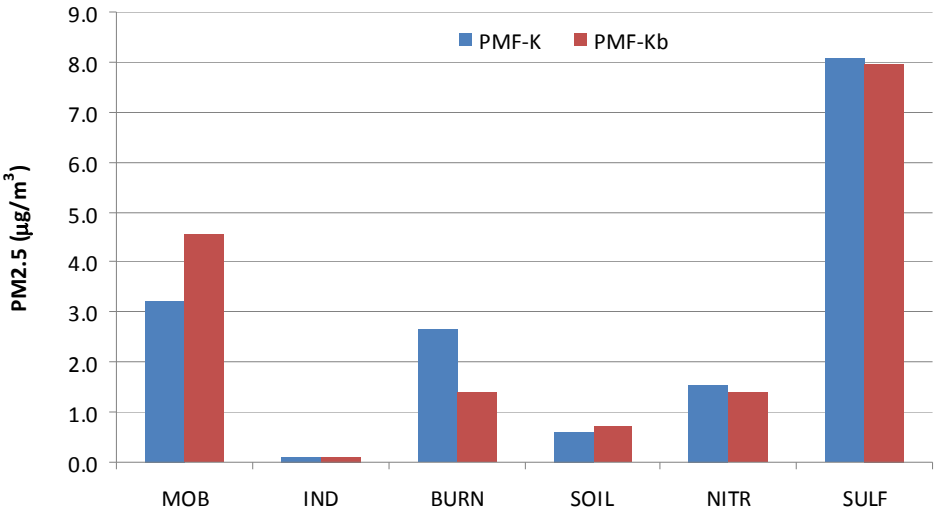

Figure 3.4 PM2.5 apportionment using K and K_b as indicator species for biomass burning

Since K constitutes less than 1% of the PM2.5 mass, the changes in the PM2.5 apportionment are attributed to the re-distribution of major species in the factors. EC, and especially OC, had the largest changes when PMF is implemented with K_b (Figure 3.5). EC from BURN is apportioned to GV while OC from BURN and SOIL is redistributed to GV and DV. This re-distribution is explained by the change in correlations between major species used to resolve the factors. In fact, the correlation between OC and K (R^2=0.31) decreases with K_b (R^2=0.1) resulting in a transfer of OC from BURN to MOB where the

correlation between OC and EC is higher (R^2=0.66). Similar changes in correlations are observed between factor contributions and major species supporting the previous analysis. The OC/EC ratio for biomass burning increases from 4.1 in PMF-K to 5.1 in PMF-K_b more consistent with OC/EC ratios found in biomass burning emissions (Lee et al., 2005).

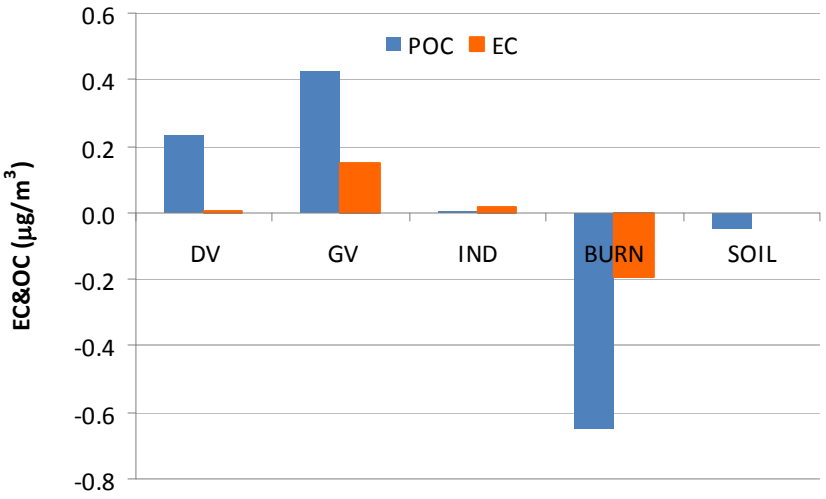

Figure 3.5 Changes in carbonaceous species (EC and OC) estimated as the contribution in PMF-K_b minus the contribution in PMF-K.

3.4.6. Comparison with similar studies

The use of K_b in PMF resulted in 9% of the PM2.5 mass apportioned to biomass burning versus 16% using total K from 1999-2004 (Table 3.5). Both estimates are within the range found in other studies (7-22%), but the larger fraction is probably an overestimation of the biomass impact given the use of total K as indicator of the source. Our estimate of the mobile source impact (28%) is larger than previous studies (17-22%) which may be more realistic for a source that is ubiquitous in Atlanta. Analysis of emission inventories shows that 92% of EC emissions in the metro area are from mobile sources and approximately 50% of the primary PM2.5 is emitted by vehicles (Air Resources Specialists, 2007). Such large

emissions explain the large impact of vehicles to ambient PM2.5. The application of CMB in Atlanta, using specific source profiles for mobile and biomass burning sources, finds that mobile sources contribute approximately 4.0 μg/m^3 to total PM2.5 mass and biomass burning contributes 1.2 μg/m^3 (Lee et al., 2008), similar to here. The same study points out the overestimation of biomass burning impacts and underestimation of mobile source contributions by PMF.

Table 3.5 Comparison of factor impacts from PMF in similar studies

Study	**SULF**	**NITR**	**MOB**	**BURN**	**IND**	**SOIL**	**MIX***	**UND***	**Ref.**
Atlanta (1998-2000)	8.85 (56%)	1.15 (7%)	3.53 (22%)	1.72 (11%)	0.08 (0.5%	0.18 (1%)	0.36 (2%)	-	(Kim et al., 2003)
Atlanta (1998-2000)	56%	9%	17%	7%	3%	2%	7%	-	(Kim et al., 2004)
Atlanta (2000-2002)	37%	8%	17%	13%	9%	2%	3%	11%	(Liu et al., 2005)
Atlanta (2000-2002)	4.93 (30%)	1.53 (9%)	2.83 (17%)	3.68 (22%)	1.0 (6%)	0.52 (3%)	0.42 (2%)	1.81 (11%)	(Liu et al., 2006)
Atlanta (1999-2004)	8.08 (45%)	1.53 (9%)	3.23 (20%)	2.67 (16%)	0.1 (1%)	0.6 (4%)	-	0.5 (3%)	PMF-K
Atlanta (1999-2004)	7.95 (49%)	1.41 (9%)	4.55 (28%)	1.40 (9%)	0.1 (1%)	0.73 (5%)	-	0.5 (3%)	PMF-K_b

* MIX: mixed source, UND: unidentified

3.4.7. Association of K and K_b with health impacts

A significant association of biomass burning source impacts with CVD is observed when the epidemiologic model is implemented with results from PMF-K (Table 3.6). This association may have been influenced by the presence of traffic in the biomass burning factor solved by PMF-K as suggested above. Using the estimated K_b fraction in PMF, biomass burning source impacts loses significance in the association with CVD, however, the subtle differences in

the associations between PMF-K and PMF-K_b do not permit to confirm the influence of traffic in the association of biomass burning with CVD outcomes.

Table 3.6 Association of biomass burning source impacts with CVD outcomes

Indicator	IQR	RR per IQR	Lower RR	Upper RR	p-value
PMF-K	0.91	1.010	1.001	1.020	0.038
PMF-K_b	1.57	1.008	0.999	1.018	0.066

3.5. Implications

This study finds that a simple transformation of ambient potassium is more strongly associated with biomass burning activities and produces significant changes in the source apportionment of PM2.5. The K_b fraction can be estimated at any monitoring site where K and Fe concentrations are available, for example, any of the EPA-STN sites throughout the US, not impacted by sea-salt. Future studies of source apportionment may benefit from the use of K_b instead of K, especially when local source profiles are not available. In areas where measurement of levoglucosan is not available, K_b constitutes a good indicator of biomass burning.

Health studies can also benefit from the use of K_b. PM2.5 from mobile sources and biomass burning has been associated with cardiovascular diseases (CVD) and EC and OC have been found to have somewhat stronger associations with CVD outcomes than other species (Peng et al., 2009; Sarnat et al., 2008). However, similar characteristics of traffic and vegetative burning sources profiles do not permit precisely delineating between the health impacts of these sources and it is suggested that mobile sources might have influenced the association of biomass burning with CVD (Sarnat et al., 2008). Our preliminary results

suggest the influence of traffic in the association of biomass source impacts with CVD, but further analyses are necessary.

3.6. References

Georgia Department of Natural Resources, 2007. Visibility Improvement State and Tribal Association of the Southeast (VISTAS) conceptual description support document.Asheville, NC.

Andreae, M. O., 1983. Soot carbon and excess fine potassium: long-range transport of combustion-derived aerosols. Science 220, 1148-1151.

Edgerton, E. S., Hartsell, B. E., Saylor, R. D., Jansen, J. J., Hansen, D. A. and Hidy, G. M., 2005. The Southeastern aerosol research and characterization study: Part II. Filter-based measurements of fine and coarse particulate matter mass and composition. Journal of the Air & Waste Management Association 55, 1527-1542.

Hansen, D. A., Edgerton, E. S., Hartsell, B. E., Jansen, J. J., Kandasamy, N., Hidy, G. M. and Blanchard, C. L., 2003. The Southeastern aerosol research and characterization study: Part 1-overview. Journal of the Air & Waste Management Association 53, 1460-1471.

Jordan, T. B., Seen, A. J. and Jacobsen, G. E., 2006. Levoglucosan as an atmospheric tracer for woodsmoke. Atmospheric Environment 40, 5316-5321.

Kim, E., Hopke, P. K. and Edgerton, E. S., 2003. Source identification of Atlanta aerosol by positive matrix factorization. Journal of the Air & Waste Management Association 53, 731-739.

Kim, E., Hopke, P. K. and Edgerton, E. S., 2004. Improving source identification of Atlanta aerosol using temperature resolved carbon fractions in positive matrix factorization. Atmospheric Environment 38, 3349-3362.

Lee, D., Balachandran, S., Pachon, J., Shankaran, R., Lee, S., Mulholland, J. A. and Russell, A. G., 2009. Ensemble-trained PM2.5 source apportionment approach for health studies. Environmental Science & Technology 43, 7023-7031.

Lee, S., Baumann, K., Schauer, J. J., Sheesley, R. J., Naeher, L. P., Meinardi, S., Blake, D. R., Edgerton, E. S., Russell, A. G. and Clements, M., 2005. Gaseous and particulate emissions from prescribed burning in Georgia. Environmental Science & Technology 39, 9049-9056.

Lee, S., Liu, W., Wang, Y. H., Russell, A. G. and Edgerton, E. S., 2008. Source apportionment of PM2.5: comparing PMF and CMB results for four ambient monitoring sites in the Southeastern United States. Atmospheric Environment 42, 4126-4137.

Lee, S. and Russell, A. G., 2007. Estimating uncertainties and uncertainty contributors of CMB PM2.5 source apportionment results. Atmospheric Environment 41, 9616-9624.

Lewis, C. W., Baumgardner, R. E., Stevens, R. K., Claxton, L. D. and Lewtas, J., 1988. Contribution of woodsmoke and motor vehicle emissions to ambient aerosol mutagenicity. Environmental Science & Technology 22, 968-971.

Li, Z., Sjodin, A., Porter, E. N., Patterson Jr, D. G., Needham, L. L., Lee, S., Russell, A. G. and Mulholland, J. A., 2009. Characterization of PM2.5-bound polycyclic aromatic hydrocarbons in Atlanta. Atmospheric Environment 43, 1043-1050.

Liu, W., Wang, Y. H., Russell, A. and Edgerton, E. S., 2005. Atmospheric aerosol over two urban-rural pairs in the southeastern United States: chemical composition and possible sources. Atmospheric Environment 39, 4453-4470.

Liu, W., Wang, Y. H., Russell, A. and Edgerton, E. S., 2006. Enhanced source identification of southeast aerosols using temperature-resolved carbon fractions and gas phase components. Atmospheric Environment 40, S445-S466.

Majestic, B. J., Anbar, A. D. and Herckes, P., 2009. Elemental and iron isotopic composition of aerosols collected in a parking structure. Science of The Total Environment 407, 5104-5109.

Marmur, A., Mulholland, J. A. and Russell, A. G., 2007. Optimized variable source-profile approach for source apportionment. Atmospheric Environment 41, 493-505.

Marmur, A., Park, S. K., Mulholland, J. A., Tolbert, P. E. and Russell, A. G., 2006. Source apportionment of PM2.5 in the southeastern United States using receptor and emissions-based models: Conceptual differences and implications for time-series health studies. Atmospheric Environment 40, 2533-2551.

Marmur, A., Unal, A., Mulholland, J. A. and Russell, A. G., 2005. Optimization-based source apportionment of PM2.5 incorporating gas-to-particle ratios. Environmental Science & Technology 39, 3245-3254.

Metzger, K. B., Tolbert, P. E., Klein, M., Peel, J. L., Flanders, W. D., Todd, K., Mulholland, J. A., Ryan, P. B. and Frumkin, H., 2004. Ambient air pollution and cardiovascular emergency department visits. Epidemiology 15, 46-56.

Miranda, J., Cahill, T. A., Morales, J. R., Aldape, F., Flores, J. M. and Díaz, R. V., 1994. Determination of elemental concentrations in atmospheric aerosols in Mexico city using proton induced x-ray emission, proton elastic scattering, and laser absorption. Atmospheric Environment 28, 2299-2306.

Norris, G. and Vedantham, R., 2008. EPA Positive Matrix Factorization (PMF) 3.0. U.S. Environmental Protection Agency, Research Triangle Park, NC.

Peel, J. L., Tolbert, P. E., Klein, M., Metzger, K. B., Flanders, W. D., Todd, K., Mulholland, J. A., Ryan, P. B. and Frumkin, H., 2005. Ambient air pollution and respiratory emergency department visits. Epidemiology 16, 164-174.

Peng, R. D., Bell, M. L., Geyh, A. S., McDermott, A., Zeger, S. L., Samet, J. M. and Dominici, F., 2009. Emergency admissions for cardiovascular and respiratory diseases and the chemical composition of fine particle air pollution. Environ. Health Perspect. 117, 957-963.

Pio, C. A., Legrand, M., Alves, C. A., Oliveira, T., Afonso, J., Caseiro, A., Puxbaum, H., Sanchez-Ochoa, A. and Gelencsér, A., 2008. Chemical composition of atmospheric aerosols during the 2003 summer intense forest fire period. Atmospheric Environment 42, 7530-7543.

Puxbaum, H., Caseiro, A., Sánchez-Ochoa, A., Kasper-Giebl, A., Claeys, M., Gelencsér, A., Legrand, M., Preunkert, S. and Pio, C., 2007. Levoglucosan levels at background sites in Europe for assessing the impact of biomass combustion on the European aerosol background. J. Geophys. Res. 112, D23S05.

R Development Core Team. R Development Core Team, 2011. R: A language and environment for statistical computing.Vienna, Austria.

Reff, A., Eberly, S. I. and Bhave, P. V., 2007. Receptor modeling of ambient particulate matter data using Positive Matrix Factorization: review of existing methods. Journal of the Air & Waste Management Association 57, 146-154.

Sarnat, J. A., Marmur, A., Klein, M., Kim, E., Russell, A. G., Sarnat, S. E., Mulholland, J. A., Hopke, P. K. and Tolbert, P. E., 2008. Fine particle sources and cardiorespiratory morbidity: An application of chemical mass balance and factor analytical source-apportionment methods. Environ. Health Perspect. 116, 459-466.

Simoneit, B. R. T., Schauer, J. J., Nolte, C. G., Oros, D. R., Elias, V. O., Fraser, M. P., Rogge, W. F. and Cass, G. R., 1999. Levoglucosan, a tracer for cellulose in biomass burning and atmospheric particles. Atmospheric Environment 33, 173-182.

Tian, D., Wang, Y. H., Bergin, M., Hu, Y. T., Liu, Y. Q. and Russell, A. G., 2008. Air quality impacts from prescribed forest fires under different management practices. Environmental Science & Technology 42, 2767-2772.

Watson, J. G., Chen, L. W. A., Chow, J. C., Doraiswamy, P. and Lowenthal, D. H., 2008. Source apportionment: findings from the US supersites program. Journal of the Air & Waste Management Association 58, 265-288.

Watson, J. G. and Chow, J. C., 2001. Source characterization of major emission sources in the Imperial and Mexicali Valleys along the US/Mexico border. Science of The Total Environment 276, 33-47.

Watson, J. G., Chow, J. C. and Houck, J. E., 2001. PM2.5 chemical source profiles for vehicle exhaust, vegetative burning, geological material, and coal burning in Northwestern Colorado during 1995. Chemosphere 43, 1141-1151.

Zhang, X., Hecobian, A., Zheng, M., Frank, N. H. and Weber, R. J., 2010. Biomass burning impact on PM2.5 over the Southeastern US during 2007: integrating chemically speciated FRM filter measurements, MODIS fire counts and PMF analysis. Atmos. Chem. Phys. 10, 6839-6853.

Zheng, M., Cass, G. R., Ke, L., Wang, F., Schauer, J. J., Edgerton, E. S. and Russell, A. G., 2007. Source apportionment of daily fine particulate matter at Jefferson street, Atlanta, GA, during summer and winter. Journal of the Air & Waste Management Association 57, 228-242.

CHAPTER 4 DEVELOPMENT OF OUTCOME-BASED, MULTIPOLLUTANT MOBILE SOURCE INDICATORS

(Pachon, J. E., Balachandran, S., Hu, Y. T., Mulholland, J. A., Darrow, L. A., Sarnat, J. A., Tolbert, P. E. and Russell, A. G., 2011. Journal of the Air & Waste Management Association. Submitted)

4.1. Abstract

Multipollutant indicators of mobile source impacts are developed from readily available CO, NOx, and elemental carbon (EC) data for use in air quality and epidemiologic analysis. Two types of outcome-based integrated mobile source indicators (IMSI) are assessed. The first is derived from analysis of emissions of EC, CO and NOx such that pollutant concentrations are mixed and weighted based on emission ratios for both gasoline and diesel vehicles. This emission-based indicator (EB-IMSI) captures the impact of mobile sources estimated from receptor models and its uncertainty is comparable to measurement and source apportionment uncertainties. The EB-IMSIs have less spatial variability than single pollutants, suggesting they are better indicators of the regional impact of mobile sources. A sensitivity analysis of fractions of pollutants in a two-pollutant mixture and the inclusion in an epidemiologic model is conducted to develop a second type of indicators based on health outcomes. The health-based indicators (HB-IMSI) are weighted combinations of CO, NOx and EC pairs that have the lowest p-value in their association with cardiovascular disease emergency department visits, possibly due to their better spatial representativeness. These outcome-based, multipollutant indicators can provide support for the setting of multipollutant air quality standards and other air quality management activities.

4.2. Introduction

Air quality standards, such as the National Ambient Air Quality Standards (NAAQS) in the US, have traditionally focused on setting maximum limits to ambient concentrations of individual pollutants The NAAQS, and air quality standards in general, are developed from exhaustive studies, both mechanistic and epidemiologic, that seek to deduce the impacts to human health from air pollution. To date, most air pollution epidemiologic work has examined associations between health outcomes and individual pollutants. However, human exposure to air pollution occurs in a multipollutant setting. Thus, a multipollutant approach may be more realistic to understanding risks and regulating urban air pollution.

Multipollutant approaches have been extensively applied in controlling emissions of pollutants to the atmosphere. Pollutants are rarely emitted in isolation by a source and control devices for one pollutant can usually modify emissions of all of the compounds. For example, methods that remove NOx and SOx in electrical generating units can also remove Hg from the flue gas (US-EPA, 2007b). Furthermore, multipollutant control has been demonstrated to be cost-effective.

Multipollutant regulations already exist for primary standards and are being utilized for secondary standards. For example, heavy and light-duty fleets are required to meet NOx, CO, PM, HC, NMHC standards(US-EPA). In addition, EPA recently created the aquatic acidification index (AAI), a multipollutant index developed based on analysis of ecological effects, to be used as part of a potential combined NAAQS standard considering the combined effects of NOx and SOx deposition on aquatic ecosystems (US-EPA, 2011).

In the past years, substantial progress has been made to move towards a result-oriented, risk-based multipollutant approach in air quality management (NARSTO, 2010). A

consistent limitation of adopting this multipollutant approach has been in the identifying mixtures of relevance in the atmosphere and the health effects of such mixtures (Hidy and Pennell, 2010; National Research Council, 2004; US-EPA, 2007b). Statistical tools such as factor analysis (FA) have been suggested to overcome this limitation. Receptor models are also useful with the constraint of conserving mass. However, these techniques rely on an abundant amount of air quality data including availability of specific components that are not routinely measured.

Multipollutant models in epidemiologic analysis have generally included two or more pollutants at a time within a model, with the goal of identifying confounders in the associations with health rather than the effects of a mixture of pollutants (Bell et al., 2011; Dominici et al., 2010; Mauderly et al., 2010; Mauderly and Samet, 2009). Multipollutant models are subject to exposure measurement error in the same way that single pollutant models are, but can also have differential errors (e.g., where the pollutant measured with the least amount of error is the one with the strongest signals) and reduced statistical power (when more than one pollutant at a time is included) (Vedal and Kaufman, 2011). Moreover, the mixtures included in multipollutant models do not always represent an actual or unique source of emissions which complicates designing effective measures to improve public health (Franklin et al., 2008; Hart et al., 2011; Lenters et al., 2010; Metzger et al., 2004; Peng et al., 2009).

Mobile source emissions have been identified as a key urban air pollution component adversely affecting public health (Beelen et al., 2008; Tonne et al., 2007). In the Atlanta area, elevated NO_2, CO, $PM_{2.5}$, organic carbon (OC) and EC concentrations, pollutants traditionally related to traffic, have been associated with Emergency Department (ED) visits

for cardiovascular disease (CVD) (Health Effects Institute, 2010; Metzger et al., 2004). Results from using receptor models in epidemiologic analysis provide further support that combustion-related sources are associated with CVD (Sarnat et al., 2008).

The adverse impact of mobile sources on health is due to the magnitude of these sources in the Atlanta area, where traffic emissions are estimated to account for 30% of the $PM_{2.5}$, 84% of NOx emissions and 97% of CO emissions (US-EPA, 2007a). Results from source apportionment indicate that the contribution of tailpipe mobile source emissions to ambient $PM_{2.5}$ varies from 17 to 26% and the total impact from mobile sources is likely larger considering that a significant amount of crustal material (i.e. Al, Si, Ca, Fe, K) originates from the re-suspension of dust due to vehicles (Kim et al., 2003, 2004; Lee et al., 2008b; Liu et al., 2005).

Our objective in this work is to develop and assess outcome-based, multipollutant indicators for mobile sources here called Integrated Mobile Source Indicators (IMSI). IMSIs are simple to construct and calculate from readily available data and are for use in air quality and epidemiologic analyses. The species considered are CO, NOx and EC available from routine air quality monitoring networks. Two types of IMSIs are developed: the first is based on outcomes from analysis of pollutant emissions and observed concentrations (here called EB-IMSI). EB-IMSI are developed for Atlanta, GA and compared to Dallas, TX. A sensitivity analysis is used to refine the indicators based on two-pollutant mixtures of NOx-EC, NOx-CO and CO-EC and develop a second type of indicators based on health outcomes (here called HB-IMSI) exclusively in Atlanta. Temporal and spatial variability of IMSIs are assessed and compared with source impacts from receptor models. While developed for mobile sources, such integrated indicators could be developed for other sources as well.

4.3. Methods

IMSI development and assessment follows four steps: i) selection of pollutants and analysis of emission inventories, ii) development of the emission-based integrated indicators (EB-IMSI), iii) comparison of air pollutant impact analysis using indicators with results from receptor models, iv) inclusion in models examining associations with acute health responses in Atlanta and development of health-based indicators (HB-IMSI).

4.3.1. Pollutant selection and analysis of emission inventories

Traditionally, CO and NOx have been used as gaseous indicators of vehicular activity. CO is emitted primarily by gasoline-fueled engines, while both gasoline and diesel engines have substantial NOx emissions. Mobile source based $PM_{2.5}$ is generated not only via combustion processes but also mechanical grinding and secondary formation (i.e. formation in the atmosphere from $PM_{2.5}$ precursors under photochemical conditions). Since $PM_{2.5}$ can have several sources, it is preferable to use components that are better indicators of $PM_{2.5}$ from combustion sources. $PM_{2.5}$ EC and OC are formed during combustion, with OC being produced in early stages of combustion and EC at later stages and higher temperatures. OC is also formed from other processes, including secondary formation from biogenic emissions. Gasoline vehicles (GV) usually have a higher OC/EC ratio than diesel vehicles (DV), with values around 3.0-4.0 for GV and below 1.0 for DV (Lee and Russell, 2007; Zheng et al., 2007). Because diesel exhaust contains much higher EC concentrations than gasoline exhaust, EC has been used as a tracer for diesel impacts on PM (Marmur et al., 2005).

Other $PM_{2.5}$ components, including heavy metals such as zinc (Zn), nickel (Ni), vanadium (V), copper (Cu) and lead (Pb), have also been used as tracers to identify mobile source impacts on air quality, and specifically to split calculated impacts between gasoline

and diesel vehicles (Lee et al., 2008b). Zn is used as a tracer of GV and is an additive in lubricating oil, Pb and Cu are produced from brake wear and road traffic, and Ni and V are found in diesel exhaust. Organic compounds, such as hopanes and polycyclic aromatic hydrocarbons (PAHs), are used as tracers of traffic-related PM impacts as well (Brook et al., 2007; Zheng et al., 2002). While these organic compounds are very useful in the identification of specific source impacts, their measurement is more resource intensive and their concentrations are not as widely available.

We chose CO, NOx and EC to develop the traffic-related IMSI because these species are ubiquitous to monitoring stations in the US and emissions inventories. A detailed analysis of CO, NOx and EC emissions and ambient air concentrations in downtown Atlanta (Fulton County) and downtown Dallas (Dallas County) was conducted for the period 1999-2007. Emissions from mobile sources (on-road and non-road) were obtained from the EPA National Emission Inventory (NEI) (US-EPA, 2007a) and the Visibility Improvement State and Tribal Association (VISTAS) project (Air Resources Specialists, 2007). Additionally, we applied the EPA Motor Vehicle Emissions Simulator (MOVES 2010) to identify the fraction of emissions from on-road GV and DV (US-EPA, 2010). Both NEI and MOVES use nation-wide information of vehicle miles traveled (VMT) to estimate on-road emissions, but emissions factors used in MOVES 2010 have been revised from those used in NEI.

Ambient air quality data in Atlanta were obtained from the Jefferson Street monitoring location (JST), a site operated by the Southeastern Aerosol Research and Characterization Study (SEARCH). Description of the measurement methods is found elsewhere (Edgerton et al., 2005; Hansen et al., 2003). Briefly, elemental carbon (EC) is measured on 24-hour PM2.5 samples using quartz filters from a particle composition monitor

(PCM) and analyzed by the thermal-optical reflectance (TOR) method at the Desert Research Institute (DRI) following the Interagency Monitoring of Protected Visual Environments (IMPROVE) protocol (Chow et al., 1993). CO, NO and NO_2 are measured every minute and averaged to the hour. CO is measured using non-dispersive infrared spectrophotometry. NO_2 is measured via photolytic conversion to NO, followed by chemiluminescence. NO and NO_2 are summed and reported as NOx. O_3 is measured using UV-absorption. For the period 1999-2004, a total of 1701 days were selected for use after removing days with missing data or data with high uncertainty. An additional site, the South DeKalb (SD) monitoring station from the EPA's Speciation Trends Network (STN) located 15.3 km to the southeast of JST (Figure 4.1) was examined to assess the spatial variability of EB-IMSIs. Both JST and SD are heavily impacted by traffic emissions and have daily ambient CO, NOx and EC measurements, with the exception of EC at SD where it is measured every third day.

In Dallas, air quality data is collected from the US EPA's Air Quality System (AQS) for the Hinton site located four miles northwest of downtown Dallas (Figure B.1 in Appendix B). Air quality from Hinton has been used in several studies because Hinton is the main monitoring site in the area (Qin et al., 2007; Smith et al., 2011). PM2.5 is sampled following the Federal Reference Method (FRM) and, at that time, EC and OC were measured using the STN thermal optical transmittance (TOT) method, similar to the National Institute of Occupational Safety and Healthy (NIOSH) method (Birch and Cary, 1996). Continuous monitoring for CO is performed by use of the FRM non-dispersive infrared correlation method and NO_2 is measured using the FRM chemiluminescence and UV methods. CO and NOx at the Hinton site were available from 1999 to 2007, while EC was only available for the period 2003-2008

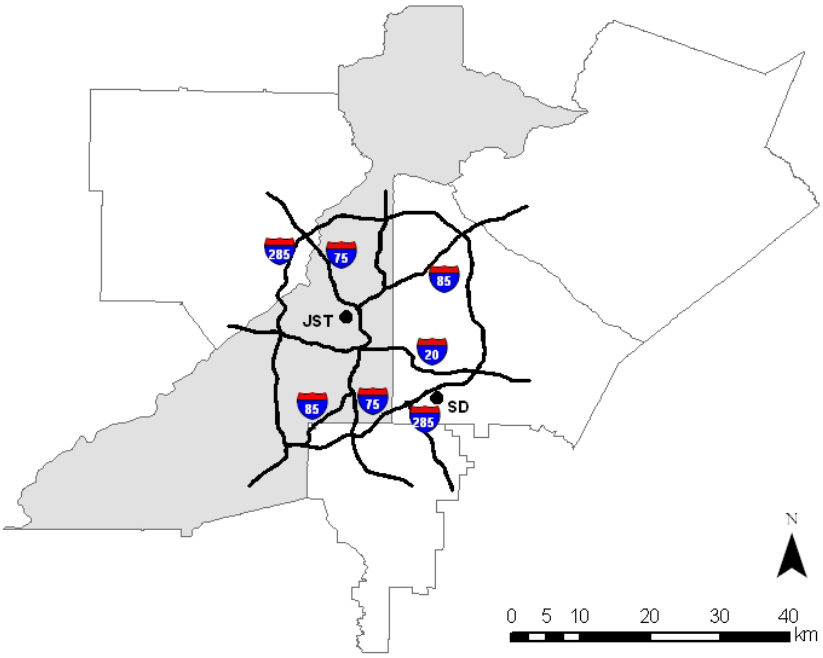

Figure 4.1 Location of Jefferson Street (JST) and South DeKalb (SD) monitoring stations in Atlanta, GA. Area in gray is Fulton County.

4.3.2. Carbon Monoxide (CO)

The NEI reports total CO emissions of 294,932 tons/year for Fulton County in 2002, of which 97% are from mobile sources (75% on-road and 22% non-road). The on-road CO emissions estimated with MOVES are slightly lower (189,664 tons/year) due to revisions in the emission factors from 1992 to 2002. MOVES estimates that 98% of the on-road CO emissions are from GV and 2% are from DV.

On a daily basis, on-road CO emission estimates are 20% higher during weekdays than weekends, indicating a decrease in GV travel during weekends. On a monthly basis, CO emissions from GV have two periods of increase during the year (Figure 4.2a): June through

August due to the use of air conditioning in summer, and December through February as result of cold start emissions.(US-EPA, 2008)

Ambient CO concentrations are the lowest during the summer months (Figure 4.2a), especially during June and July when dispersion of contaminants is favored and CO photochemical destruction is faster. The highest concentrations are found from October through December when wind speeds are slower (Figure B.3 in the Appendix B) and thermal inversion episodes trap pollutants nearer the ground. From January through March inversions are still present, but wind speeds are significantly higher than prior months resulting in greater dispersion of pollutants.

On an annual basis, there is a clear trend between reductions in ambient air concentrations of CO and emission reductions from 1999 to 2007 (Figure 4.2b). Comparison of CO emission estimates from MOVES and NEI in 1999, 2002 and 2005 shows good agreement between both methods. The reduction of CO emissions in 2007 with respect to 1999 was 48% in NEI and 45% in MOVES.

These results support using CO concentrations as an indicator of GV impacts, though this indicator is limited to local sources and can lead to potential biases in a regional assessment.

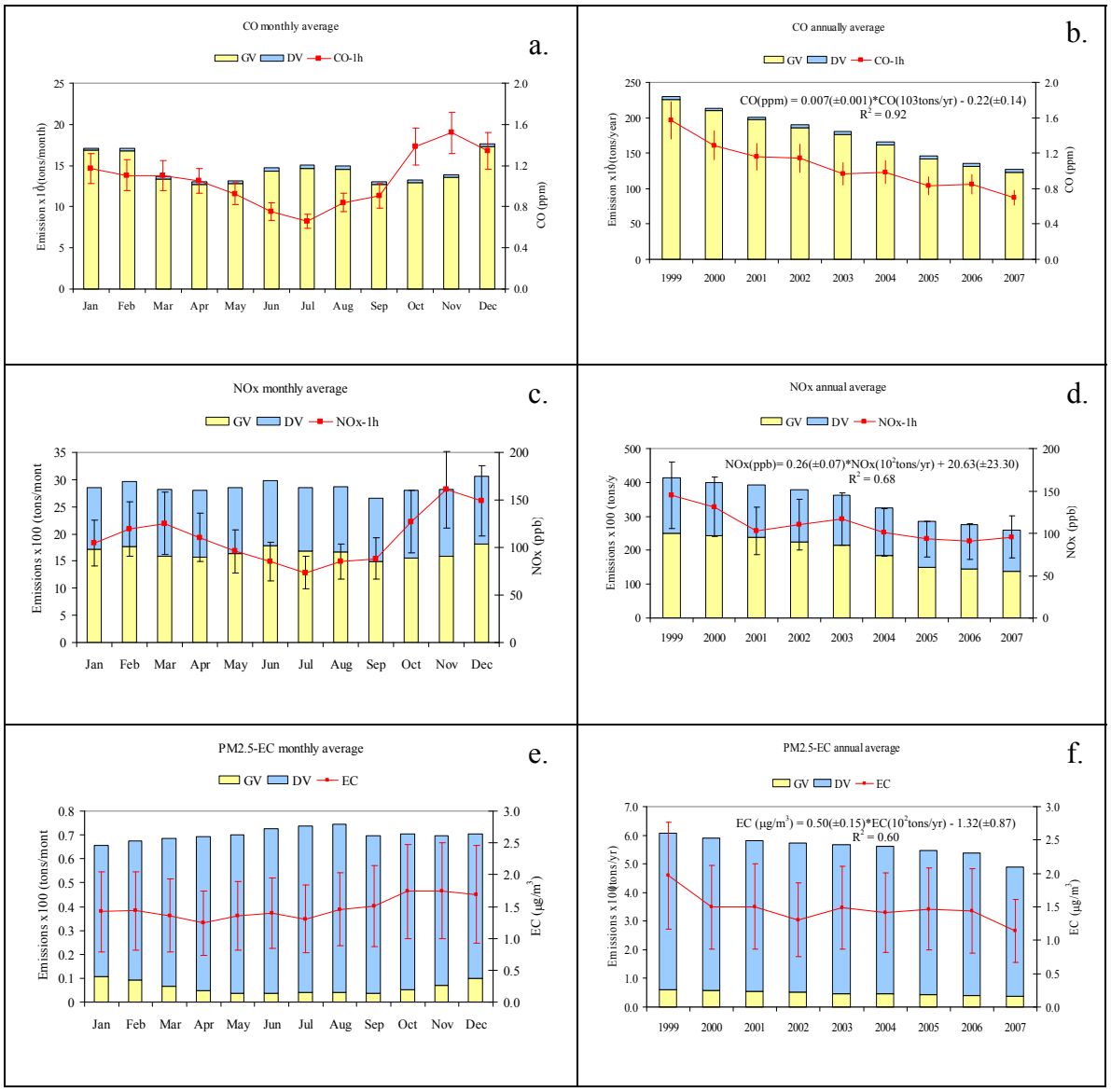

Figure 4.2 Monthly and annual trends of CO, NOx and EC. Bars represent emissions estimates from MOVES in tons/month (a, c, e) or tons/yr (b, d, f). Bold line represents ambient air concentrations of CO (ppm), NOx (ppb) and EC ($\mu g/m^3$) on right vertical scale. Error bars are the root mean square (RMS) error of daily uncertainties from measurements. R^2 denotes the correlation between annual emissions and annual average concentrations.

4.3.3. Nitrogen Oxides (NOx)

The NEI reports total NOx emissions of 47,103 tons/year for Fulton County in 2002, of which 87% are from mobile sources (72% on-road and 15% non-road). NOx emissions estimated with MOVES are slightly lower than the NEI estimates (37,781 tons/year) due to

lower exhaust emissions from heavy-duty vehicles.(US-EPA, 2010) MOVES estimates that 60% of the on-road NOx emissions are from GV and 40% are from DV. Although diesel engines emit more NOx than spark ignition engines per mile traveled, the gasoline fleet is significantly larger (about 10 times) than the diesel fleet for Fulton County.(Blanchard et al., 2010) Other sources contributing to NOx emissions are classified as area and point sources, in particular fuel combustion in electrical generating utilities (EGU) and biomass burning. It is expected, however, that most of the NOx impacting the receptor stations come from mobiles sources, because EGU have high effective stack heights such that pollutants are better dispersed before impacting the monitor station at the surface. Further, NOx emissions from point sources were 13% of the total emissions in 1999, but only 2% in 2007.

On a weekly basis, NOx ambient air concentrations are 24% higher on weekdays than on weekends, consistent with a larger reduction of DV than GV traffic during weekends. On a monthly basis, NOx follows a similar trend to CO, with higher concentrations in winter and lower concentrations during summer (Figure 4.2c) when NOx is more rapidly removed by photochemical reactions. NOx emissions from DV are relatively constant throughout the year, whereas NOx emissions from GV have a similar trend to CO emissions, increasing in summer months due to the use of A/C systems and in winter months due to cold start emissions.(US-EPA, 2008)

On a yearly basis, NOx ambient concentrations decreased from 1999 to 2001, increased during 2002 and 2003, and decreased again until 2007 (Figure 4.2d). The significant reduction during the period 1999-2001 (from 154 to 103 ppb) is likely a result of the implementation of the EPA acid rain program and stationary controls to reduce ozone, combined with mobile source reductions.(US-EPA, 2005) From 2002-2007, reductions in

ambient NOx are attributed largely to decreases in on-road NOx emissions. NOx emissions from on-road sources have a stronger correlation with ambient NOx during the period 2002-2007 (R^2=0.65) than 1999-2007 (R^2=0.36).

These results indicate that mobile source NOx emissions have a large impact on ambient NOx concentrations, but are not as dominant as mobile source CO emissions on ambient CO concentrations.

4.3.4. Elemental Carbon (EC)

VISTAS estimates of EC emissions for 2002 is 92% from mobiles sources (on-road and non-road) and 8% from other sources, such as biomass burning. From the on-road fraction, MOVES estimates 91% from DV and 9% from GV. On a weekly basis, EC concentrations are 30% higher during weekdays than weekends, due to the higher fraction of diesel vehicle traffic on weekdays. On a monthly basis, EC concentrations are lowest in spring and summer as compared to the October-December period. During the cooler months, dispersion of pollutants is not favored due to increased thermal inversions and reduced wind speeds (Figure 4.2e).

EC emissions from DV increase in summer due to an increase in VMT and greater construction activity with the subsequent increase in non-road emissions. Although not as large as emissions from DV, EC emissions from GV can be an important source during winter time because of cold starts (US-EPA, 2008).

On an annual basis, EC concentrations decreased from 1.97 $\mu g/m^3$ in 1999 to 1.13 $\mu g/m^3$ in 2007 (Figure 4.2f) as a result of changes in fuel composition and controls on mobile sources, such as the introduction of low and ultra low sulfur diesel in 2002 and 2006, respectively. Controls in point and open fires might also have helped on this reduction, such

as the open burning ban implemented in the 13-county metro Atlanta area in 1996. These results indicate that EC emissions are dominated by mobile sources for Fulton County, particularly by DV.

In summary, data from Atlanta using a number of emissions and monitoring databases show that CO and EC are likely good indicators of GV and DV, respectively. NOx appears to be an indicator of overall mobile sources and cannot be easily used to discern between GV and DV. Since only 20% of the total OC emissions are from mobiles sources (on-road and non-road) (Air Resources Specialists, 2007) and a fraction between 26%-47% of ambient OC can be formed secondarily (Pachon et al., 2010), our development of EB-IMSI does not use OC, though the indicators can be used to estimate the OC from mobile sources.

A similar analysis of ambient concentrations and emissions of CO, NOx and EC is conducted for Dallas and presented in Appendix B.1.

4.4. Development of the emission-based integrated indicators

We propose a multipollutant indicator of CO, NOx and EC to assess mobile source impacts on air quality. In this work, the 1hr maximum values for CO and NOx were chosen because the 1hr metric has been found more associated with health outcomes than other metrics (Metzger et al., 2004). The EB-IMSI uses ratios of mobile-source-to-total emissions for each pollutant as weighting coefficients. Mobile source fractions of each pollutant can be estimated by multiplying these ratios by the ambient air concentrations. For example, the fraction of EC from mobile sources is estimated here as the total EC concentration multiplied by the ratio $(EC_{mob}/EC_{tot})_{Emis}$. Since the original pollutants have different units ($\mu g/m^3$ for EC

and ppm for CO and NOx), a scaling of the ambient air concentrations by the standard deviation of each variable was performed:

$$EB-IMSI=\frac{\left(\frac{EC_{mob}}{EC_{tot}}\right)_{Emis}EC'+\left(\frac{NOx_{mob}}{NOx_{tot}}\right)_{Emis}NOx'+\left(\frac{CO_{mob}}{CO_{tot}}\right)_{Emis}CO'}{\left(\frac{EC_{mob}}{EC_{tot}}\right)_{Emis}+\left(\frac{NOx_{mob}}{NOx_{tot}}\right)_{Emis}+\left(\frac{CO_{mob}}{CO_{tot}}\right)_{Emis}} \quad (4.1)$$

where $EC'=\frac{EC}{\sigma_{EC}}$, $CO'=\frac{CO}{\sigma_{CO}}$, $NOx'=\frac{NOx}{\sigma_{NOx}}$ represent the scaled concentrations (i.e., divided by the standard deviation) and the ratios correspond to emission ratios. The EB-IMSI uses normalization by the sum of the emission ratios in such a way that the indicator can be easily compared with other IMSI.

The weighting coefficients (ratios between mobile sources and total emissions) for NOx and CO, obtained from the NEI database, are 0.84±0.03 and 0.97±0.01, respectively. The weighting coefficient for EC was estimated from VISTAS in 2002 to 0.92±0.04. The fractional contribution of each one of the weighting coefficients is approximately the same (0.33 for EC, 0.31 for NOx, 0.36 for CO).

We were also interested in differentiating impacts from gasoline and diesel exhaust emissions, since the contribution at the receptor site can be quite different and the control mechanisms are specific to each type of vehicle. Therefore, we define integrated indicators for gasoline vehicles (EB-IMSI-GV) and diesel vehicles (EB-IMSI-DV) using specific emission ratios from gasoline and diesel emissions estimated with MOVES.

The ratio of gasoline-to-mobile emissions was used as a weighting coefficient for each species, being 0.58±0.02 for NOx and 0.98±0.01 for CO, obtained from the application of MOVES. For EC, the ratio of gasoline-to-mobile emissions is more seasonally dependent, with a summer value of 0.06±0.01 and a winter value of 0.12±0.04. The fractional contribution of each weighting coefficient is 0.05 for EC, 0.32 for NOx and 0.63 for CO, which indicates more weight on the CO and NOx than EC. Therefore, EB-IMSI-GV was defined as a weighting mixture of CO and NOx only:

$$EB-IMSI_{GV}=\frac{\left(\frac{NOx_{GV}}{NOx_{tot}}\right)_{Emis}NOx'+\left(\frac{CO_{GV}}{CO_{tot}}\right)_{Emis}CO'}{\left(\frac{NOx_{GV}}{NOx_{tot}}\right)_{Emis}+\left(\frac{CO_{GV}}{CO_{tot}}\right)_{Emis}} \tag{4.2}$$

where $\left(\frac{NOx_{GV}}{NOx_{tot}}\right)=\left(\frac{NOx_{GV}}{NOx_{mob}}\right)\left(\frac{NOx_{mob}}{NOx_{tot}}\right), \left(\frac{CO_{GV}}{CO_{tot}}\right)=\left(\frac{CO_{GV}}{CO_{mob}}\right)\left(\frac{CO_{mob}}{CO_{tot}}\right)$

Similarly, the ratios of diesel-to-total mobile emissions obtained from MOVES, used as weighting coefficients, for NOx was 0.42±0.02 and for CO 0.02±0.01. For EC, the ratio of diesel-to-total mobile emissions was more seasonally dependent, with a summer value of 0.94±0.01 and a winter value of 0.88±0.04. The contribution of each weighting coefficient was 0.69 for EC, 0.29 for NOx, 0.02 for CO, which implies more weight on EC and NOx than CO. Therefore, EB-IMSI-DV was defined as a weighting mixture of EC and NOx only:

$$EB-IMSI_{DV}=\frac{\left(\frac{EC_{DV}}{EC_{tot}}\right)_{Emis}EC'+\left(\frac{NOx_{DV}}{NOx_{tot}}\right)_{Emis}NOx''}{\left(\frac{EC_{DV}}{EC_{tot}}\right)_{Emis}+\left(\frac{NOx_{DV}}{NOx_{tot}}\right)_{Emis}} \tag{4.3}$$

where $\left(\frac{EC_{DV}}{EC_{tot}}\right)=\left(\frac{EC_{DV}}{EC_{mob}}\right)\left(\frac{EC_{mob}}{EC_{tot}}\right), \left(\frac{NOx_{DV}}{NOx_{tot}}\right)=\left(\frac{NOx_{DV}}{NOx_{mob}}\right)\left(\frac{NOx_{mob}}{NOx_{tot}}\right)$

Specification of the EB-IMSIs has limitations. First, the emission fraction for a pollutant is translated to an ambient fraction assuming that the average source and receptor fractions are the same. This assumption has been tested in the past with good results: gas-to-$PM_{2.5}$ emission ratios were used to optimize source profiles in Atlanta, finding a more accurately apportionment of $PM_{2.5}$ from mobile sources and coal-fire power-plants.(Marmur et al., 2005) A second limitation is the use of an annual average emission ratio across the time series; however daily estimates of emissions are not available at this time.

The EB-IMSI expressions for Dallas use the same values for the weighting coefficients than Atlanta since emissions estimates were obtained from the same sources.

4.5. Comparison of air pollutant impact analysis using indicators with results from receptor models

The EB-IMSIs were compared with source impacts from receptor models. The chemical mass balance method CMBv.8.2 (Watson et al., 1984) and the Positive Matrix Factorization method PMFv3.0 (Norris and Vedantham, 2008) were applied to the same period of time as the indicators. For PMF, strong species were NO_3, SO_4, NH_4, EC, four OC thermal fractions, Al, Si, Fe, K, Ca, Br, Mn, Zn and weak species were $PM_{2.5}$, Cu, Pb, Se. The temperature-resolved OC fractions were chosen to help on the separation between gasoline and diesel source impacts.(Kim et al., 2004; Liu et al., 2005) Missing data were replaced by their geometric mean to conserve the original number of samples for better performance of the PMF algorithm.(Reff et al., 2007) For CMB, optimized source profiles were chosen from a previous study in Atlanta and sources were eliminated to avoid negative source impacts.(Marmur et al., 2005)

4.6. Inclusion in models examining associations between pollutant mixtures and acute health responses in Atlanta

Based on the combination of pollutants in the EB-IMSI-GV and EB-IMSI-DV, a sensitivity analysis was performed between two-pollutant mixtures. For EB-IMSI-GV, mixtures of CO and NOx were evaluated and for EB-IMSI-DV mixtures of EC and NOx were chosen. In addition, mixtures of EC and CO were also evaluated. The sensitivity analysis was performed as follows.

$$\text{NOx-EC} = \alpha * \text{NOx'} + (1-\alpha) * \text{EC'} \quad (4.4)$$

$$\text{NOx-CO} = \alpha * \text{NOx'} + (1-\alpha) * \text{CO'} \quad (4.5)$$

$$\text{CO-EC} = \alpha * \text{CO'} + (1-\alpha) * \text{EC'} \quad (4.6)$$

where EC', CO' and NOx' represent the scaled concentrations and α is a parameter that varies from 0 to 1, in such a way that allows comparing pollutants individually (when α is equal to 0 or 1) versus two-pollutant mixtures. The combination of NOx-EC at α=0.3 corresponds to EB-IMSI-DV and the mixture of NOx-CO at α=0.3 corresponds to EB-IMSI-GV.

The impact of multipollutant metrics associated with mobile sources on health was assessed in an epidemiologic analysis. CVD ED visits were chosen as the health endpoint for this analysis given as those have been found to be associated with combustion-related activities in Atlanta.(Metzger et al., 2004; Sarnat et al., 2008) Briefly, ED visits for CVD were collected from 41 hospitals in metro Atlanta from 1999 to 2004. Daily ED counts are regressed with air pollution indicators using a Poisson generalized linear model (GLM).

$$\log[E(Y)] = \alpha + \beta * IMSI + \sum_k \lambda_k day - of - week_k + \sum_m v_m hospital_m \quad (4.7)$$

$$+ \sum_P \zeta_P holiday_p + g_1(\gamma_1,....,\gamma_N; time) + g_2(\partial_1,....,\partial_N; temperature) + g_3(\eta_1,.....,\eta_N; dewpoint)$$

where E(Y) is the predicted count of CVD visit and β is the regression coefficient of the indicator of interest. Day of week, holiday and hospital entry and exit are modeled using indicator variables (as the hospitals provided data for varying amounts of time). Long-term temporal trends are accounted for using cubic splines with monthly knots (g_1). Daily (lag 0) temperature is controlled using indicator variables for each degree Celsius and cubic terms for lag1 and lag 2 moving average temperature (g_2); dew point is controlled using cubic terms for lag 0-1-2 moving average (g_3). The model specifications are described, in detail, elsewhere.(Metzger et al., 2004; Sarnat et al., 2008)

Unlike traditional multipollutant models that solve for different regression coefficients, our approach solves for only one β for a multipollutant indicator. The points at which the two-pollutant mixtures show the strongest association with CVD define the health-based integrated indicators (HB-IMSI).

4.7. Results

The assessment and relevance of the EB-IMSIs was conducted as follows: i) analysis of EB-IMSI trends, ii) comparison with mobile source impacts from receptor models, iii) uncertainties in the estimation of the indicators, iv) comparison with HB-IMSI derived from associations with CVD ED visits and v) implication for multipollutant air quality standards.

4.7.1. EB-IMSI trends

EB-IMSIs exhibit similar temporal trends as ambient EC, CO and NOx, with a decrease during summer and increase during fall and reduction in annual averages from 1999 to 2007 (Fig 3). The total EB-IMSI was strongly correlated with EC (R^2=0.74), CO (R^2=0.86) and NOx (R^2=0.81), which was expected since they are the species forming the indicator. EB-IMSI-GV was most strongly correlated with CO (R^2=0.94) whereas EB-IMSI-DV was more strongly correlated with EC (R^2=0.91). On a monthly basis, EB-IMSI-GV showed a larger reduction in concentrations during summer than EB-IMSI-DV, consistent with less commuting from light-duty traffic during the summer months. On an annual basis, there is a larger decrease in EB-IMSI-GV than EB-IMSI-DV, explained by a more rapid introduction of new control technologies in the gasoline fleet than diesel vehicles. The comparison of EB-IMSIs annual averages with reduction in emissions of CO, NOx and EC with respect to 1999 shows a similar trend suggesting a good agreement between indicators estimated with ambient air concentrations and emissions from mobile sources.

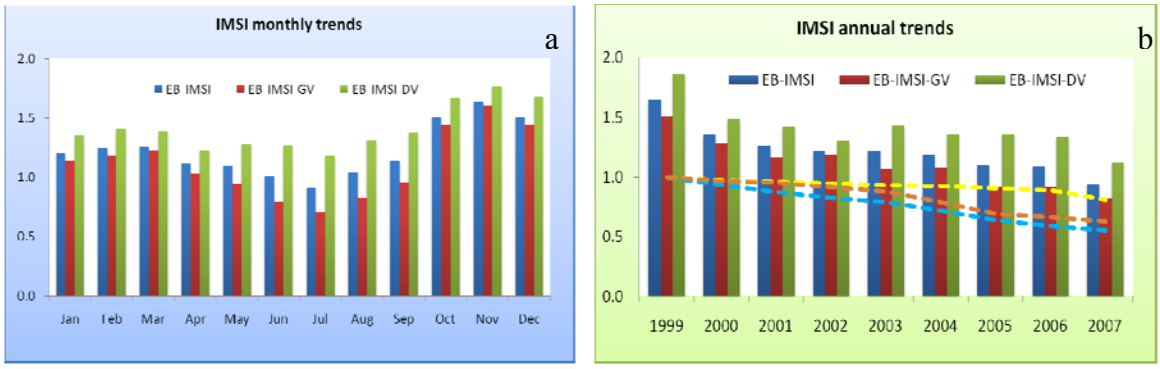

Figure 4.3 Temporal trends (a. monthly; b. annual) of EB-IMSI, EB-IMSI-GV and EB-IMSI-GV (unitless). The indicators are normalized such as they have a standard deviation of one. Annual trend is compare with reduction in emissions of CO, NOx and EC with respect to 1999 (on right y axes).

On a daily basis, EB-IMSI is 22% larger during weekdays than weekends, capturing the increase in traffic during the week. The EB-IMSI-DV trend has a large decrease during weekends (30%) than EB-IMSI-GV (14%) and is explained by reduced diesel traffic during the weekend.

In Dallas, EB-IMSI annual trends peak in 2005, similar to CO, NOx and EC (Fig. B.2 in the Appendix B) due to dry conditions during this year. A slight increase in EB-IMSI and EB-IMSI-DV is also observed in 2007 and explained by lower wind speeds during that year. On a weekly basis, EB-IMSIs are greater on weekdays than weekends, similar to traffic trends. EB-IMSI-DV has a larger weekday/weekend ratio than EB-IMSI-GV (1.39 and 1.20 respectively), suggesting a larger reduction of heavy-duty traffic during weekends, as expected.

4.7.2. Comparison with results from receptor models

CMB and PMF methods yield similar estimates for PM air quality impacts for the chosen sources (Table B.1 in the Appendix B). The correlation between gasoline and diesel source impacts resolved by CMB and PMF (Table 4.1) was substantially lower than the correlation of the combined fractions into one mobile source (R^2=0.83) in both summer and winter, which demonstrates the difficulty of receptor models to adequately capture the split between gasoline and diesel daily contributions. The proposed EB-IMSI correlates strongly with total mobile source impacts from CMB (R^2=0.86 in winter and R^2=0.73 in summer) and PMF (R^2=0.85 in winter and R^2=0.69 in summer). The EB-IMSI-DV correlates stronger with diesel source impacts from CMB and PMF than the corresponding correlation of EB-IMSI-GV with gasoline source impacts from the receptor models. This is due to both CMB and PMF using EC as a fitting species to solve for diesel contributions, and EB-IMSI-DV is

heavily weighted by EC, whereas EB-IMSI-GV uses CO, a species that is typically not used to fit the CMB or PMF gasoline source categories.

Table 4.1 Correlations between EB-IMSI, EB-IMSI-GV and EBIMSI-DV with single species and daily source impacts from CMB and PMF

R	EC	Nox-1h	CO-1h	PMF-DV	PMF-GV	PMFmob	CMB-GV	CMB-DV	CMBmob	EB-IMSI	EB-IMSIGV	EB-IMSIDV
EC	**1.00**	0.68	0.76	0.70	0.75	0.85	0.65	0.94	0.93	0.88	0.80	0.95
Nox-1h	0.61	**1.00**	0.73	0.57	0.63	0.70	0.51	0.62	0.67	0.89	0.87	0.87
CO-1h	0.53	0.70	**1.00**	0.64	0.66	0.76	0.63	0.64	0.76	0.93	0.97	0.82
PMF-DV	0.58	0.48	0.41	**1.00**	0.45	0.87	0.68	0.56	0.75	0.70	0.67	0.71
PMF-GV	0.50	0.32	0.33	0.07	**1.00**	0.83	0.53	0.69	0.71	0.74	0.70	0.77
PMFmob	0.74	0.56	0.52	0.79	0.66	**1.00**	0.71	0.73	0.86	0.85	0.80	0.86
CMB-GV	0.41	0.32	0.28	0.45	0.12	0.41	**1.00**	0.37	0.88	0.66	0.64	0.65
CMB-DV	0.93	0.52	0.45	0.47	0.51	0.66	0.08	**1.00**	0.76	0.79	0.70	0.88
CMBmob	0.88	0.56	0.48	0.62	0.40	0.71	0.79	0.67	**1.00**	0.86	0.80	0.90
EB-IMSI	0.81	0.90	0.88	0.57	0.44	0.69	0.39	0.72	0.73	**1.00**	0.99	0.96
EB-IMSIGV	0.62	0.87	0.96	0.48	0.37	0.59	0.32	0.54	0.57	0.96	**1.00**	0.90
EB-IMSIDV	0.95	0.82	0.66	0.61	0.48	0.75	0.42	0.87	0.85	0.93	0.79	**1.00**

*Values in the upper right represent correlations during winter time (Oct-Mar); values in the lower left represent correlations during summer time (Apr-Sep).

In the southeastern US, biomass burning can also be a significant source of EC, CO and NOx to ambient air.(Lee et al., 2008a) EB-IMSI does not seem to be influenced by daily impacts from this source. On selected days with biomass burning activity over 4.0 $\mu g/m^3$ of PM2.5 identified by both CMB and PMF, the integrated indicators were more strongly correlated with source impacts from mobile sources than wood burning. On those days, the correlation between EB-IMSI and mobile source impacts from CMB (R^2=0.86) or PMF (R^2=0.83) were significantly higher than the correlation between EB-IMSI and source impacts from biomass burning from CMB (R^2=0.13) or PMF (R^2=0.34). This result supports the emissions estimates and analyses detailed above that found emissions of EC, CO and NOx in Atlanta predominantly from mobile sources.

4.7.3. Uncertainties in mobile source indicators

Uncertainties are involved in several steps of the calculations (e.g. emission estimates, ambient measurements, receptor models), and we estimate uncertainties in EB-IMSIs and compared them with uncertainties from singles species and receptor model source contributions. Uncertainties in ambient measurements (EC, CO, NOx) were estimated as one-third of the detection limit (μg/m^3 or ppm) plus the product of analytical uncertainty (percentage) and concentration. Both detection limit and instrument uncertainty were obtained from the SEARCH study.(Hansen et al., 2003) Uncertainties in CMB source impacts are estimated using the effective variance method which considers uncertainties in both source profiles and ambient concentrations.(Lee and Russell, 2007) In PMF, uncertainties in factor contributions are not given explicitly by the model, so a bootstrapping procedure is used(Norris and Vedantham, 2008). Uncertainties in EB-IMSIs are propagated from individual uncertainties taking into account that CO, NOx and EC are correlated between each other and therefore, covariance terms need to be included.(International Organization for Standardization, 1993)

$$\sigma_c^2(f) = \sum_{i=1}^{N}\left(\frac{\delta f}{\delta x_i}\right)^2 \sigma^2(x_i) + 2\sum_{i=1}^{N-1}\sum_{j=i+1}^{N}\frac{\delta f}{\delta x_i}\frac{\delta f}{\delta x_j}\mathrm{cov}(x_i, x_j) \qquad (4.8)$$

Application of the propagation of errors in the estimation of the EB-IMSI uncertainties is explained in detail in the Appendix B.2.

Among single species, CO and NOx have lower uncertainties than EC because gas species are typically more accurately measured than filter-based $PM_{2.5}$ species measurements (Table 4.2). The EB-IMSIs show uncertainties larger than the ambient measurements since

uncertainties in emissions ratios are involved in addition to the ambient measurement uncertainties. Furthermore, the calculation of uncertainties in EB-IMSIs includes the uncertainty provided by correlated quantities, as it has been demonstrated they can impact uncertainty results (Espinosa et al., 2010). Here, the uncertainty in EB-IMSIs is primarily driven by the uncertainties in the covariance relationships between EC, CO and NOx. For EB-IMSI-GV, the uncertainties are driven by the covariance relationships of CO and NOx. For EB-IMSI-DV, uncertainties are mostly driven by uncertainties in EC measurements and emissions ratios and the covariance relationships of EC and NOx.

Table 4.2 Comparison of uncertainties between indicators

Indicator	Indicator value	Standard deviation	Uncertainty*	Relative uncertainty
CO-1h (ppm)	1.16	1.00	0.16	0.14
NOx-1h (ppm)	0.12	0.10	0.03	0.25
EC (μg/m3)	1.53	0.97	0.64	0.42
EB-IMSI	1.31	0.90	0.72	0.55
EB-IMSI-GV	1.17	0.96	0.80	0.68
EB-IMSI-DV	1.48	0.94	0.76	0.51
PMF-mob ($\mu g/m^3$)	2.94	2.30	1.11	0.38
PMF-GV ($\mu g/m^3$)	1.37	1.21	0.36	0.26
PMF-DV ($\mu g/m^3$)	1.57	1.65	1.05	0.67
CMB-mob ($\mu g/m^3$)	2.54	1.70	2.53	1.00
CMB-GV ($\mu g/m^3$)	1.35	1.15	2.00	1.48
CMB-DV ($\mu g/m^3$)	1.27	1.02	1.60	1.26

* Uncertainties are estimated as the RMS average $\left(\overline{\sigma_i} = \sqrt{\frac{1}{N}\sum \sigma_i^2}\right)$ of daily uncertainties from 1999-2004.

The range of uncertainties of EB-IMSIs (0.51-0.68) is comparable to the range of uncertainties in PMF (0.26-0.67) which is a standard method to estimate contributions from

mobile sources. The high range of uncertainties in CMB (1.00-1.48) is mostly explained by uncertainties in the source profiles (Lee and Russell, 2007).

4.7.4. HB-IMSIs derived from associations with CVD ED visits

The epidemiologic model (Equation 4.7) was implemented with time series of pollutant concentrations (CO, NOx, EC), sources impacts (from CMB and PMF), EB-IMSIs and the two-pollutant mixtures from the sensitivity analysis. A total of 40 metrics were evaluated and compared for the daily association between the metric and corresponding ED visits for CVD in the period 1999-2004. Within the single species, NOx-1hr was most strongly associated with CVD, followed by CO-1hr (Table 4.3). Pollutants that are better measured such as CO and NOx typically have stronger associations in a epidemiologic model,(Vedal and Kaufman, 2011) and NOx has been proposed as indicator of toxic species emitted by traffic.(Brook et al., 2007) When the three pollutants are combined to form the EB-IMSI, the strength of association is greater than either for EC or CO-1hr separately, but less than NOx-1hr. Using EB-IMSI-GV as a predictor of CVD-related ED visits in model resulted in greater statistical significance than EB-IMSI-DV. In this study, gasoline and diesel source impacts from CMB and PMF were not shown to be significantly associated with CVD. This may be explained as both CMB and PMF use EC as a fitting species for mobile fractions, and the association between this pollutant and CVD in this particular analysis was only borderline significant. Differences in time periods, health outcomes and analytic methods (e.g., tighter controls in the epidemiologic analyses) may explain the significant association between mobile source daily contributions and CVD found in other studies in the Atlanta area.(Metzger et al., 2004; Sarnat et al., 2008)

Table 4.3 Results for the associations of ED for CVD with mobile source impacts metrics (sorted by p-value)

Indicator	IQR	RR per IQR	95% CI	p-value
CMB-DV	1.0 μg/m^3	1.005	0.997 – 1.014	0.206
PMF-GV	2.3 μg/m^3	1.005	0.997 – 1.012	0.206
PMF-DV	2.3 μg/m^3	1.006	0.998 – 1.014	0.168
CMB-GV	1.0 μg/m^3	1.006	0.999 – 1.012	0.079
EC	1.0 μg/m^3	1.008	1.000 – 1.017	0.054
CO-1h	0.9 ppm	1.007	1.001 – 1.014	0.033
EB-IMSI	2.3	1.007	1.001 – 1.014	0.029
EB-IMSI-DV	0.7	1.010	1.001 – 1.018	0.022
NOx-1h	0.1 ppm	1.008	1.001 – 1.015	0.018
EB-IMSI-GV	0.8	1.009	1.002 – 1.017	0.018

The inclusion of the two-pollutant mixtures (NOx-EC, NOx-CO, CO-EC) in the epidemiologic model is represented in three curves with a minimum point where the association with CVD is strongest (Figure 4.4). The minimum point suggests that the combinations of pollutants at specific fractions are more prone to explain associations with health outcomes than individual species.

The minimum point in the curves occurs at α=0.6 for NOx-CO, at α=0.7 for NOx-EC and at α=0.5 for CO-EC. It would seem reasonable that a large fraction of NOx in the NOx-CO and NOx-EC pairs would give a more strongly significance to the association with CVD outcomes. However, at larger NOx fractions than the minimum point the significance actually decreases. Similarly, for the CO-EC pair one could also expect that a larger fraction of CO in the mixture would give greater significance. The minimum occurs when both pollutants are approximately equally weighted.

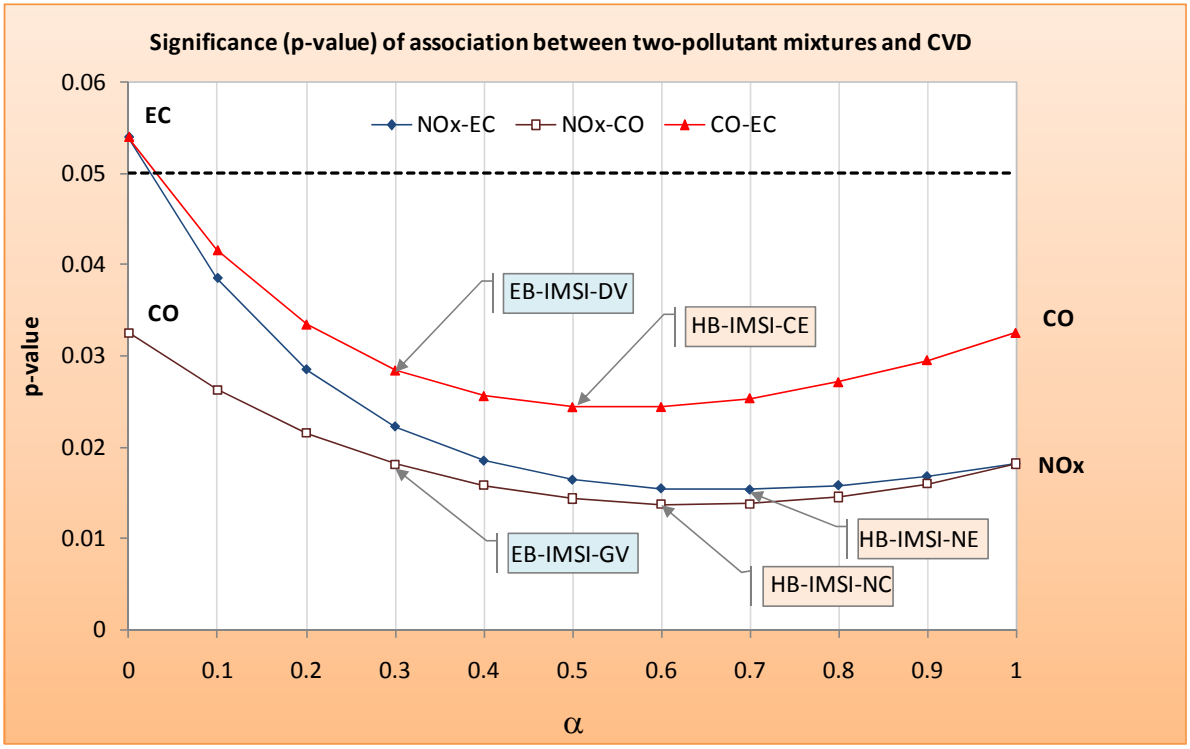

Figure 4.4 Sensitivity analysis of the association between pairs of pollutants and CVD outcomes; the dashed line represents p-value = 0.05.

The points where the association of the two-pollutant mixtures and CVD is strongest defined the health-based indicators. That is, we define HB-IMSI-NC at α=0.6 for NOx-CO, HB-IMSI-NE at α=0.7 for NOx-EC, and HB-IMSI-CE at α=0.5 for CO-EC. Pollutants used in the two-pollutant HB-IMSIs are denoted by a suffix, e.g., "-NE" for NOx and EC. The HB-IMSIs hold different fractions of pollutants than the EB-IMSIs, suggesting that other sources, besides traffic, may be contributing in the association with CVD though the p-values are relatively constant between the both integrated indicators. The advantage of using EB-IMSIs is that specific control mechanisms can be suggested to mobile sources facilitating the work of policy-makers.

The IMSIs and the two-pollutant mixtures showing different associations with CVD outcomes at different α values can be partially explained by the correlations between

individual pollutants and the two-pollutant mixture and more clearly by the spatial variability analysis.

With respect to the first explanation, the correlation of each pair of pollutants and the third pollutant not included in the pair changes with the α fraction (Figure 4.5). For example, the correlation between NOx-EC and CO has a maximum value at α=0.5 (R^2=0.63) which is larger than the correlation between CO-EC (R^2=0.49) or CO-NOx (R^2=0.55). Similarly, NOx-CO and CO-EC have stronger correlations with EC and NOx at α=0.4 and α=0.6 respectively.

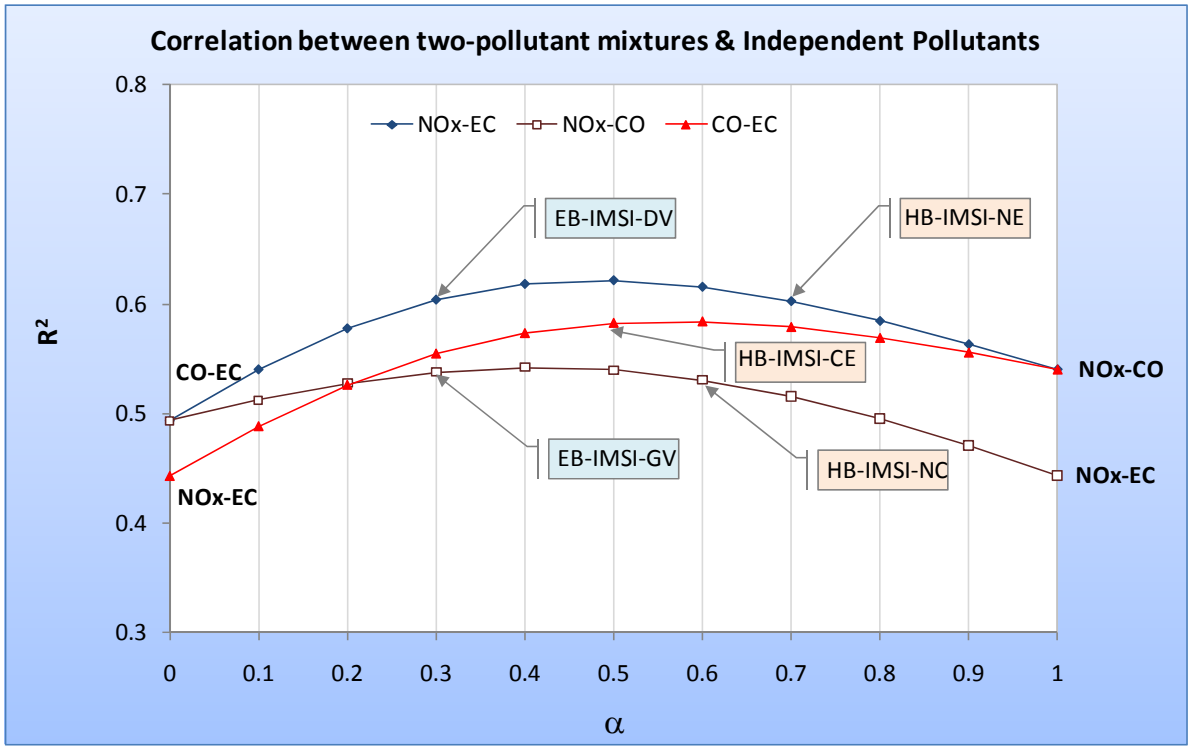

Figure 4.5 Correlation (R^2) between pair of pollutants and the third pollutant not included in the two-pollutant mixture (NOx-EC vs CO; NOx-CO vs EC; CO-EC vs NOx). Vertical scale starts at 0.3 to emphasize correlations.

A higher correlation of a pair of pollutants with a third pollutant more strongly associated with CVD, may explain the higher association of that pair with the health outcome. For example, the strongest association of CO-EC with CVD at α=0.5 (Figure 4.4) might be explained by the higher correlation of the CO-EC pair and NOx at that fraction (Figure 4.5). However, this is not the case for NOx-EC and NOx-CO pairs which already include the statistical power of NOx in the health association.

A more clear explanation can be found in the spatial variability analysis. We observe that the correlations between pairs of pollutants estimated at JST and the corresponding pairs calculated at SD are stronger at certain value of α than others (Figure 4.6). These values are α=0.5 for NOx-EC (R^2=0.72) and NOx-CO (R^2=0.72) and α=0.4 for CO-EC (R^2=0.76). The correlations between pair of pollutants at JST and SD are stronger than the correlations between single pollutants at both sites (R^2=0.64 for EC; R^2=0.55 for CO; R^2=0.59 for NOx) suggesting that mixtures of pollutants have a greater spatial representativeness than individual species. Previous studies have found that for pollutants with large spatial error, health associations are likely attenuated(Goldman et al., 2010). Pollutant mixtures having a more robust spatial representativeness than single pollutants may offer a better explanation of the stronger association with health.

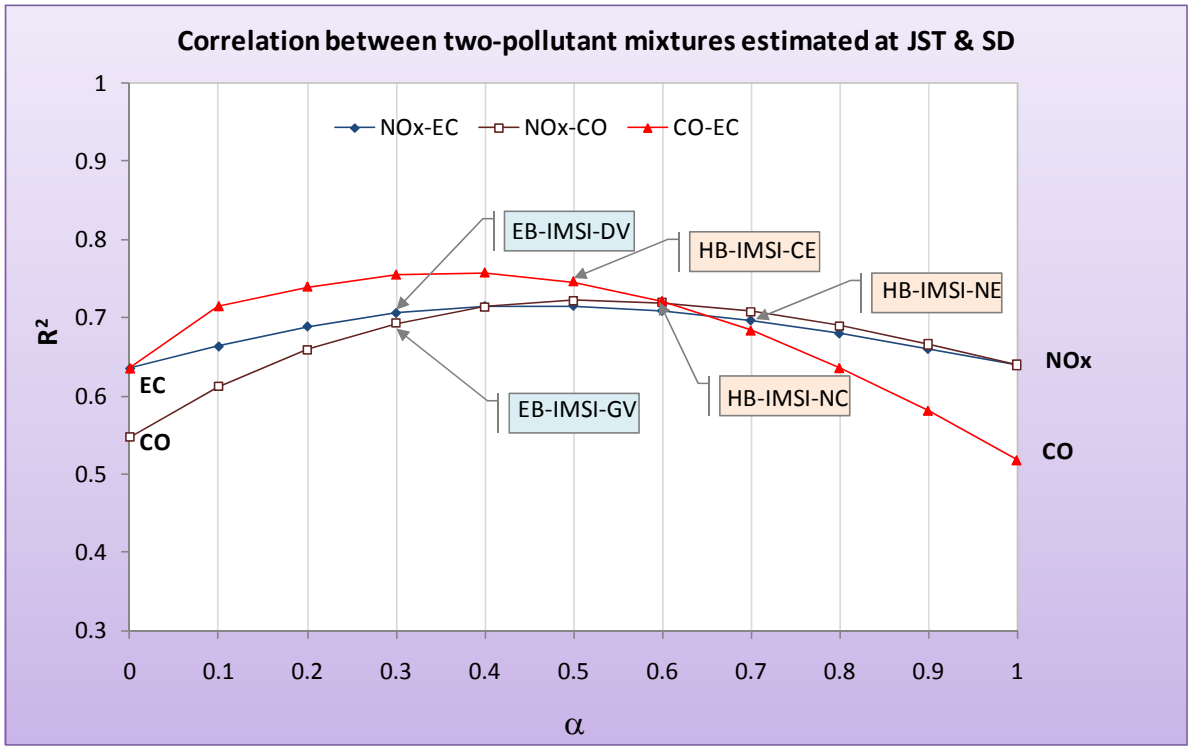

Figure 4.6 Correlation (R^2) between pair of pollutants calculated at JST and the corresponding pair estimated at SD. Vertical scale starts at 0.3 to emphasize correlations.

As a result of the greater spatial representativeness, EB-IMSI-GV and EB-IMSI-DV constitute better indicators for mobile sources which are expected to be ubiquitous in the area. This result complements a previous spatial analysis in which mobile source impacts were classified as having "intermediate" spatial representativeness of the Atlanta area due to the lack of a unique marker (EC was used as the only mobile tracer) (Marmur et al., 2006). Using EB-IMSIs, mobile source impacts show a more robust representativeness in the area.

Finally, the association of pollutant mixtures with health outcomes could be related to interaction between pollutants as has been shown in laboratory studies (Mauderly and Samet, 2009). This hypothesis needs further study.

4.7.5. Implications for multipollutant air quality standards

EB-IMSIs and HB-IMSIs can provide support to the setting of multipollutant air quality standards in a manner similar to that used in the development of the aquatic acidification index (AAI)(US-EPA, 2011) (Figure 4.7). The AAI was designed to take into account the combined effects of NOx and SOx in the acidification of aquatic ecosystems, given that these two species are linked from atmospheric chemistry. Similarly, HB-IMSIs assess the effects of mixtures of pollutants associated with mobile sources on health and EB-IMSIs assess mixtures representing the gasoline and diesel vehicle impacts on air quality. Since mobile sources and their composition are ubiquitous, it is expected that the integrated indicators can be applied in other cities. IMSIs are simple to construct and calculate and can be estimated at any monitoring site where EC, CO and NOx concentrations are available.

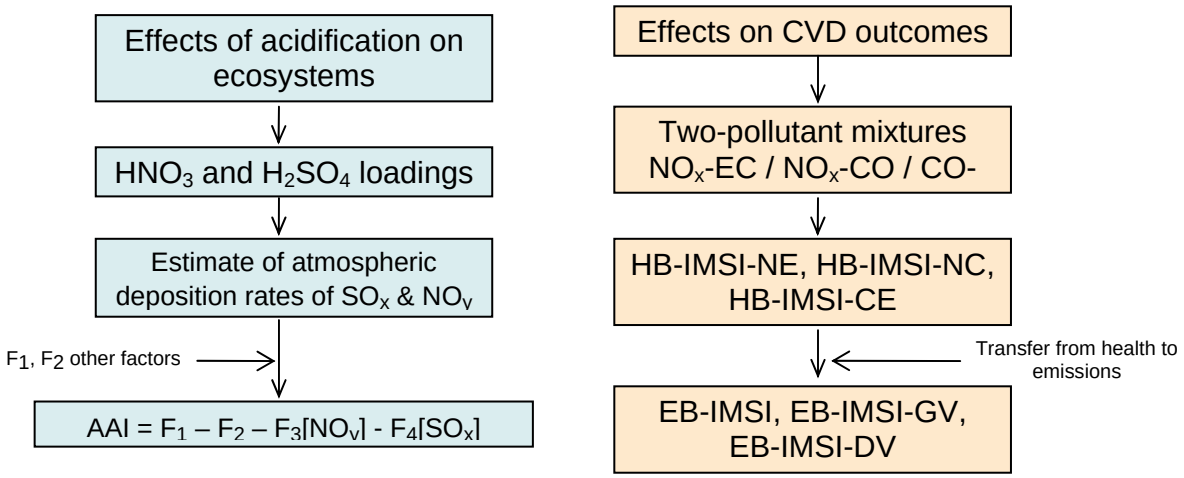

Figure 4.7 Analogy between the design of the AAI and IMSIs

4.8. References

Georgia Department of Natural Resources, 2007. Visibility Improvement State and Tribal Association of the Southeast (VISTAS) conceptual description support document.Asheville, NC.

Beelen, R., Hoek, G., van den Brandt, P. A., Goldbohm, R. A., Fischer, P., Schouten, L. J., Jerrett, M., Hughes, E., Armstrong, B. and Brunekreef, B., 2008. Long-term effects of traffic-related air pollution on mortality in a Dutch cohort (NLCS-AIR study). Environ Health Perspect 116, 196-202.

Bell, M. L., Cifuentes, L. A., Davis, D. L., Cushing, E., Gusman Telles, A. and Gouveia, N., 2011. Environmental health indicators and a case study of air pollution in Latin American cities. Environmental Research 111, 57-66.

Birch, M. E. and Cary, R. A., 1996. Elemental carbon-based method for monitoring occupational exposures to particulate diesel exhaust. Aerosol Science and Technology 25, 221-241.

Blanchard, C. L., Hidy, G. M., Tanenbaum, S., Rasmussen, R., Watkins, R. and Edgerton, E., 2010. NMOC, ozone, and organic aerosol in the southeastern United States, 1999-2007: 1. Spatial and temporal variations of NMOC concentrations and composition in Atlanta, Georgia. Atmospheric Environment 44, 4827-4839.

Brook, J. R., Burnett, R. T., Dann, T. F., Cakmak, S., Goldberg, M. S., Fan, X. and Wheeler, A. J., 2007. Further interpretation of the acute effect of nitrogen dioxide observed in Canadian time-series studies. J Expos Sci Environ Epidemiol 17, S36-S44.

Chow, J. C., Watson, J. G., Pritchett, L. C., Pierson, W. R., Frazier, C. A. and Purcell, R. G., 1993. The DRI thermal optical reflectance carbon analysis system - description, evaluation and applications in United-States air quality studies. Atmospheric Environment Part a-General Topics 27, 1185-1201.

Dominici, F., Peng, R. D., Barr, C. D. and Bell, M. L., 2010. Protecting human health from air pollution: shifting from a single-pollutant to a multipollutant approach. Epidemiology 21, 187-194

Edgerton, E. S., Hartsell, B. E., Saylor, R. D., Jansen, J. J., Hansen, D. A. and Hidy, G. M., 2005. The Southeastern aerosol research and characterization study: Part II. Filter-based measurements of fine and coarse particulate matter mass and composition. Journal of the Air & Waste Management Association 55, 1527-1542.

Espinosa, A., Miranda, J. and Pineda, J. C., 2010. Evaluation of uncertainty in correlated quantities: application to elemental analysis of atmospheric aerosols. Rev. Mex. Fis. E. 56, 134-140.

Franklin, M., Koutrakis, P. and Schwartz, P., 2008. The role of particle composition on the association between PM2.5 and mortality. Epidemiology 19, 680-689.

Goldman, G. T., Mulholland, J. A., Russell, A. G., Srivastava, A., Strickland, M. J., Klein, M., Waller, L. A., Tolbert, P. E. and Edgerton, E. S., 2010. Ambient air pollutant measurement error: characterization and impacts in a time-series epidemiologic study in Atlanta. Environmental Science & Technology 44, 7692-7698.

Hansen, D. A., Edgerton, E. S., Hartsell, B. E., Jansen, J. J., Kandasamy, N., Hidy, G. M. and Blanchard, C. L., 2003. The Southeastern aerosol research and characterization study: Part 1-overview. Journal of the Air & Waste Management Association 53, 1460-1471.

Hart, J. E., Garshick, E., Dockery, D. W., Smith, T. J., Ryan, L. and Laden, F., 2011. Long-term ambient multipollutant exposures and mortality. Am. J. Respir. Crit. Care Med. 183, 73-78.

Health Effects Institute, 2010. HEI Panel on the health effects of traffic-related air pollution. A critical review of the literature on emissions, exposure, and health effects. Boston, MA.

Hidy, G. M. and Pennell, W. T., 2010. Multipollutant air quality management. Journal of the Air & Waste Management Association 60, 645-674.

International Organization for Standardization, 1993. Guide to the expression of uncertainty in measurements, ISO, Geneva, Switzerland.

Kim, E., Hopke, P. K. and Edgerton, E. S., 2003. Source identification of Atlanta aerosol by positive matrix factorization. Journal of the Air & Waste Management Association 53, 731-739.

Kim, E., Hopke, P. K. and Edgerton, E. S., 2004. Improving source identification of Atlanta aerosol using temperature resolved carbon fractions in positive matrix factorization. Atmospheric Environment 38, 3349-3362.

Lee, S., Kim, H. K., Yan, B., Cobb, C. E., Hennigan, C., Nichols, S., Chamber, M., Edgerton, E. S., Jansen, J. J., Hu, Y., Zheng, M., Weber, R. J. and Russell, A. G., 2008a. Diagnosis of aged prescribed burning plumes impacting an urban area. Environmental Science & Technology 42, 1438-1444.

Lee, S., Liu, W., Wang, Y. H., Russell, A. G. and Edgerton, E. S., 2008b. Source apportionment of PM2.5: comparing PMF and CMB results for four ambient monitoring sites in the Southeastern United States. Atmospheric Environment 42, 4126-4137.

Lee, S. and Russell, A. G., 2007. Estimating uncertainties and uncertainty contributors of CMB PM2.5 source apportionment results. Atmospheric Environment 41, 9616-9624.

Lenters, V., Uiterwaal, C. S., Beelen, R., Bots, M. L., Fischer, P., Brunekreef, B. and Hoek, G., 2010. Long-term exposure to air pollution and vascular damage in young adults. Epidemiology 21, 512-520

Liu, W., Wang, Y. H., Russell, A. and Edgerton, E. S., 2005. Atmospheric aerosol over two urban-rural pairs in the southeastern United States: chemical composition and possible sources. Atmospheric Environment 39, 4453-4470.

Marmur, A., Park, S. K., Mulholland, J. A., Tolbert, P. E. and Russell, A. G., 2006. Source apportionment of PM2.5 in the southeastern United States using receptor and emissions-based models: Conceptual differences and implications for time-series health studies. Atmospheric Environment 40, 2533-2551.

Marmur, A., Unal, A., Mulholland, J. A. and Russell, A. G., 2005. Optimization-based source apportionment of PM2.5 incorporating gas-to-particle ratios. Environmental Science & Technology 39, 3245-3254.

Mauderly, J. L., Burnett, R. T., Castillejos, M., Özkaynak, H., Samet, J. M., Stieb, D. M., Vedal, S. and Wyzga, R. E., 2010. Is the air pollution health research community prepared to support a multipollutant air quality management framework? Inhalation Toxicology 22, 1-19.

Mauderly, J. L. and Samet, J. M., 2009. Is there evidence for synergy among air pollutants in causing health effects? Environ. Health Perspect. 117, 1-6.

Metzger, K. B., Tolbert, P. E., Klein, M., Peel, J. L., Flanders, W. D., Todd, K., Mulholland, J. A., Ryan, P. B. and Frumkin, H., 2004. Ambient air pollution and cardiovascular emergency department visits. Epidemiology 15, 46-56.

NARSTO, 2010. Technical challenges of multipollutant air quality management, Springer, Dordretch.

National Research Council, 2004. Air quality management in the United States, The National Academie Press, Washington DC.

Norris, G. and Vedantham, R., 2008. EPA Positive Matrix Factorization (PMF) 3.0. U.S. Environmental Protection Agency, Research Triangle Park, NC.

Pachon, J. E., Balachandran, S., Hu, Y., Weber, R. J., Mulholland, J. A. and Russell, A. G., 2010. Comparison of SOC estimates and uncertainties from aerosol chemical composition and gas phase data in Atlanta. Atmospheric Environment 44, 3907-3914.

Peng, R. D., Bell, M. L., Geyh, A. S., McDermott, A., Zeger, S. L., Samet, J. M. and Dominici, F., 2009. Emergency admissions for cardiovascular and respiratory

diseases and the chemical composition of fine particle air pollution. Environ. Health Perspect. 117, 957-963.

Qin, Y., Walk, T., Gary, R., Yao, X. and Elles, S., 2007. C2-C10 nonmethane hydrocarbons measured in Dallas, USA--Seasonal trends and diurnal characteristics. Atmospheric Environment 41, 6018-6032.

Reff, A., Eberly, S. I. and Bhave, P. V., 2007. Receptor modeling of ambient particulate matter data using Positive Matrix Factorization: review of existing methods. Journal of the Air & Waste Management Association 57, 146-154.

Sarnat, J. A., Marmur, A., Klein, M., Kim, E., Russell, A. G., Sarnat, S. E., Mulholland, J. A., Hopke, P. K. and Tolbert, P. E., 2008. Fine particle sources and cardiorespiratory morbidity: An application of chemical mass balance and factor analytical source-apportionment methods. Environ. Health Perspect. 116, 459-466.

Smith, L. A., Mukerjee, S., Chung, K. C. and Afghani, J., 2011. Spatial analysis and land use regression of VOCs and NO2 in Dallas, Texas during two seasons. J. Environ. Monit. 13, 999-1007.

Tonne, C., Melly, S., Mittleman, M., Coull, B., Goldberg, R. and Schwartz, J., 2007. A case-control analysis of exposure to traffic and acute myocardial infarction. Environ Health Perspect 115, 53-57.

Emission Standards Reference Guide. U.S. Environment Protection Agency.

U.S. Environmental Protection Agency, 2005. Acid rain program, 2004 progress report.Research Triangle Park, NC. EPA 430-R-05-012.

U.S. Environment Protection Agency, 2007a. 2002 National Emissions Inventoriy Data & documentation.

U.S. Environmental Protection Agency, 2007b. The Multi-pollutant report: technical concepts & examples.Research Triangle Park, NC.

U.S. Environmental Protection Agency, 2008. Analysis of particulate matter emissions from light-duty gasoline vehicles in Kansas city.Research Triangle Park, NC. EPA420-R-08-010.

U.S. Environmental Protection Agency, 2010. Motor Vehicle Emission Simulator (MOVES): user guide.Office of Transportation and Air Quality, Research Triangle Park, NC. EPA-420-B-09-041.

U.S. Environmental Protection Agency, 2011. Policy assessment for the review of the secondary National Ambient Air Quality Standards for oxides of nitrogen and oxides of sulfur.Research Triangle Park, NC. EPA-452/R-11-005a.

Vedal, S. and Kaufman, J. D., 2011. What does multi-pollutant air pollution research mean? Am. J. Respir. Crit. Care Med. 183, 4-6.

Watson, J. G., Cooper, J. A. and Huntzicker, J. J., 1984. The effective variance weighting for least-squares calculations applied to the mass balance receptor model. Atmospheric Environment 18, 1347-1355.

Zheng, M., Cass, G. R., Ke, L., Wang, F., Schauer, J. J., Edgerton, E. S. and Russell, A. G., 2007. Source apportionment of daily fine particulate matter at Jefferson street, Atlanta, GA, during summer and winter. Journal of the Air & Waste Management Association 57, 228-242.

Zheng, M., Cass, G. R., Schauer, J. J. and Edgerton, E. S., 2002. Source apportionment of PM2.5 in the Southeastern United States using solvent-extractable organic compounds as tracers. Environmental Science & Technology 36, 2361-2371.

CHAPTER 5 MOBILE SOURCE AIR QUALITY IMPACT INDICATOR SETS FOR POLICY UTILIZATION: EVALUATION AND UNCERTAINTIES

(Jorge E. Pachon, Marissa Maier, Sivaraman Balachandran, Yongtao Hu, James A. Mulholland, Jeremy A. Sarnat, Lyndsey A. Darrow, Armistead G. Russell. In preparation)

5.1. Abstract

The analysis of long-term emission trends and pollutant concentrations is used to develop relationships between traffic emissions and single and multipollutant indicators of mobile sources. Using concentration-response functions, a direct link between emissions and health outcomes is developed for single and multipollutant indicators and then is translated into health benefits using estimates of illness costs. The comparison of human health benefits (HHB) associated with CO versus NOx and EC suggests that emission controls on gasoline vehicles have been more effective to improve public health than emission controls on diesel vehicles. The evaluation of HHB using integrated indicators supports the previous finding. In addition, HHB estimated using integrated indicators were found more consistent than using single species, supporting our selection of multipollutants as better surrogates of mobile sources. A vehicular ozone indicator was developed from sensitivities of ozone to mobile NOx emissions in a chemical transport model. An inverse response of ozone concentrations to NOx emissions overall was found, which is expected for NOx-rich areas. Together, this information is grouped into indicator sets for use by policy-makers.

5.2. Introduction

Assessing the effectiveness of policies designed to reduce adverse outcomes of human activities is becoming increasingly central to environmental management. Quantitative evaluation of the steps in the air quality chain, from emission sources to ambient measurements to exposure and to health effects (i.e., the accountability paradigm), is an important task for policy makers in order to show that specific policy decisions have produced the desired benefits. However, the intended outcomes are not always quantifiable, or even observable. As a result of this limitation, surrogate measures of the environmental impacts are traditionally used as indicators of the range of outcomes experienced.

Environmental indicators, as defined by EPA, are numerical values whose time trends represent the condition of the environment on a particular geographic location (US-EPA, 2008). Bell et al. (2011) reviews environmental indicators related to human health at each step in the health system (i.e., from emissions through exposure and health endpoint), finding that indicators are useful for policy-makers and the general public to assess the state of the environment and the associated health and socio-economic impacts. The authors also note the limitations of environmental indicators such as the spatial and temporal representativeness of single pollutant indicators and the lack of consideration to the simultaneous exposure to multiple pollutants. Since impacts on the environment at times lead to impacts on human health, environmental indicators are often linked to health outcomes in the form of health outcome-based indicators. These indicators not only represent the state of the environment, but also describe their relationships to

particular health outcomes (US-EPA, 2006), facilitating the evaluation of public health policy effectiveness as result of improvement in environmental conditions

Associations between air pollutant exposures within a population and health effects are characterized using a range of epidemiologic approaches (Brook et al., 2010; Laden et al., 2006; Pope et al., 2002) and used in the development of policies aiming to reduce pollutant concentrations and improve public health. However, pollutants are emitted by multiple sources or formed in the atmosphere from primary precursors, and are differentially removed, obscuring the association of health outcomes with specific emission sources. To overcome this limitation, several epidemiologic studies have used results from source apportionment (SA) modeling (Laden et al., 2000; Mar et al., 2000; Sarnat et al., 2008). This approach has found that mobile sources, for example, are generally more associated with cardiovascular diseases than other primary sources (Sarnat et al., 2008).

The accountability in the air quality chain is conducted through the evaluation of environmental indicators at different stages in the link from air pollution sources to adverse health effects (Health Effects Institute, 2003). In order to evaluate how emission changes may impact health response, a two-step process is traditionally conducted. First, ambient concentrations are estimated from first principles using emission inventories, meteorology and photochemistry in chemical transport models (CTM), such as CMAQ. Second, data from CTMs is used in conjunction with concentration-response functions (CRF) from epidemiologic models to estimate how emission changes affect human health, such as in BenMAP (Davidson et al., 2007; Fann et al., 2011; Tagaris et al., 2009; Voorhees et al., 2011). This two-step process has been commonly applied for single

pollutants and more recently for multipollutants. Wesson et al. (2010) assessed and compared benefits from single and multipollutant control strategies and concluded greater health benefits from multipollutant controls. Their work, however, do not include multipollutant analysis at other steps in the air quality chain, for example, in the estimation of health-impact functions.

Ozone (O_3) is a secondary pollutant formed from volatile organic compounds (VOC) and NOx in the presence of sunlight. Automobiles have a marked impact on ozone because they emit a large fraction of both VOC and NOx emissions in urban areas. In Atlanta, for example, estimates suggest that 84% of the NOx and 36% of the anthropogenic VOCs are emitted by mobile sources (US-EPA, 2007). Understanding the impact of automobile emissions on O_3 is difficult, since other emission sources participate significantly in its formation (e.g., power plants and biogenic sources) and emissions can lead to a net formation or destruction of ozone under different meteorological conditions, emission densities and other factors (Chameides et al., 1988; Cohan et al., 2005; Lin et al., 1988).

One approach to determine the impact of vehicles on ozone is by quantifying the responsiveness or "sensitivities" of ozone to its precursors (e.g., NOx, VOCs) in CTMs (Hakami et al., 2004). The sensitivities represent how pollutant concentrations would respond to reductions in precursors if the system were linear, which is typically the case for emission reductions of 25-50% (Cohan et al., 2005). Using sensitivity analysis, Tian et al (2010) found that reductions in mobile on-road NOx emission would contribute most to corresponding decreases in Atlanta ozone concentrations, followed by reductions in mobile non-road and point NOx emissions. Further, Liao et al (2008) found that

sensitivities of ozone to NOx emissions are typically correlated with the corresponding ozone concentration.

In previous work, we discussed the use of EC, CO and NOx as indicators of mobile sources in Atlanta, observing that CO concentrations respond closely to the change in emissions of gasoline vehicles (GV); ambient EC had a relatively good response to the change in emissions of diesel vehicles (DV); and NOx was found an indicator of the overall fleet (GV+DV) (Pachon et al., 2011). That work also examined multispecies indicators finding that mixtures of CO and NOx were more spatially representative of the GV source impacts and mixtures of EC and NOx were more representative of DV source impacts than using single species. Those traffic emission indicator mixtures were also more strongly associated with cardiovascular diseases (CVD) in epidemiologic models than single species indicators, possibly be due to their greater spatial representativeness.

In the current analysis, we estimate HHB using single and multipollutant indicators of mobile sources in two steps. First, long-term relationships between ambient concentrations and emissions are examined to evaluate the response in single and multipollutant indicators as a result of the change in emissions (separate and integrated respectively). Such relationships are used along with CRF to estimate how emission changes may impact health response. For this analysis, CRF for multipollutant indicators were obtained using mixtures of pollutants in an epidemiologic model, providing a framework to evaluate multipollutants throughout the air quality chain. This is the first time, to our knowledge, that a comprehensive air quality analysis is conducted comparing single and multipollutant indicators.

Indicators sets for single and multipollutant indicators are presented to facilitate their application in air quality management. Indicator sets include not only indicator values and uncertainties, but also relationships between indicators at different stages, from emission to ambient concentrations to health outcomes. The attributes accompanied the indictor sets include type of information needed to estimate the indicator, ease of use, range of validity or appropriate references. The indicator sets are expected to be useful for policy makers who are interested not only in the value of the indicators, but also in their associated uncertainties and their applicability at other times and other regions.

5.3. Methods

Our previous work discussed indicator development strategies for single and multipollutant species, conducted health association modeling and sensitivity analysis, and explored the propagation of uncertainties from emissions and ambient concentrations in the indicators using data for Atlanta during 1999-2004 (Pachon et al., 2011). The proposed approach includes: i) the quantification of relationships between emissions and ambient concentrations using both single and multipollutant indicators of mobile sources in Atlanta; ii) an estimation of human health benefits associated with reductions in these single and multipollutant indicators, iii) the development of a vehicular ozone indicator, iv) the construction of indicator sets and v) the evaluation of uncertainties in different metrics.

5.3.1. Development of relationships between emission and ambient concentrations for single and multipollutant indicators of mobiles sources

The development of emission-based integrated mobile source indicators (EB-IMSI) builds on our previous work using ratios of mobile-source-to-total emissions as

weighting coefficients in the combinations of ambient EC, CO and NOx (Pachon et al., 2011).

$$EB-IMSI=\frac{\left(\frac{EC_{mob}}{EC_{tot}}\right)_{Emis}EC'+\left(\frac{NOx_{mob}}{NOx_{tot}}\right)_{Emis}NOx'+\left(\frac{CO_{mob}}{CO_{tot}}\right)_{Emis}CO'}{\left(\frac{EC_{mob}}{EC_{tot}}\right)_{Emis}+\left(\frac{NOx_{mob}}{NOx_{tot}}\right)_{Emis}+\left(\frac{CO_{mob}}{CO_{tot}}\right)_{Emis}} \quad (5.1)$$

$$EB-IMSI_{GV}=\frac{\left(\frac{NOx_{GV}}{NOx_{tot}}\right)_{Emis}NOx'+\left(\frac{CO_{GV}}{CO_{tot}}\right)_{Emis}CO'}{\left(\frac{NOx_{GV}}{NOx_{tot}}\right)_{Emis}+\left(\frac{CO_{GV}}{CO_{tot}}\right)_{Emis}} \quad (5.2)$$

$$EB-IMSI_{DV}=\frac{\left(\frac{EC_{DV}}{EC_{tot}}\right)_{Emis}EC'+\left(\frac{NOx_{DV}}{NOx_{tot}}\right)_{Emis}NOx'}{\left(\frac{EC_{DV}}{EC_{tot}}\right)_{Emis}+\left(\frac{NOx_{DV}}{NOx_{tot}}\right)_{Emis}} \quad (5.3)$$

where EC′, CO′ and NOx′ are scaled concentrations (divided by the standard deviation). For the period 1999-2004, normalized values of IMSI were: EB-IMSI: 3.58 ± 1.38, EB-IMSI-GV: 1.81 ± 0.42 and EB-IMSI-DV: 1.52 ± 0.67.

The rate of change in pollutant concentrations as a result of the change in emissions is estimated as the regression slope between long-term concentrations and emissions for EC, CO and NOx ('m'). Estimated emissions are normalized by the area of the city (i.e., Fulton County in Atlanta or 210 km^2) to facilitate comparison with other cities. To evaluate a relationship between emissions and multipollutant indicators, mobile emissions of EC, CO and NOx are integrated using a similar approach in the construction of EB-IMSI (Equations 5.1-5.3).

$$IMSE = CO_{mob} + NOx_{mob} + EC_{mob} \tag{5.4}$$

$$IMSE - GV = \left(\frac{CO_{GV}}{CO_{mob}}\right) * CO_{mob} + \left(\frac{NOx_{GV}}{NOx_{mob}}\right) * NOx_{mob} + \left(\frac{EC_{GV}}{EC_{mob}}\right) * EC_{mob} \tag{5.5}$$

$$IMSE - DV = \left(\frac{CO_{DV}}{CO_{mob}}\right) * CO_{mob} + \left(\frac{NOx_{DV}}{NOx_{mob}}\right) * NOx_{mob} + \left(\frac{EC_{DV}}{EC_{mob}}\right) * EC_{mob} \tag{5.6}$$

The rate of change in integrated mobile source emissions (IMSE) is regressed against the rate of change in ambient values of EB-IMSIs.

5.3.2. Estimation of human health benefits using single and multipollutant indicators in Atlanta

From previous work, we have obtained the CVD-ED risk per change of pollutant concentrations (EC, CO, NOx) and multipollutant indicators (EB-IMSI) in Atlanta during 1999-2004 (Pachon et al., 2011). This concentration-response function (β) along with the concentration-emission relationship, '*m*', is used to model the influence of changing emissions and corresponding incidences on adverse health impacts (here called 'h'):

$$h\left(\frac{risk}{emissions}\right) = \beta\left(\frac{risk}{conc}\right) * m\left(\frac{conc}{emissions}\right) \tag{5.7}$$

where 'risk' is a unitless variable. The evaluation of the uncertainty in this metric is conducted using propagation of errors, assuming that β and *m* are uncorrelated, which is strongly likely to be the case because β and *m* are the result of different health and emission analyses.

$$\sigma_h^2 = \beta^2\sigma_m^2 + m^2\sigma_\beta^2 \tag{5.8}$$

where σ_m is the uncertainty in the relationship between ambient concentrations and emissions obtained from the slope standard error of the regression and σ_β is the uncertainty in the risk signal obtained from the standard error in the epidemiologic model.

Estimates of HHB are expressed as the number of CVD-ED visits avoided per year during 1999-2004 as a result of reductions in mobile source emissions of EC, CO and NOx. The HHB is estimated as the product of 'h' $(ton/yr)^{-1}$ and emission reduction $\Delta E = (E_{1999} - E_{2004})/6$ from 1999 to 2004 in ton/yr.

$$HHB = h\left(\frac{risk}{ton/yr}\right) * \Delta E\left(\frac{ton}{yr}\right) * 25{,}000\frac{visits}{yr} \tag{5.9}$$

The factor 25,000 accounts for the average number of CVD-ED visits per year in Atlanta during 1999-2004 (Tolbert et al., 2007). The uncertainty in HHB can be expressed as follows.

$$\sigma_{HHB} = 25{,}000 * \sqrt{h^2 * \sigma_{\Delta E}^2 + \Delta E^2 * \sigma_h^2} \tag{5.10}$$

where σ_h is the uncertainty obtained from Equation 5.8 and $\sigma_{\Delta E}$ is the uncertainty in reduction of emissions $\sigma_{\Delta E} = \sqrt{\sigma_{E1999}^2 + \sigma_{E2004}^2}/6$.

The annual savings in costs of HHB (S) can then be estimated applying the typical cost of treating one CVD visit. Our calculations are based on the cost of illness (COI) for CVD provided by EPA (2004), which considers only direct expenditures (costs of treating or mitigating the health effect) and not the value of avoided pain and suffering or

premature mortality, which are considered in more comprehensive cost-benefit analyses of air pollution.

$$S\left(\frac{\$}{yr}\right) = HHB\left(\frac{visits}{yr}\right) * COI(\$) \qquad (5.11)$$

with respective uncertainty estimated as $\sigma_S = COI * \sigma_{HHB}$.

5.3.3. Development of the vehicular ozone indicator

Ozone concentrations typically do not have a linear response to the change in precursor emissions as described for EC, CO and NOx. Therefore, the estimation of a concentration-emission relationship for ozone is not feasible using the same approach (i.e., long-term analysis of concentrations and emissions). The use of sensitivities from CTMs can be used to assess such relationship. Sensitivities in CTMs are defined as the rate of change in ambient concentrations as a result of the perturbation in model parameters (Dunker, 1981; Hakami et al., 2003). The first-order sensitivity ($S_{i,j}$) of pollutant concentration *i* (C_i) to source emissions *j* (E_j) is calculated as (Hakami et al., 2003):

$$S_{ij} = E_j \frac{\partial C_i}{\partial E_j} \qquad (5.12)$$

Liao et al (2008) calculated first-order sensitivities of daily maximum 8-h ozone concentrations to anthropogenic NOx ($S_{MDA8hO3,ANOx}$) and VOC ($S_{MDA8hO3,AVOC}$) for Atlanta during 2001. The $S_{MDA8hO3,ANOx}$ was found linearly correlated with ozone concentrations.

$$S_{MDA8hO3,ANOx} = \left[a + b * O_3\right] \quad (5.13)$$

The sensitivity of ozone to mobile NOx can be estimate from the previous relationship and using the ratio between mobile-source-to-total NOx emissions.

$$S_{MDA8hO3,mobNOx} = \left(\frac{NOx_{mob}}{NOx_{tot}}\right)_{Emis} * S_{MDA8hO3,ANOx} \quad (5.14)$$

The sensitivities of ozone to NOx are significantly greater in magnitude to the sensitivities of ozone to anthropogenic VOCs, due to higher biogenic VOC emissions and subsequently lower sensitivity of ozone to anthropogenic VOC emissions (Tian et al., 2010). Furthermore, sensitivities of ozone to anthropogenic VOCs do not exhibit a linear relationship with ozone concentrations. Therefore, in this work the vehicular ozone indicator (VOI) corresponds to the sensitivity of ozone to mobile NOx emissions plus a fixed value of the sensitivity of ozone to anthropogenic VOCs.

5.3.4. Construction of indicator sets

Indicators sets for single and multipollutant indicators are presented to facilitate their application in air quality management. Indicator sets include not only indicator values and uncertainties, but also relationships between indicators at different stages of the air quality chain, from emission to ambient concentrations to health outcomes (Fig. 5.1). The attributes accompanied the indictor sets include type of information needed to estimate the indicator, ease of use, range of validity or appropriate references. The indicator sets are expected to be useful for policy makers who are interested not only in the value of the

indicator, but also in their associated uncertainties and their applicability at other times and other regions.

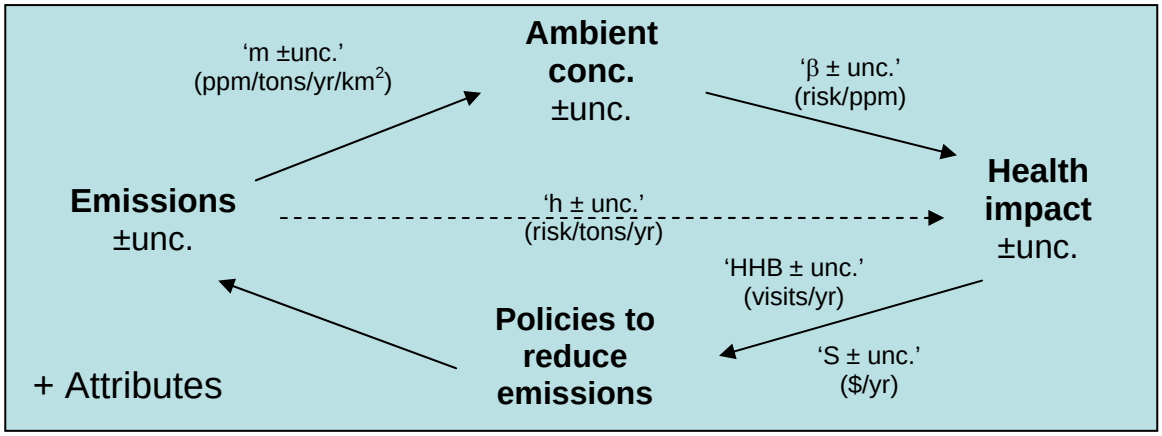

Figure 5.1 Conceptual framework of Indicator Sets

Indicator sets, as opposite to single indicators, provides a framework to assess policy effectiveness throughout the air quality chain. It is applicable to both single and multipollutant indicators, since information at every step is available from this and previous work (Pachon et al., 2011).

5.3.5. Estimation of uncertainties

Uncertainties in the indicator sets are estimated at every step of the air quality chain: from emission sources to ambient measurements to exposure and to health effects. Although comparison of uncertainties is complicated since they were obtained from different approaches, an assessment of relative uncertainties (uncertainty/indicator value) offers some insights. To facilitate the comparison, uncertainties are assessed in five different groups: emissions, emission-concentration response functions, ambient concentrations, HHB and receptor models.

5.3.6. Air quality and emissions data

Single and multipollutant indicators were developed for Atlanta during the period 1999-2004 in previous work. This study expands the indicators throughout 2007 using air quality data from the Jefferson Street site (JST), a highly-instrumented monitoring site near downtown and part of the SEARCH project (located at 33.8 degrees North and -84.4 degrees West). Description of the measurement methods is found elsewhere (Edgerton et al., 2005; Hansen et al., 2003). Briefly, elemental carbon (EC) is measured on 24-hour $PM_{2.5}$ samples using quartz filters from a particle composition monitor (PCM) and analyzed by the thermal-optical reflectance (TOR) method at the Desert Research Institute (DRI) following the Interagency Monitoring of Protected Visual Environments (IMPROVE) protocol (Chow et al., 1993). CO, NO and NO_2 are measured every minute and averaged to the hour. CO is measured using non-dispersive infrared spectrophotometry. NO_2 is measured via photolytic conversion to NO, followed by chemiluminescence. NO and NO_2 are summed and reported as NOx. O_3 is measured using UV-absorption.

Emissions from mobile sources were estimated in Atlanta using the EPA-MOVES 2010 model (US-EPA, 2010). Nationwide vehicle information was used to determine emissions for GV and DV from 2005 to 2007 for Fulton County in Georgia. Emissions of EC, NOx and CO for other sources were obtained from the Visibility Improvement State and Tribal Association of the Southeast (VISTAS) project (Air Resources Specialists, 2007).

5.4. Results

Results are presented in the development of long-term relationships between ambient concentrations and emissions for single and multipollutant indicators of mobiles sources, the estimation of human health benefits of emission controls, the development of indicator sets and uncertainties, and the vehicular fraction of the ozone.

5.4.1. Development of relationships between ambient concentrations and emissions for single and multipollutant indicators of mobiles sources

Ambient concentrations of CO, NOx and EC are plotted versus CO, NOx and EC emissions respectively in Atlanta from 1999 to 2007 observing high correlation coefficients (R^2=0.94 for CO, R^2=0.68 for NOx, R^2=0.60 for EC) (Fig. 5.2). Concentration-emission regression slopes are statistically significant at the 95% confidence interval (CI), but regression intercepts are not. The rate of change in ambient concentrations of CO as a result of change in CO emissions is 1.51 ± 0.17 ppm/10^3 tons/yr/km^2, which is equivalent to $7.2 \times 10^{-6} \pm 8.1 \times 10^{-7}$ ppm/(ton/yr) when de-normalized by the area of Fulton County. For NOx, the rate of change in ambient concentrations as a result of change in emissions is 0.54 ± 0.14 ppm/10^3 tons/yr/km^2 ($2.6 \times 10^{-6} \pm 6.7 \times 10^{-7}$ ppm/ton/yr). The rate of change in ambient CO is greater than the rate of change in ambient NOx as a result of change in emissions, which is explained by higher CO concentrations in the atmosphere than NOx (1.05ppm CO and 0.11ppm NOx averages during 1999-2007).

The rate of change in ambient concentrations of EC as a result of change in EC emissions is 1.04 ± 0.32 (μg/m^3)/(tons/yr/km^2), which is equivalent to $5.9 \times 10^{-3} \pm 1.5 \times 10^{-3}$

($\mu g/m^3$)/(ton/yr). The relative uncertainty (uncertainty/slope) of the regression slopes is larger for EC and NOx (approx. 30%) than CO (10%).

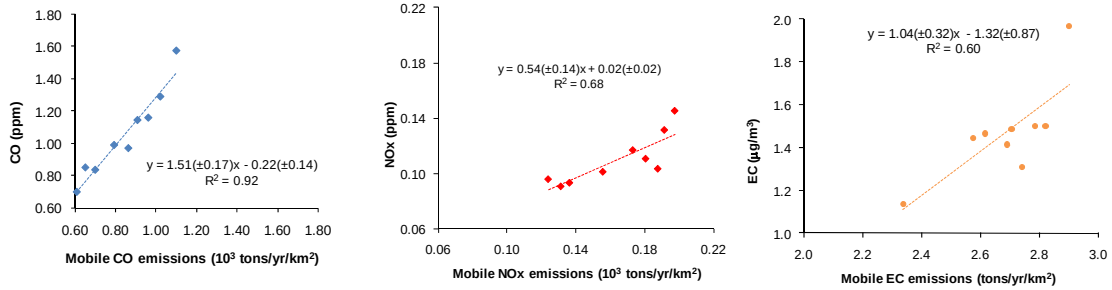

Figure 5.2 Ambient pollutants vs. emissions in Atlanta for 1999-2007

Estimated EB-IMSIs (Equations 5.1-5.3) are plotted versus IMSEs (Equations 5.4-5.6) for Atlanta (Fig. 5.3). Significant correlations are observed for the three integrated indicators, with concentration-emission regression slopes statistically significant at the 95% CI, buy intercepts not significant (i.e., not different than zero).

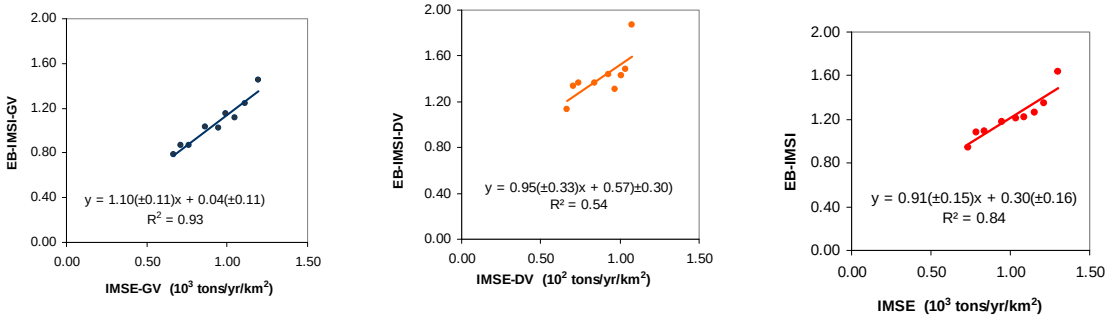

Figure 5.3 Ambient multipollutants vs. integrated emissions in Atlanta during 1999-2007 period.

The rates of change in ambient concentrations of EB-IMSIs as a result of change in IMSEs, after de-normalizing by the area, are: $4.36x10^{-6}\pm7.1x10^{-7}$ EB-IMSI/(ton/yr), $5.2x10^{-6}\pm5.2x10^{-7}$ EB-IMSI-GV/(ton/yr), $4.5x10^{-5}\pm1.6x10^{-5}$ EB-IMSI-DV/(ton/yr), which denotes a larger response in EB-IMSI-DV per ton of integrated pollutants reduced than EB-IMSI and EB-IMSI-GV. The similarity in the rate of changes for EB-IMSI and EB-IMSI-GV is explained by the weight of CO and NOx in both indicators and suggests that most of the vehicles source impacts are from GV.

The relative uncertainties in the regression slopes are about 20% for EB-IMSI, 10% for EB-IMSI-GV and 30% for EB-IMSI-DV.

5.4.2. Human health benefits of emission controls using single and multipollutant indicators of mobile sources

The changes in incidences on adverse cardiovascular impacts associated with the increase in mobile emissions 'h' $(ton/yr)^{-1}$ is substantially larger for EC than CO or NOx (Table 5.1), due to the greater health signal per $\mu g/m^3$ (β) observed for EC compared to that for CO ($7.41x10^{-6}$ $(\mu g/m^3)^{-1}$) or NOx ($6.1x10^{-5}$ $(\mu g/m^3)^{-1}$), though signal for EC was borderline significant at the 95% CI (Table 5.1).

The savings in costs of CVD visits avoided per ton of pollutant reduced (S') ($/ton) is the largest for EC. Fann et al. (2009) also found larger health benefits ($/ton) in the reduction of directly emitted carbonaceous particles over gases (NOx, NH_3, SOx and VOC) in the US. They suggested that particles are more stable in the atmosphere and emitted more closely to the population than gases, resulting in larger health effects.

Table 5.1 Savings in CVD visits avoided by reduction in emissions of CO, NOx and EC in Atlanta

	CO	**NOx**	**EC**
β estimate for CVD outcomes (p-value)	0.0085 ± 0.004 ppm^{-1} (0.033)	0.095 ± 0.04 ppm^{-1} (0.018)	0.0078 ± 0.004 $(ug/m^3)^{-1}$ (0.054)
Rate of change in ambient conc. to change in emissions 'm'	$7.2x10^{-6} \pm 8.1x10^{-7}$ (ppm/ton/yr)	$2.6x10^{-6} \pm 6.7x10^{-7}$ (ppm/ton/yr)	$5.0x10^{-3} \pm 1.5x10^{-3}$ $(\mu g/m^3)/(ton/yr)$
Risk per ton of emission 'h' $(ton/yr)^{-1}$	$6.1x10^{-8} \pm 2.9x10^{-8}$	$2.4x10^{-7} \pm 1.2x10^{-7}$	$3.9x10^{-5} \pm 2.3x10^{-5}$
Average emission reduction 1999-2004 (ton/yr)	$10,690 \pm 5,000$ $(5.4\%)^{\&}$	$1,450 \pm 330$ $(3.8\%)^{\&}$	7.3 ± 4.7 $(1.3\%)^{\&}$
HHB (CVD-ED visits avoided/yr) from 1999-2004	16 (5-27)	9 (4-14)	7 (1-13)
Annual savings in costs of CVD visits avoided from 1999-2004 'S' (million $)	0.30 (0.10-0.50)	0.16 (0.07-0.25)	0.13 (0.02-0.24)
Savings in CVD per ton of emissions (S') ($/ton)	28 (15-41)	112 (56-168)	17,800 (7200-28400)

* Cost of Illness (COI) for all-cardiovascular diseases estimated at $18,387 per unit (US-EPA, 2004) $^{\&}$ (percentage with respect to average emissions during 1999-2007)

However, reduction in emissions of EC (average of 8 tons/yr from 1999-2004) is much less than the reduction in emissions of CO and NOx (averages of 10,000 tons/yr and 1,500 tons/yr from 1999-2004 respectively). When this reduction in emissions is taken into account, the number of CVD visits saved per year (HHB) and the respective annual savings (S) are larger for CO than NOx or EC. The largest HHB for CO is explained by the greater reduction in emissions of CO in comparison of NOx and EC. Given that CO was found to be a good indicator of GV impacts, the HHB associated with CO can be interpreted as result of the controls in GV emission from 1999-2004. Similar

analysis for DV impacts is difficult since EC was not found a robust indicator of DV and NOx is significantly emitted by both GV and DV in Atlanta. With these limitations, the HHB associated with NOx and EC are similar in magnitude and can be partially explained by the controls in DV emissions from 1999-2004.

The comparison of HHB among pollutants suggest that emission reductions in CO, likely explained by emission controls on GV, have been more effective for improving public health than emission reductions in NOx or EC, partially explained by emission controls on DV. However, improvements in public health should consider further reductions in NOx and EC emissions, and therefore controls on DV, since health benefits per ton of emission are much larger for these two pollutants than for CO.

The CVD risk associated with the increase in IMSE 'h' $(ton/yr)^{-1}$ is larger for IMSE-DV than IMSE-GV or IMSE (Table 5.2) because the EB-IMSI-DV has a larger health signal per unit of IMSI (β) than EB-IMSI and EB-IMSI-GV. The association of EB-IMSIs and CVD outcomes is statistically significant in all cases (p-value<0.05). Integrated emission reductions from 1999-2004 are larger for EB-IMSI and EB-IMSI-GV than EB-IMSI-DV, because the first two indicators include reductions of CO, which are larger than reductions in NOx or EC (Table 5.1). Nonetheless, reductions in integrated emissions are between 5-6% of their average emission for the integrated indicators, a range that is smaller than the range of reductions for single pollutants (1-6%).

Table 5.2 Savings in CVD visits avoided by reduction in integrated emissions and assessed through EB-IMSI

	EB-IMSI	**EB-IMSI-GV**	**EB-IMSI-DV**
β estimate for CVD outcomes (p-value)	0.0103 ± 0.0048 (0.029)	0.0088 ± 0.0042 (0.018)	0.0115 ± 0.0054 (0.022)
Rate of change in ambient conc. to change in emissions 'm' (IMSI/ton/yr)	$4.3x10^{-6} \pm 7.1x10^{-7}$	$5.2x10^{-6} \pm 5.2x10^{-7}$	$4.5x10^{-5} \pm 1.6x10^{-5}$
Risk per ton of emission 'h' $(ton/yr)^{-1}$	$4.5x10^{-8} \pm 2.2x10^{-8}$	$4.6x10^{-8} \pm 2.3x10^{-8}$	$5.2x10^{-7} \pm 3.0x10^{-7}$
Average emission reduction 1999-2004 (ton/yr)	12,150 ± 5,000 (6.0%)[&]	11,300 ± 5,000 (4.5%)[&]	830 ± 170 (6.0%)[&]
HHB (CVD-ED visits avoided/yr) from 1999-2004	14 (5-23)	13 (4-22)	11 (4-18)
Annual savings in costs of CVD visits avoided from 1999-2004 'S' (million $)	0.25 (0.09-0.41)	0.24 (0.08-0.40)	0.20 (0.08-0.32)
Savings in CVD per ton of emissions (S') ($/ton)	21 (11-31)	21 (11-31)	240 (100-380)

* Cost of Illness (COI) for all-cardiovascular diseases estimated at $18,387 per unit (US-EPA, 2004)

Using the integrated indicators, the calculated human health benefits (HHB) during 1999-2004 vary between 11 and 14 visits avoided per year, equivalent to $0.20-0.25 million annually, as a result of reductions in mobile source emissions (Table 5.2). EB-IMSI, as an indicator of the overall fleet, has a larger HHB than EB-IMSI-GV or EB-IMSI-DV. Although, integrated emissions for EB-IMSI are the sum of the integrated emissions for EB-IMSI-GV and EB-IMSI-DV (Equations 5.4-5.6), the HHB are not

expected to be additive, since the health response of EB-IMSI is not the sum of health signals for EB-IMSI-GV and EB-IMSI-DV.

Similar to the analysis using single species, the calculated HHB associated with the reduction in GV emissions were observed to be greater than the benefits accrued from reducing DV emissions. Using CO finds similar results than using EB-IMSI-GV (5-27 vs. 4-22 avoided CVD visits per year respectively). The slightly smaller HHB using EB-IMSI-GV is explained by the presence of NOx in the integrated indicator leading to a lower value of 'h' in comparison to CO alone. Previously, we have suggested EB-IMSI-GV as a better indicator of GV than CO, based on a larger spatial representativeness of EB-IMSI-GV that is consistent with emissions from GV spread around the metro Atlanta area (Pachon et al., 2011).

On the other hand, using EC resulted in less HHB than using EB-IMSI-DV as indicator of DV impacts (1-13 vs. 4-18 avoided CVD visits per year respectively). The larger HHB using EB-IMSI-DV is explained by the presence of NOx in the integrated indicator leading to greater average emission reductions from 1999-2004, even though the value of 'h' is substantially smaller for EB-IMSI-DV than EC. Similarly to EB-IMSI-GV, our previous work suggested EB-IMSI-DV as a better indicator of DV than EC, based on a larger spatial representativeness of EB-IMSI-DV (Pachon et al., 2011). Additionally, while the association of EC with CVD outcomes was only border line significant, EB-IMSI-DV was found significantly associated with CVD outcomes in an epidemiologic model.

NOx has been suggested as an indicator of mobile sources, without distinction between GV and DV, and it has been used to study associations between mobile source

impacts and cardio-vascular health in several studies (Brook et al., 2007; Burnett et al., 2004; Metzger et al., 2004). In previous work, we found NOx as the species most significantly associated with CVD outcomes, probably due to its larger spatial representativeness over CO and EC (Pachon et al., 2011). The calculation of HHB using NOx resulted in less number of CVD visits avoided than EB-IMSI (4-14 vs. 5-23). The larger HHB using EB-IMSI is explained by the presence of CO in the integrated indicator leading to greater average emission reductions from 1999-2004, even though the value of 'β' is substantially smaller for EB-IMSI than NOx.

5.4.3. Vehicular ozone indicator (VOI)

The daily maximum 8h O_3 concentration has decreased in Atlanta from 47 ppbv to 40 ppbv (i.e., 15% reduction) from 1999-2004, largely due to regional NOx reductions and lowering VOC levels from point sources. An estimate of 8.6±2.5 ppbv of ozone is attributed to mobile NOx (Tian et al., 2010). From the 2002 National Emission Inventory (US-EPA, 2007) a ratio of mobile-source-to-total NOx emissions of 0.84 is obtained and used to estimate the sensitivity of ozone to mobile NOx (Equation 5.14), which shows a linear correlation with ozone concentrations with a high regression coefficient and statistically significant slope and intercept (Figure 5.4). Sensitivities of ozone to mobile NOx are positive (i.e., reductions in mobile NOx decreases ozone) for estimated ozone concentrations greater than 50 ppbv, and likewise, sensitivities are negative (i.e., reduction in mobile NOx increase ozone) when estimated peak 8-hr ozone is below 50 ppbv, typically during winter months.

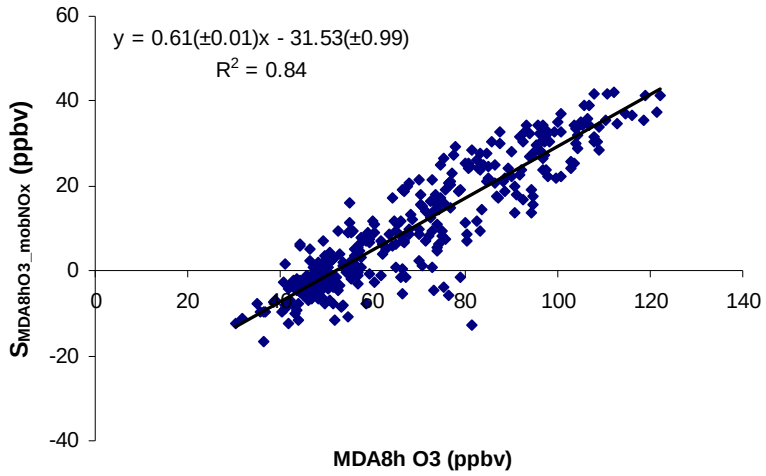

Figure 5.4 Sensitivity of daily maximum 8-h O3 to mobile NOx in downtown Atlanta during 2001 from Liao et al. (2008)

Using the linear relationship with ozone developed for 2001, the VOI is estimated for the period 1999-2004 from observed O_3 concentrations from the JST site. The estimated sensitivities are negative because annual average observed ozone concentrations are below 43 ppbv, though during the summer they are higher (56 ppbv). Negative sensitivities in NOx-rich areas, such as downtown Atlanta, are observed in several studies (Dunker et al., 2002; Hu et al., 2006; Mendoza-Dominguez et al., 2000; Xiao et al., 2010).

Mobile sources also emit VOCs to the atmosphere. From the NEI, the ratio of mobile-source-to-total VOC emissions is 0.38. However, sensitivity of ozone to VOCs does not exhibit a linear relationship with ozone concentrations as the one observed for NOx. Therefore, the impact of VOC emissions from mobile sources to ozone is estimated as the product of 0.38 (mobile-source-to-total VOC emissions ratio) and 3.22 ppbv (average sensitivity of ozone to VOCs). The result of 1.22 ppbv does not depend on the ozone concentration, unlike NOx.

The average VOI from 1999-2004 is 7.14 ppv O_3, which resulted from the sum of 5.85 ppbv O_3 (based on sensitivities of O_3 to mobile NOx) and 1.22 ppbv O_3 (based on sensitivities of O_3 to mobile VOCs). Uncertainties in the VOI have been estimated as 29%, based on uncertainties in sensitivities of ozone to mobile NOx in Atlanta (Tian et al., 2010). In this work, uncertainty in the average VOI is estimated as 2.07 ppbv.

5.4.4. Construction of Indicator sets

Indicator sets include not only indicator values and uncertainties, but also relationships between indicators at different stages of the air quality chain, from emission to ambient concentrations to health outcomes, in order to facilitate their application in air quality management. An example of indicator sets for NOx (Fig. 5.5) and EB-IMSI (Fig. 5.6) is discussed in this section that can be expanded to a more comprehensive list of indicators developed throughout this project (Table 5.3).

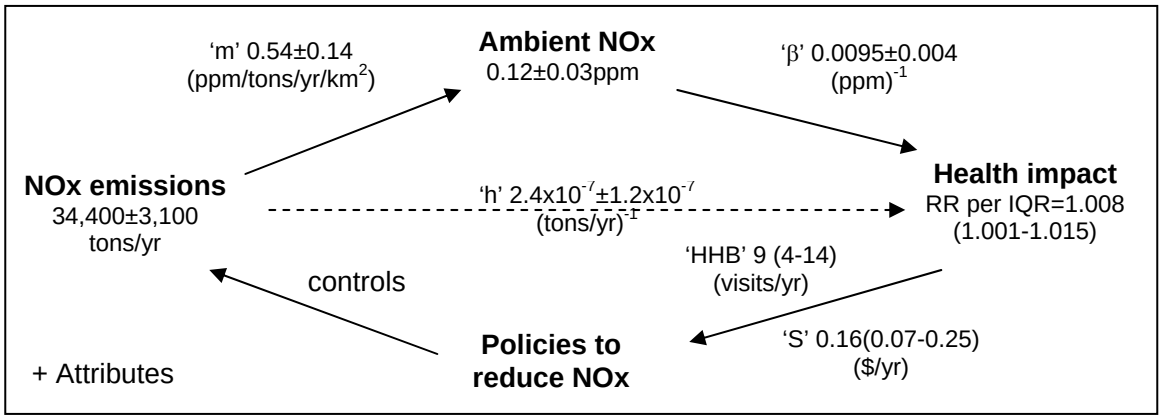

Figure 5.5 Framework of Indicator set for NOx

The indicator set for NOx is comprised of individual indicators and the relationships among them. For this study, long-term NOx emissions is an indicator of effectiveness of policies to reduce NOx from mobile sources; ambient NOx is an indicator of mobile

source impacts on air quality; the association of NOx with CVD outcomes (quantified as the RR per IQR) is an indicator of the impact of mobile source activity on cardiovascular health. The slope in the linear regression between NOx emissions and concentrations is denoted as 'm' and represents the change in NOx as a result of the change in NOx emissions from mobile sources. The use of NOx in an epidemiologic model provides a relationship between changes in NOx concentrations and changes in the incidence of adverse CVD impacts, denoted as 'β'. The 'm' and 'β' ratios are used to find the response in the incidence of adverse CVD impacts as a result of change in NOx emissions from mobile sources 'h'. The reduction in mobile source emissions in Atlanta from 1999-2004 is used along with 'h' to estimate the number of CVD visits avoided per year (HHB) and the respective savings in costs of those visits (S).

The HHB and savings are of utility for policy-makers in the setting of cost-benefits analysis of air pollution reduction. Emission controls for mobile sources and the respective costs are drawn in the indicator sets framework, but their quantification are beyond the scope of this study. The attributes in the indicator set for NOx includes information, range of validity or appropriate references to estimate each one of the individual indicators and the described relationships among them (Table 5.3).

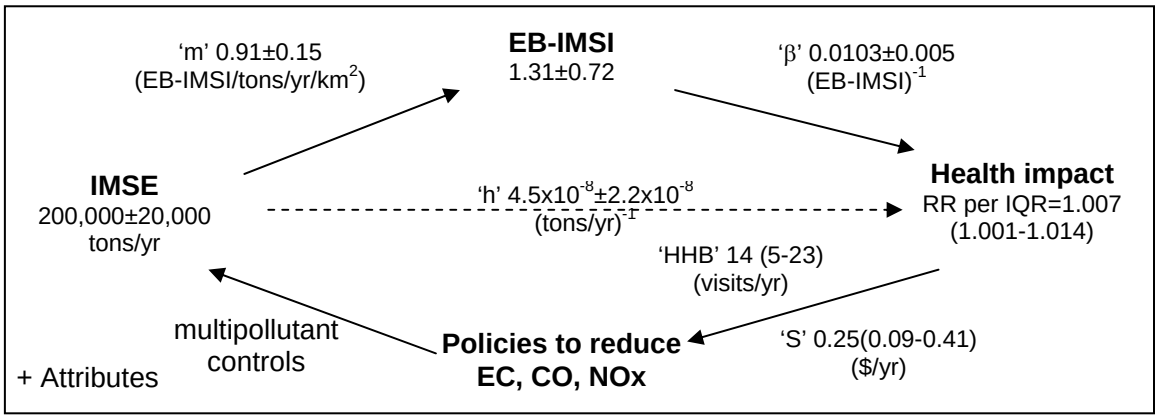

Figure 5.6 Framework of Indicator set for EB-IMSI

The indicator set for EB-IMSI is comprised of individual indicators and the relationships among them in a multipollutant framework. Integrated mobile source emissions (IMSE) trend is an indicator of effectiveness of policies to reduce emission of CO, NOx and EC from mobile sources; EB-IMSI is an indicator of mobile source impacts on air quality; the association of EB-IMSI with CVD outcomes (quantified as the RR per IQR) is an indicator of the multipollutant impact of mobile source activity on cardiovascular health. The slope in the linear regression between IMSE and EB-IMSI is denoted as 'm' and represents the change in EB-IMSI as a result of the change in emissions of NOx, CO and EC from mobile sources. The use of EB-IMSI in an epidemiologic model provides a relationship between changes in multipollutant concentrations and changes in the incidence of adverse CVD impacts, denoted as 'β'. The 'm' and 'β' ratios are used to find the response in the incidence of adverse CVD impacts as a result of change in integrated emissions of NOx, CO and EC from mobile sources 'h'. The reduction in mobile source emissions in Atlanta from 1999-2004 is used along with 'h' to estimate the number of CVD visits avoided per year (HHB) and the respective savings in costs of those visits (S).

The HHB and savings obtained from the analysis of EB-IMSI can support the setting of cost-benefits analysis of air pollution reduction in a multipollutant framework. Therefore, multipollutant emission controls for mobile sources and respective costs can be evaluated in the indicator set for EB-IMSI, but their quantification are beyond the scope of this study. The attributes in the indicator set for EB-IMSI includes information, range of validity or appropriate references to estimate each one of the individual indicators and the described relationships among them (Table 5.3).

5.4.5. Comparison of uncertainties among indicators

In general, uncertainties from mobile source emission estimates were found to be the lowest among indicators and uncertainties from mobile source impacts from receptor models were found to be the highest (Table 5.3). The reason for obtaining low uncertainties in emissions is that they were estimated as one standard deviation of emissions in the six-year period, and therefore they are only reflecting the variance over those years. Uncertainties in mobile emissions are expected to be larger if information on emissions factors, driving patterns, meteorological conditions and vehicular activity are considered, but unfortunately MOVES 2010 (US-EPA, 2010) does not provide an estimate of an uncertainty at present.

Table 5.3 Comprehensive list of indicators

Indicator	Value	Unc.	Relative unc.	Associated outcome	Attribute
NOx mobile emissions (ton/yr)	34400	3100	0.09	Long-term trend reflect effectiveness of policies. Reduction of 21% from 1999-2004	Estimated with MOVES 2010a, uncertainty provided as one standard deviation
NOx ambient (ppm)	0.12	0.03	0.25	Indicator of mobile source emissions, rate of change: 0.54±0.14 ppm/ton/yr/km^2	Correlation coefficient between emissions and concentrations R^2=0.63, regression slope significant at the 95% CI.
				Indicator of impact of mobile sources on CVD outcomes, RR per IQR=1.008 (1.001-1.015)	NOx ambient concentrations obtained at a central monitor for epidemiologic analysis.
S_{NOx} ($/ton)	112	56	0.50	Economic benefits for saving CVD-ED* visits per ton of NOx reduced	Product of concentration-health response function and emission-concentration response
CO mobile emissions (ton/yr)	170000	35000	0.21	Long-term trend reflect effectiveness of policies. Reduction of 28% from 1999-2004	Estimated with MOVES 2010a, uncertainty provided as one standard deviation
CO ambient (ppm)	1.16	0.16	0.14	Indicator of mobile source emissions, rate of change: 1.51±0.17 ppm/ton/yr/km^2	Correlation coefficient between emissions and concentrations R^2=0.93, regression slope significant at the 95% CI.
				Indicator of impact of GV sources on CVD outcomes, RR per IQR=1.007 (1.001-1.014)	CO ambient concentrations obtained at a central monitor for epidemiologic analysis.
S_{CO} ($/ton)	28	13	0.46	Economic benefits for saving CVD-ED* visits per ton of CO reduced	Product of concentration-health response function and emission-concentration response
EC mobile emissions (ton/yr)	580	17	0.03	Long-term trend reflect effectiveness of policies. Reduction of 7% from 1999-2004	Estimated with MOVES 2010a, uncertainty provided as one standard deviation
EC ambient ($\mu g/m^3$)	1.53	0.64	0.42	Indicator of mobile source emissions, rate of change: 1.04±0.32 ppm/ton/yr/km^2	Correlation coefficient between emissions and concentrations R^2=0.60, regression slope significant at the 95% CI.
				Indicator of impact of DV sources on CVD outcomes, RR per IQR=1.008 (1.000-1.017)	EC ambient concentrations obtained at a central monitor for epidemiologic analysis.
S_{EC} ($/ton)	17800	10800	0.61	Economic benefits for saving CVD-ED* visits per ton of EC reduced	Product of concentration-health response function and emission-concentration response
EB-IMSI	1.31	0.72	0.55	Indicator of mobile source integrated emissions, rate of change: 1.13±0.12 IMSI/IMSE	Integrated EC, CO and NOx concentrations scaled and weighted by mobile-to-total emissions, see Pachon et al (AWMA, 2011) Eq. 1
				Indicator of impact of mobile sources on CVD outcomes, RR per IQR=1.007 (1.001-1.014)	NOx, CO and EC ambient concentrations obtained at a central monitor for epidemiologic analysis.
$S_{EB\text{-}IMSI}$ ($/ton)	23	11	0.48	Economic benefits for saving CVD-ED* visits per ton of EB-IMSI reduced	To express IMSE in units of ton/yr, mobile emissions of EC, CO, NOx were added up.
EB-IMSI-GV	1.17	0.8	0.68	Indicator of mobile source integrated emissions, rate of change: 1.13±0.12 IMSI/IMSE	Integrated CO and NOx concentrations scaled and weighted by mobile-to-total emissions, see Pachon et al (AWMA, 2011) Eq. 2
				Indicator of impact of mobile sources on CVD outcomes, RR per IQR=1.009 (1.002-1.017)	NOx, CO and EC ambient concentrations obtained at a central monitor for epidemiologic analysis.
$S_{EB\text{-}IMSI\text{-}GV}$ ($/ton)	21	11	0.52	Economic benefits for saving CVD-ED* visits per ton of EB-IMSI-GV reduced	To express IMSE-GV in units of ton/yr, 98% of mobile CO and 58% of NOx mobile emissions were added up.

Table 5.3 Comprehensive list of indicators (cont.)

Indicator	Value	Unc.	Relative unc.	Associated outcome	Attribute
EB-IMSI-DV	1.48	0.76	0.51	Indicator of mobile source integrated emissions, rate of change: 0.92±0.3 IMSI/IMSE	Integrated EC and NOx concentrations scaled and weighted by mobile-to-total emissions, see Pachon et al (AWMA, 2011) Eq. 3
				Indicator of impact of mobile sources on CVD outcomes, RR per IQR=1.010 (1.001-1.018)	NOx, CO and EC ambient concentrations obtained at a central monitor for epidemiologic analysis.
$S_{EB\text{-}IMSI\text{-}DV}$ ($/ton)	240	140	0.58	Economic benefits for saving CVD-ED* visits per ton of EB-IMSI-DV reduced	To express IMSE-DV in units of ton/yr, 94% of mobile EC and 42% of NOx mobile emissions were added up.
HB-IMISI-NC	1.17	0.93	0.79	Indicator of impact of NOx-CO mixture on CVD outcomes, RR per IQR=1.010 (1.002-1.018)	NOx and CO ambient concentrations obtained at a central monitor for epidemiologic analysis.
HB-IMISI-NE	1.29	0.92	0.71	Indicator of impact of NOx-EC mixture on CVD outcomes, RR per IQR=1.009 (1.002-1.016)	NOx and EC ambient concentrations obtained at a central monitor for epidemiologic analysis.
HB-IMSI-CE	1.37	0.92	0.67	Indicator of impact of EC-CO mixture on CVD outcomes, RR per IQR=1.009 (1.001-1.017)	EC and CO ambient concentrations obtained at a central monitor for epidemiologic analysis.
PMF-mob ($\mu g/m^3$)	2.94	1.11	0.38	Indicator of mobile factor contribution from PMF	Uncertainty in PMF estimated using bootstrapping of 100 runs
PMF-GV ($\mu g/m^3$)	1.37	0.36	0.26	Indictor of GV factor contribution from PMF	Uncertainty in PMF estimated using bootstrapping of 100 runs
PMF-DV ($\mu g/m^3$)	1.57	1.05	0.67	Indicator of DV factor contribution from PMF	Uncertainty in PMF estimated using bootstrapping of 100 runs
CMB-mob ($\mu g/m^3$)	2.54	2.53	1.00	Indicator of mobile source impact from CMB	CMB using optimized sources profiles for Atlanta, see Marmur et al., 2007
CMB-GV ($\mu g/m^3$)	1.35	2.0	1.48	Indictor of GV factor contribution from CMB	CMB using optimized sources profiles for Atlanta, see Marmur et al., 2007
CMB-DV ($\mu g/m^3$)	1.27	1.6	1.26	Indicator of DV factor contribution from CMB	CMB using optimized sources profiles for Atlanta, see Marmur et al., 2007
SOC ($\mu g/m^3$)	1.25	0.71	0.57	Indicator of photochemical activity	Estimated using the regression method, see Pachon et al., AE, 2010
POC ($\mu g/m^3$)	2.84	1.25	0.44	Indicator of combustion activity	Estimated using the regression method, see Pachon et al., AE, 2010
$K_{b\ (\mu g/m^3)}$	30.4	26.7	0.88	Indicator of biomass burning activity	Estimated based on regression with Fe., see Pachon et al., AE, 2011
VOI	5.85	1.7	0.29	VOI estimated as the sensitivity of ozone to mobile NOx	Uncertainty estimated as 29% of VOI according to Tian et al, AWMA, 2010

* Emergency department visits for Cardiovascular diseases, economic analysis assuimg a cost of illness (COI) of $18,387 per CVD (EPA, 2004)

Estimates of health benefits as a result of reduction in mobile emissions were also found to be highly uncertain. Such estimates include uncertainties in the CRF, in the relationship between emissions and concentrations and in the estimation of illness costs. Uncertainties were in the same order of magnitude for estimates of health benefits using singles species and multipollutant indicators. While consideration of uncertainties is important, they do not obscure the choice of selecting multipollutant indicators versus singles species as better surrogates of mobile source impact on air quality, exposure and cardiovascular health.

5.5. References

Georgia Department of Natural Resources, 2007. Visibility Improvement State and Tribal Association of the Southeast (VISTAS) conceptual description support document.Asheville, NC.

Bell, M. L., Cifuentes, L. A., Davis, D. L., Cushing, E., Gusman Telles, A. and Gouveia, N., 2011. Environmental health indicators and a case study of air pollution in Latin American cities. Environmental Research 111, 57-66.

Brook, J. R., Burnett, R. T., Dann, T. F., Cakmak, S., Goldberg, M. S., Fan, X. and Wheeler, A. J., 2007. Further interpretation of the acute effect of nitrogen dioxide observed in Canadian time-series studies. J Expos Sci Environ Epidemiol 17, S36-S44.

Brook, R. D., Rajagopalan, S., Pope, C. A., III, Brook, J. R., Bhatnagar, A., Diez-Roux, A. V., Holguin, F., Hong, Y., Luepker, R. V., Mittleman, M. A., Peters, A., Siscovick, D., Smith, S. C., Jr, Whitsel, L. and Kaufman, J. D., 2010. Particulate matter air pollution and cardiovascular disease: an update to the scientific statement from the American Heart Association. Circulation 121, 2331-2378.

Burnett, R. T., Stieb, D., Brook, J. R., Cakmak, S., Dales, R., Raizenne, M., Vincent, R. and Dann, T., 2004. Associations between short-term changes in nitrogen dioxide and mortality in Canadian cities. Arch. Environ. Health 59, 228-236.

Chameides, W. L., Lindsay, R. W., Richardson, J. and Kiang, C. S., 1988. The role of biogenic hydrocarbons in urban photochemical smog - Atlanta as a case study. Science 241, 1473-1475.

Chow, J. C., Watson, J. G., Pritchett, L. C., Pierson, W. R., Frazier, C. A. and Purcell, R. G., 1993. The DRI thermal optical reflectance carbon analysis system - description, evaluation and applications in United-States air quality studies. Atmospheric Environment Part a-General Topics 27, 1185-1201.

Cohan, D. S., Hakami, A., Hu, Y. T. and Russell, A. G., 2005. Nonlinear response of ozone to emissions: Source apportionment and sensitivity analysis. Environmental Science & Technology 39, 6739-6748.

Davidson, K., Hallberg, A., McCubbin, D. and Hubbell, B., 2007. Analysis of PM2.5 using the Environmental Benefits Mapping and Analysis Program (BenMAP). J. Toxicol. Env. Health Part A 70, 332-346.

Dunker, A. M., 1981. Efficient calculation of sensitivity coefficients for complex atmospheric models. Atmospheric Environment (1967) 15, 1155-1161.

Dunker, A. M., Yarwood, G., Ortmann, J. P. and Wilson, G. M., 2002. Comparison of source apportionment and source sensitivity of ozone in a three-dimensional air quality model. Environmental Science & Technology 36, 2953-2964.

Edgerton, E. S., Hartsell, B. E., Saylor, R. D., Jansen, J. J., Hansen, D. A. and Hidy, G. M., 2005. The Southeastern aerosol research and characterization study: Part II. Filter-based measurements of fine and coarse particulate matter mass and composition. Journal of the Air & Waste Management Association 55, 1527-1542.

Fann, N., Fulcher, C. and Hubbell, B., 2009. The influence of location, source, and emission type in estimates of the human health benefits of reducing a ton of air pollution. Air Quality, Atmosphere & Health 2, 169-176.

Fann, N., Roman, H. A., Fulcher, C. M., Gentile, M. A., Hubbell, B. J., Wesson, K. and Levy, J. I., 2011. Maximizing Health Benefits and Minimizing Inequality: Incorporating Local-Scale Data in the Design and Evaluation of Air Quality Policies. Risk Analysis 31, 908-922.

Hakami, A., Odman, M. T. and Russell, A. G., 2003. High-order, direct sensitivity analysis of multidimensional air quality models. Environmental Science & Technology 37, 2442-2452.

Hakami, A., Odman, M. T. and Russell, A. G., 2004. Nonlinearity in atmospheric response: A direct sensitivity analysis approach. J. Geophys. Res.-Atmos. 109.

Hansen, D. A., Edgerton, E. S., Hartsell, B. E., Jansen, J. J., Kandasamy, N., Hidy, G. M. and Blanchard, C. L., 2003. The Southeastern aerosol research and characterization study: Part 1-overview. Journal of the Air & Waste Management Association 53, 1460-1471.

Health Effects Institute, 2003. Assessing health impact of air quality regulations: concepts and methods for accountability research. Boston, MA.

Hu, Y. T., Odman, M. T. and Russell, A. G., 2006. Re-examination of the 2003 North American electrical blackout impacts on regional air quality. Geophys. Res. Lett. 33.

Laden, F., Neas, L. M., Dockery, D. W. and Schwartz, J., 2000. Association of fine particulate matter from different sources with daily mortality in six U.S. cities. Environ. Health Perspect. 108, 941-947.

Laden, F., Schwartz, J., Speizer, F. E. and Dockery, D. W., 2006. Reduction in fine particulate air pollution and mortality: Extended follow-up of the Harvard Six Cities study. Am J Respir Crit Care Med 173, 667-672.

Liao, K. J., Tagaris, E., Napelenok, S. L., Manomaiphiboon, K., Woo, J. H., Amar, P., He, S. and Russell, A. G., 2008. Current and future linked responses of ozone and PM2.5 to emission controls. Environmental Science & Technology 42, 4670-4675.

Lin, X., Trainer, M. and Liu, S. C., 1988. On the nonlinearity of the tropospheric ozone production. J. Geophys. Res.-Atmos. 93, 15879-15888.

Mar, T. F., Norris, G. A., Koenig, J. Q. and Larson, T. V., 2000. Associations between air pollution and mortality in Phoenix, 1995-1997. Environ. Health Perspect. 108, 347-353.

Mendoza-Dominguez, A., Wilkinson, J. G., Yang, Y. J. and Russell, A. G., 2000. Modeling and direct sensitivity analysis of biogenic emissions impacts on regional ozone formation in the Mexico-US border area. Journal of the Air & Waste Management Association 50, 21-31.

Metzger, K. B., Tolbert, P. E., Klein, M., Peel, J. L., Flanders, W. D., Todd, K., Mulholland, J. A., Ryan, P. B. and Frumkin, H., 2004. Ambient air pollution and cardiovascular emergency department visits. Epidemiology 15, 46-56.

Pachon, J. E., Balachandran, S., Hu, Y. T., Mulholland, J. A., Darrow, L. A., Sarnat, J. A., Tolbert, P. E. and Russell, A. G., 2011. Development of Outcome-based, Multipollutant mobile source indicators. Jornal of the Air & Waste Management Association *Submitted*.

Pope, C. A., Burnett, R. T., Thun, M. J., Calle, E. E., Krewski, D., Ito, K. and Thurston, G. D., 2002. Lung cancer, cardiopulmonary mortality, and long-term exposure to fine particulate air pollution. JAMA 287, 1132-1141.

Sarnat, J. A., Marmur, A., Klein, M., Kim, E., Russell, A. G., Sarnat, S. E., Mulholland, J. A., Hopke, P. K. and Tolbert, P. E., 2008. Fine particle sources and cardiorespiratory morbidity: An application of chemical mass balance and factor analytical source-apportionment methods. Environ. Health Perspect. 116, 459-466.

Tagaris, E., Liao, K. J., Delucia, A. J., Deck, L., Amar, P. and Russell, A. G., 2009. Potential Impact of Climate Change on Air Pollution-Related Human Health Effects. Environmental Science & Technology 43, 4979-4988.

Tian, D., Cohan, D. S., Napelenok, S., Bergin, M., Hu, Y. T., Chang, M. and Russell, A. G., 2010. Uncertainty Analysis of Ozone Formation and Response to Emission Controls Using Higher-Order Sensitivities. Journal of the Air & Waste Management Association 60, 797-804.

Tolbert, P. E., Klein, M., Peel, J. L., Sarnat, S. E. and Sarnat, J. A., 2007. Multipollutant modeling issues in a study of ambient air quality and emergency department visits in Atlanta. J. Expo. Sci. Environ. Epidemiol. 17, S29-S35.

U.S. Environment Protection Agency, 2004. Final Regulatory Analysis: control of emissions from nonroad diesel engines.Office of Transportation and Air Quality, http://www.epa.gov/nonroad-diesel/2004fr.htm#ria

U.S. Environmental Protection Agency, 2006. Development of Environmental Health Outcome Indicators.Office of Research and Development, Washington, D.C. Available on the internet at: http://www.epa.gov/ncer/rfa/2006/2006_star_ephi.html

U.S. Environment Protection Agency, 2007. 2002 National Emissions Inventoriy Data & documentation.

U.S. Environmental Protection Agency, 2008. EPA's Report on the Environment.National Center for Environmental Assessment, Washington, D.C.

U.S. Environmental Protection Agency, 2010. Motor Vehicle Emission Simulator (MOVES): user guide.Office of Transportation and Air Quality, Research Triangle Park, NC. EPA-420-B-09-041.

Voorhees, A. S., Fann, N., Fulcher, C., Dolwick, P., Hubbell, B., Bierwagen, B. and Morefield, P., 2011. Climate Change-Related Temperature Impacts on Warm Season Heat Mortality: A Proof-of-Concept Methodology Using BenMAP. Environmental Science & Technology 45, 1450-1457.

Wesson, K., Fann, N., Morris, M., Fox, T. and Hubbell, B., 2010. A multi–pollutant, risk–based approach to air quality management: case study for Detroit. Atmospheric Pollution Research 1, 296-304.

Xiao, X., Cohan, D. S., Byun, D. W. and Ngan, F., 2010. Highly nonlinear ozone formation in the Houston region and implications for emission controls. J. Geophys. Res.-Atmos. 115.

CHAPTER 6 CONCLUSIONS AND FUTURE RESEARCH

Environmental indicators were developed and evaluated to assess the impact of mobile sources on emissions, air quality, exposure and health. Different levels of indicators are discussed, from single species to multipollutant indicators. Human health benefits of reducing mobile source emissions were assessed and compared using single and multipollutant indicators. Indicator sets, including the indicator value and uncertainties, accompanied with their associated outcomes and attributes were developed. The indicator sets are expected to be useful for policy makers who are interested not only in the indicator, but also in their associated uncertainties and their applicability at other times and other regions.

Comparison of SOC estimates and uncertainties from aerosol chemical composition and gas phase data in Atlanta.

Comparison of four methods to estimate the SOC fraction in the $PM_{2.5}$ suggests that between 26 and 47% of the OC in Atlanta is secondary in origin on a year-around basis. Uncertainties in the estimated SOC fraction range from 51% to more than 100% and are largely influenced by estimation of SOC in winter time. The SOC fraction estimated by the regression method has the lowest uncertainty, a greater value in summer than winter, shows less day-to-day variability and has a more similar trend to the WSOC measurements as compared to the other methods, suggesting the regression method is the most accurate method for developing multi-year SOC estimates useful in epidemiologic analysis and evaluation of air quality policy effectiveness. The regression method only

requires readily measured speciated $PM_{2.5}$ components (i.e., EC, OC, K, sulfate and nitrate), ozone and CO data.

Revising the use of potassium (K) in the source apportionment of PM2.5.

We apply a method to estimate the fraction of potassium attributable to biomass burning and demonstrated that K_b is a more robust indicator of this source than total potassium. The analysis of temporal variability shows a larger concentration of K_b during spring when biomass burning is more intense and greater correlation with levoglucosan, an organic compound found to be a good tracer of biomass burning. The examination of spatial variability suggests that K_b is an important fraction in urban areas not impacted by sea-salt where K has multiple sources, but not as important in rural areas where most of the K is from biomass burning. The application of PMF with total potassium appears to overestimate the contribution of biomass burning in urban sites and underestimate the impact of other sources such as traffic. This limitation is avoided when PMF is implemented with K_b, resulting in a modified allocation of PM2.5 mass as a result of the re-distribution of the carbonaceous species within factors.

Development of outcome-based, multipollutant mobile source indicators.

This study proposed an approach to develop multipollutant indicators based on analysis of emissions inventories and health outcomes. The EB-IMSIs are simple to construct and calculate and demonstrate advantages over the use of single species: EB-IMSIs have stronger spatial representativeness, suggesting they are better indicators of the regional impact of mobile sources, they agree well with the observed trends of traffic and they have stronger associations with observed health effects, possibly due to their better spatial representativeness. Uncertainties in EB-IMSIs are similar to uncertainties in

ambient measurements and receptor models. A sensitivity analysis of fractions in EB-IMSIs led to the development of HB-IMSIs, suggesting mixtures of pollutants more strongly associated with CVD outcomes. The use of IMSIs in epidemiologic modeling constitutes an alternative approach to assess the health impact of pollutant mixtures. Although the approach presented in this manuscript was developed for mobile sources, this work can be extended to other sources. IMSI can support the setting of multipollutant air quality standards since they represent the impact of traffic on health.

Using independent air quality from Dallas, TX we observed CO and NOx as indicators of mobile sources, with NOx being more indicator of regional mobile source impact than CO. The Dallas basin was found more ventilated than Atlanta, favoring dispersion of pollutants and lower ambient air concentrations. EB-IMSIs estimated in Atlanta and Dallas followed traffic trends adequately.

Mobile source air quality impact indicator sets for policy utilization: evaluation and uncertainties.

We have examined changes in the incidence of adverse CVD impacts as result of change in indicators of mobile source activity. We have compared single and multipollutant indicators, finding that a multipollutant framework is more consistent to understanding health risk from mobiles source emissions than using single species. Our results contribute in the setting of multipollutant approaches for air quality management.

The concept of indicator sets, which include a group of indicators and their relationships, along with associated attributes, facilitates a comprehensive analysis of the air quality chain, from emissions to ambient concentrations and to health outcomes. This

proposed framework is of great utility for policy makers in the setting of cost-benefit analysis of air pollution reduction.

Uncertainties in estimates of emissions were found the lowest and uncertainties in source impacts from receptor models were found the highest. The estimation of health benefits were found also highly uncertain. While consideration of uncertainties is important, they do not obscure the choice of selecting multipollutant indicators versus singles species as surrogates of mobile source impact on air quality, exposure and cardiovascular health.

6.1. FUTURE RESEARCH

This work developed and evaluated single and multipollutant indicators for mobile sources, given the large impact of vehicles to air quality in urban centers. The approaches developed here are extendable to other emission sources, which may have a greater impact in other areas. Outcome-based indicators can provide links between expected direct policy impacts, atmospheric concentration and health.

Comparison of SOC estimates and uncertainties from aerosol chemical composition and gas phase data in Atlanta.

The use of water soluble organic carbon (WSOC), as a surrogate of SOC, was useful in the evaluation of methods to estimate SOC. The availability of additional measurements of WSOC in the future can facilitate the comparison of estimates of SOC in longer periods of time.

New methods for quantifying organic aerosols in short time scales, such as the aerosol mass spectrometer (AMS), are expected to be available in the Atlanta area. Such

methods will quantify oxygenated and hydrogenated organic species that can be used for more specific estimations of primary and secondary organic fractions.

The ensemble of estimates of SOC from different methods is expected to provide an accurate estimate of SOC, as it has been found with source impacts from primary and secondary emissions sources. Such estimate can be compared with results from the regression method for refining of the SOC fraction. Furthermore, the comparison of individual estimates with the ensemble can provide estimates of uncertainties that are more comparable between methods.

Associations of organic carbon (OC) with health outcomes have found OC linked with the increase in CVD. However, our preliminary analyses suggest that the primary fraction is more responsible of such health outcomes. The availability of more extensive SOC estimates will permit health researchers to clarify this complexity.

Revising the use of potassium (K) in the source apportionment of PM2.5.

Levoglucosan was useful in the evaluation of K_b as a better tracer of biomass burning than total potassium. However, measurements of levoglucosan concentrations are limited. The availability of more levoglucosan data will allow stronger analysis of biomass burning impacts and validation of indicators.

Biomass burning source impacts estimated using total potassium in receptor models have been associated with the increase in CVD in epidemiologic models. However, given the multiple sources of potassium to the atmosphere, it is not clear whether this association is due exclusively to biomass burning impacts or is also impacted by different sources emitting K. The use of Kb in receptor modeling and

subsequent epidemiologic analysis will provide information on the associations between impact on health endpoint and more refined source impacts.

Development of outcome-based, multipollutant mobile source indicators.

The outcome-based approach discussed as part of this work to assess the impacts of mobile sources on emissions, air quality and health, can be extended to the evaluation of other sources. Sources such as biomass burning, power plants, industrial processes, agriculture, are suitable to be evaluated on their impact to air quality through the use of outcome-based indicators, in places where information on emissions and ambient pollutants is available

This work contributed to the multipollutant risk science providing new approaches to combine pollutants and evaluating the health effects of such combinations. Since our focus was indicators for mobile sources, we limited our approach to EC, CO and NOx, but multiple species can be selected to form integrated indicators of other emissions sources. Of particular interest will be the integration of organic species that are identified as specific tracers of emission sources.

This study found a greater significance in the association of mixtures of pollutants with health outcomes than single species, possibly explained by their larger spatial representativeness of the mixtures. However, synergistic effects may be playing a role in the increase of association with mixtures. Toxicological studies can be conducted to investigate this potential.

Uncertainties in mobile source emissions were estimated as one standard deviation from the mean. However, a comprehensive estimate of the uncertainties from mobile sources should include information on emission factors, activity data, driving

patterns and meteorological conditions. Currently, such uncertainty estimates are not available from MOVES 2010, but as they become available, better estimates of uncertainties on emission and relationships with concentrations can be obtained.

Mobile source air quality impact indicator sets for policy utilization: evaluation and uncertainties.

Our preliminary estimates of human health benefits are based on local relationships between emissions and concentrations and local association between pollutants and health outcomes. The availability of air quality and health data in other urban centers will facilitate the replication of these analyses. In this estimation, only benefits due to reduced CVD-ED visits were captured, and not for reduced premature mortality. The inclusion of mortality impact will contribute to strength the benefits of air pollution management through the use of indicators.

Indicator sets, that are expected to be useful for policy makers, were developed for Atlanta in this project. Concurrently with the development of additional indicators for mobile and other emission sources, indicator sets can refined to include new information associated with the application of the indicators and estimates of uncertainty.

Emission-based integrated mobile source indicators were estimated for Dallas, TX during 2003-2008 to support an ongoing epidemiologic work in the area. Results from that epidemiologic work can be used to develop health-based IMSI in a similar way it was discussed in Atlanta, GA. Specific characteristics of these cities will facilitate the evaluation of health outcome-based indicators for use in policy analysis.

APPENDIX A

SUPPORTING INFORMATION FOR CHAPTER 3

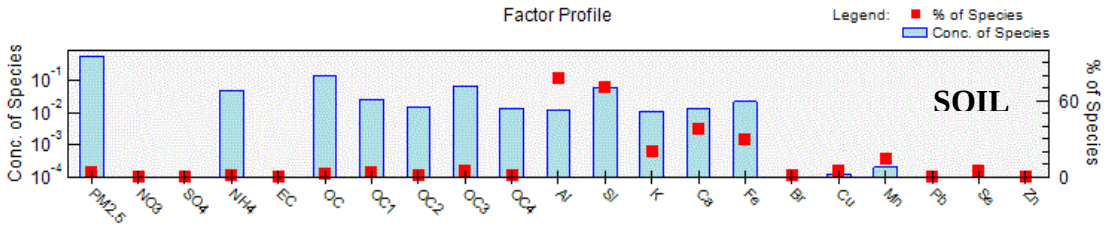

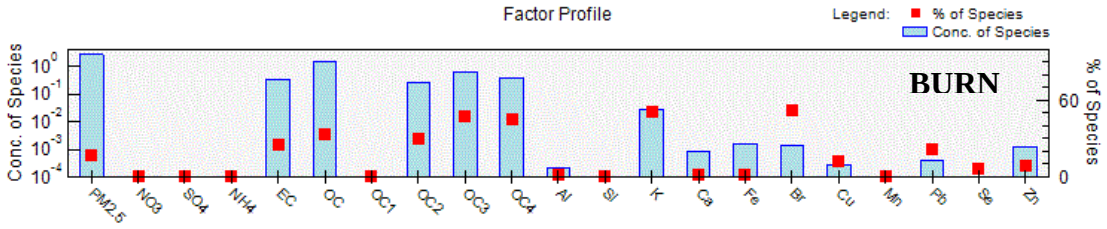

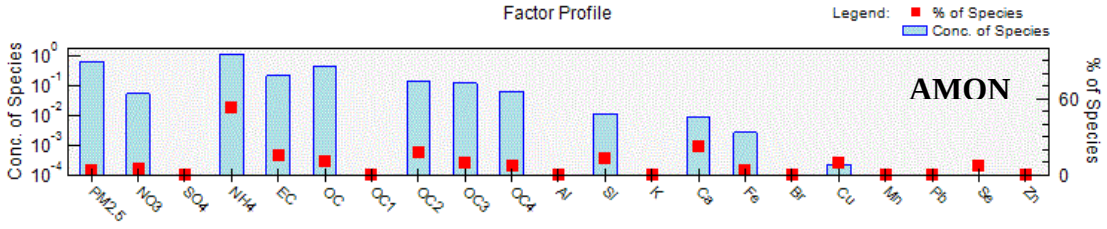

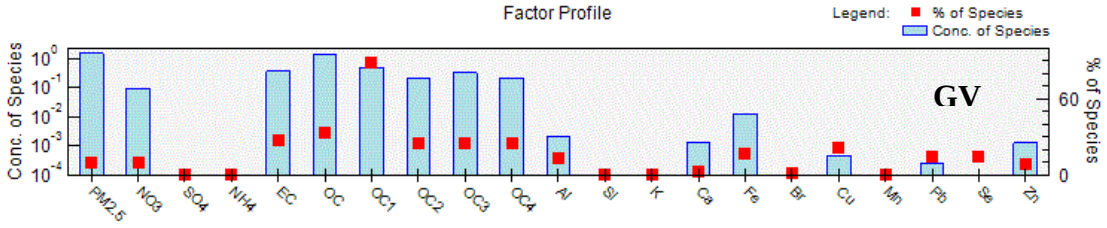

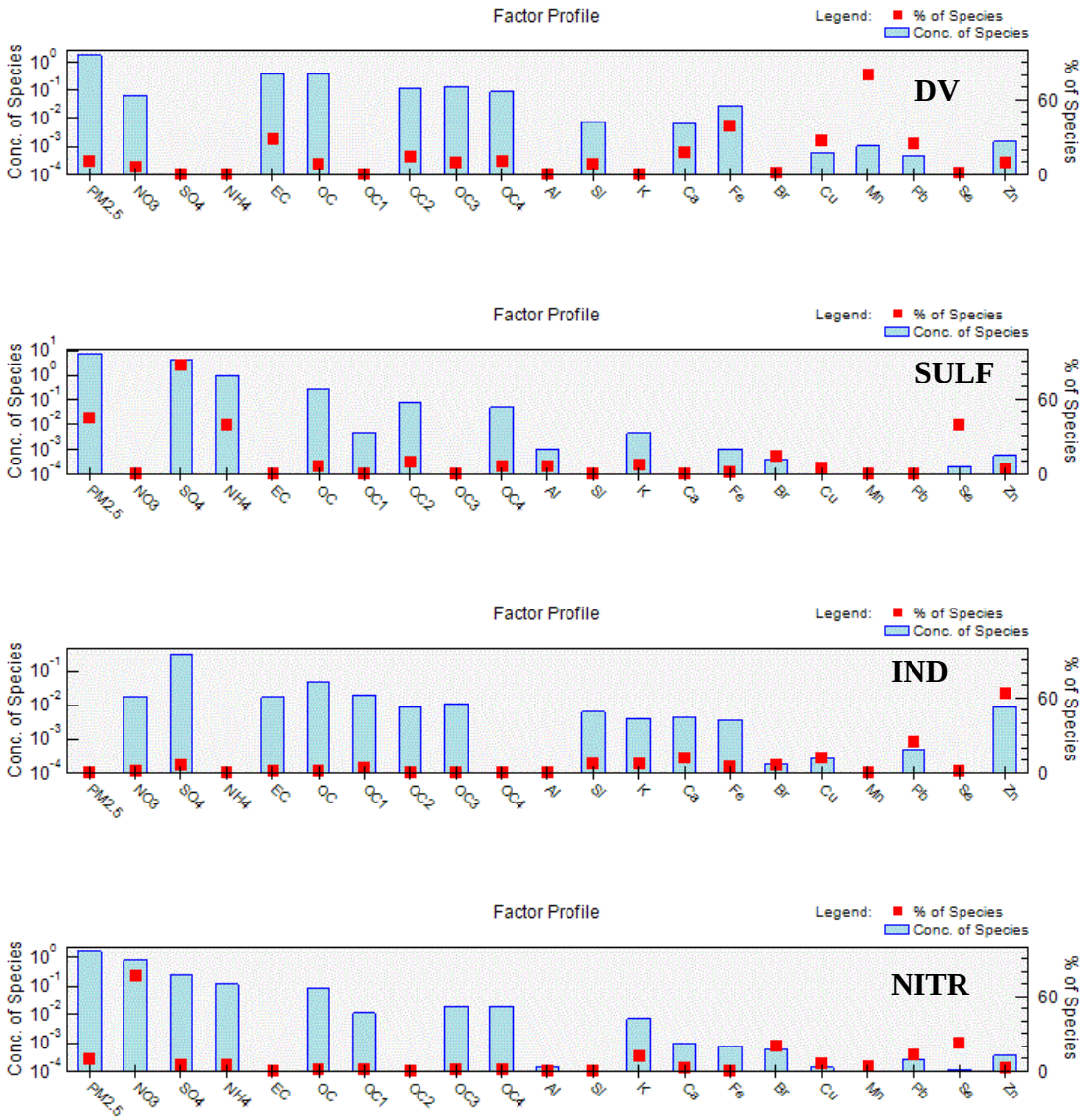

Figure A.1 Factor profiles for PMF-K

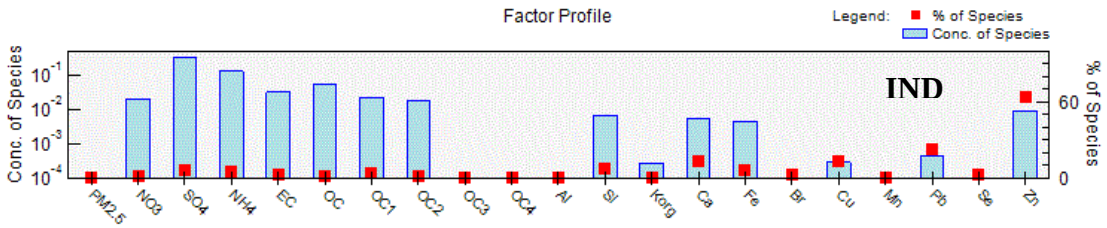
Factor Profile
Legend:
% of Species
Conc. of Species
IND
Conc. of Species
% of Species
PM2.5
NO3
SO4
NH4
EC
OC
OC1
OC2
OC3
OC4
Al
Si
Korg
Ca
Fe
Br
Cu
Mn
Pb
Se
Zn

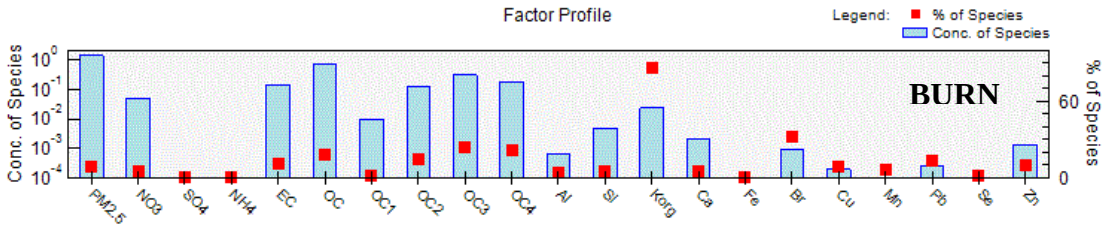
Factor Profile
Legend:
% of Species
Conc. of Species
BURN
Conc. of Species
% of Species
PM2.5
NO3
SO4
NH4
EC
OC
OC1
OC2
OC3
OC4
Al
Si
Korg
Ca
Fe
Br
Cu
Mn
Pb
Se
Zn

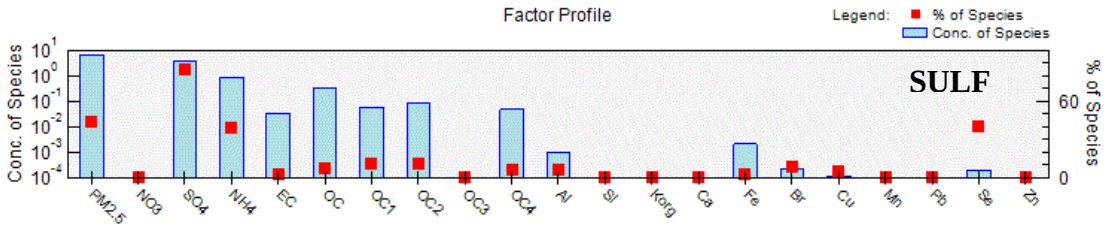
Factor Profile
Legend:
% of Species
Conc. of Species
SULF
Conc. of Species
% of Species
PM2.5
NO3
SO4
NH4
EC
OC
OC1
OC2
OC3
OC4
Al
Si
Korg
Ca
Fe
Br
Cu
Mn
Pb
Se
Zn

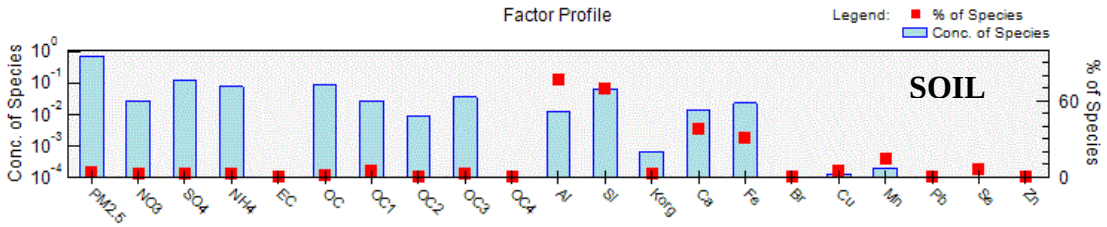
Factor Profile
Legend:
% of Species
Conc. of Species
SOIL
Conc. of Species
% of Species
PM2.5
NO3
SO4
NH4
EC
OC
OC1
OC2
OC3
OC4
Al
Si
Korg
Ca
Fe
Br
Cu
Mn
Pb
Se
Zn

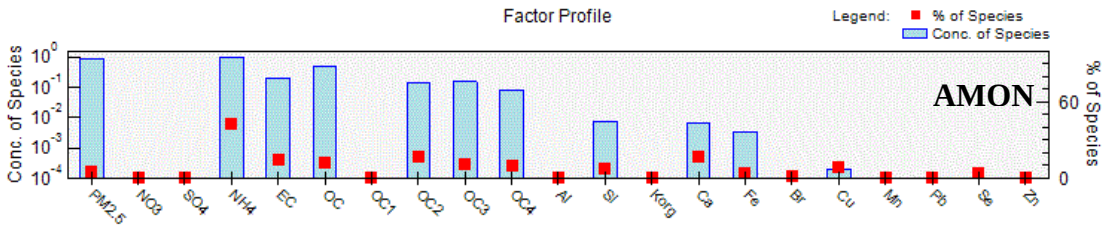
Factor Profile
Legend:
% of Species
Conc. of Species
AMON
Conc. of Species
% of Species
PM2.5
NO3
SO4
NH4
EC
OC
OC1
OC2
OC3
OC4
Al
Si
Korg
Ca
Fe
Br
Cu
Mn
Pb
Se
Zn

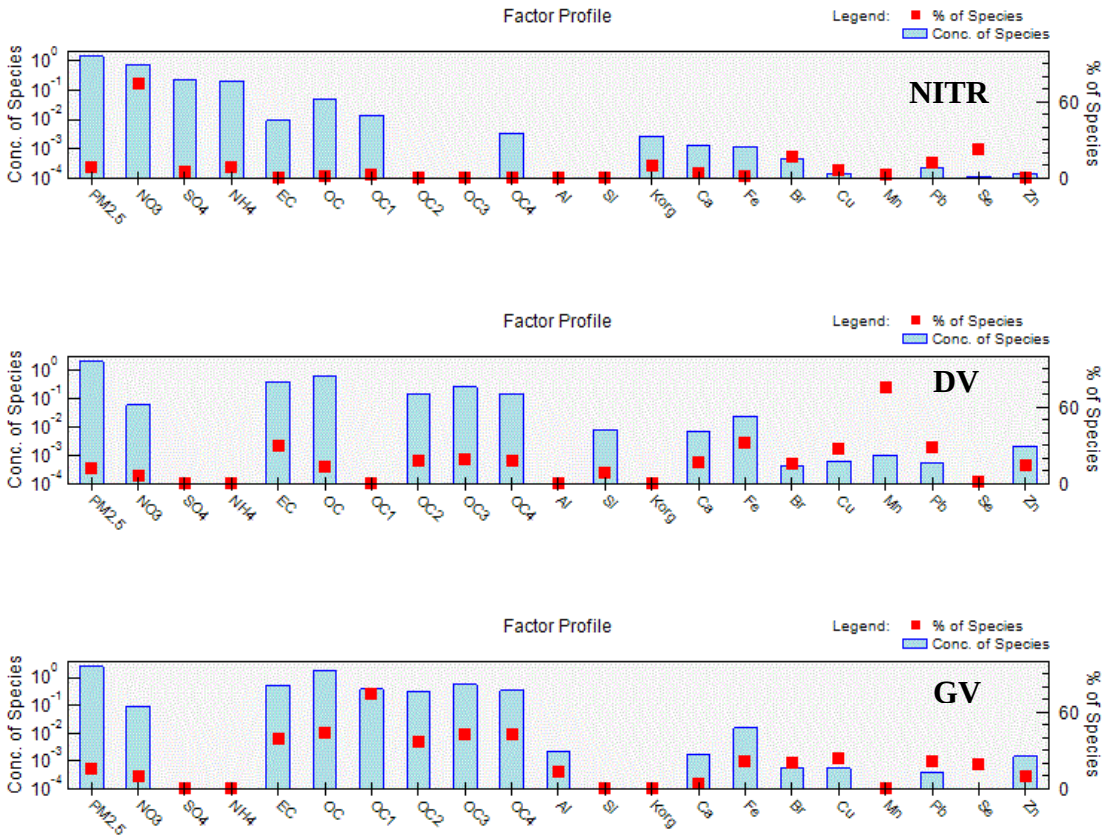

Figure A.2 Factor profiles for PMF-K_b

Table A.1 Correlations between factor contributions in PMF-K and PMF-K_b and PM2.5 species

R	*GV*	*DV*	*Biomass*	*Soil dust*	*Industrial*	*Sec. sulf*	*Sec. Ammon.*	*Sec. Nitrate*	*GV*	*DV*	*Biomass*	*Soil dust*	*Industrial*	*Sec. sulf*	*Sec. Ammon.*	*Sec. Nitrate*
GV	1.00															
DV	0.56	1.00														
BURN	0.46	0.46	1.00													
SOIL	0.04	0.12	0.04	1.00												
IND	0.52	0.36	0.35	-0.01	1.00											
SULF	-0.06	0.04	-0.16	0.06	-0.06	1.00										
AMMON	0.22	-0.01	0.03	-0.09	0.15	0.46	1.00									
NITR	-0.01	0.01	0.07	-0.20	0.12	-0.16	-0.06	1.00								
GV	1.00	0.57	0.46	0.04	0.52	-0.07	0.21	-0.03	1.00							
DV	0.62	0.98	0.48	0.10	0.42	-0.03	0.02	-0.01	0.63	1.00						
BURN	-0.01	0.12	0.82	0.04	0.06	-0.03	-0.02	0.11	-0.03	0.05	1.00					
SOIL	0.04	0.09	0.02	1.00	-0.01	0.06	-0.09	-0.20	0.03	0.07	0.03	1.00				
IND	0.57	0.42	0.33	0.01	0.99	-0.01	0.17	0.10	0.57	0.49	0.00	0.01	1.00			
SULF	-0.05	0.04	-0.17	0.05	-0.06	1.00	0.46	-0.16	-0.07	-0.03	-0.04	0.05	-0.01	1.00		
AMMON	0.21	-0.03	-0.09	-0.08	0.13	0.46	0.98	-0.08	0.20	0.00	-0.17	-0.07	0.16	0.46	1.00	
NITR	0.01	0.01	0.05	-0.19	0.13	-0.19	-0.08	1.00	0.00	0.00	0.07	-0.20	0.12	-0.18	-0.10	1.00
PM2.5	0.43	0.46	0.36	0.12	0.32	0.73	0.55	0.08	0.41	0.42	0.24	0.11	0.37	0.73	0.50	0.06
NO3	0.15	0.14	0.20	-0.18	0.24	-0.17	-0.01	**0.98**	0.14	0.13	0.16	-0.19	0.22	-0.16	-0.05	0.98
SO4	0.04	0.08	-0.11	0.05	0.01	**0.99**	0.57	-0.10	0.03	0.02	-0.03	0.06	0.06	0.99	0.56	-0.12
NH4	0.11	0.01	-0.06	-0.02	0.08	0.80	**0.86**	0.04	0.09	-0.02	-0.01	-0.02	0.11	0.80	0.86	0.01
EC	**0.73**	**0.71**	**0.58**	0.08	0.54	0.10	0.33	0.04	**0.73**	**0.74**	**0.22**	0.06	0.58	0.10	0.29	0.04
OC	**0.63**	**0.85**	**0.75**	0.10	0.45	0.13	0.26	0.02	**0.63**	**0.84**	**0.45**	0.07	0.48	0.13	0.18	0.01
Al	-0.01	0.09	-0.02	**0.90**	-0.06	0.02	-0.16	-0.18	-0.01	0.06	0.01	**0.90**	-0.04	0.01	-0.13	-0.17
Si	0.16	0.16	0.09	**0.97**	0.12	0.08	0.02	-0.18	0.15	0.14	0.06	**0.97**	0.14	0.07	0.03	-0.18
K	0.40	0.41	**0.83**	0.39	0.37	0.05	0.07	0.11	0.39	0.41	0.70	0.37	0.36	0.04	-0.02	0.09
Kb	-0.03	0.07	0.72	0.09	0.06	0.04	-0.02	0.16	-0.04	0.02	**0.88**	0.07	0.01	0.04	-0.13	0.13
Ca	0.36	0.24	0.19	0.45	0.43	0.10	0.21	-0.03	0.35	0.27	0.03	0.44	0.45	0.10	0.20	-0.02
Fe	0.68	0.58	0.38	0.63	0.51	0.10	0.18	-0.09	0.68	0.64	-0.02	0.62	0.56	0.09	0.19	-0.07
Br	0.39	0.33	0.49	-0.03	0.36	0.01	0.09	0.20	0.38	0.35	0.33	-0.04	0.36	0.01	0.04	0.19
Cu	0.15	0.14	0.09	0.02	0.10	0.00	0.06	-0.01	0.15	0.15	0.01	0.02	0.11	0.00	0.05	0.00
Mn	0.51	0.40	0.29	0.39	0.49	0.06	0.20	0.03	0.52	0.45	-0.03	0.38	0.53	0.06	0.21	0.04
Pb	0.30	0.25	0.26	-0.03	0.41	-0.06	0.05	0.10	0.31	0.27	0.10	-0.03	0.41	-0.06	0.03	0.11
Se	0.19	0.16	0.07	0.03	0.15	0.33	0.20	0.14	0.18	0.15	0.00	0.02	0.17	0.33	0.19	0.14
Zn	0.53	0.41	0.44	0.00	**0.98**	-0.02	0.16	0.16	0.53	0.46	0.18	-0.01	**0.98**	-0.02	0.11	0.17

Area in gray is PMF implemented with K_b

APPENDIX B

SUPPORTING INFORMATION FOR CHAPTER 4

B.1 Analysis of ambient concentrations and emissions of CO, NOx and EC in Dallas, TX

In Dallas, air quality data is collected from the US EPA's Air Quality System (AQS) for the Hinton site located four miles northwest of downtown Dallas (Figure B1 in Appendix B).

Figure B.1 Location of Hinton site in downtown Dallas, TX

Estimated NOx mobile emissions in Dallas decrease from 88,500 tons in 2000 to 61,900 tons in 2007, representing a 30% decrease (Fig. B.2a), with 57% from GV and 43% from DV. On a monthly basis, NOx emissions from GV increase in summer months due to the use of air conditioning (A/C) while NOx emissions from DV are relatively constant throughout the year (Fig B.2b).

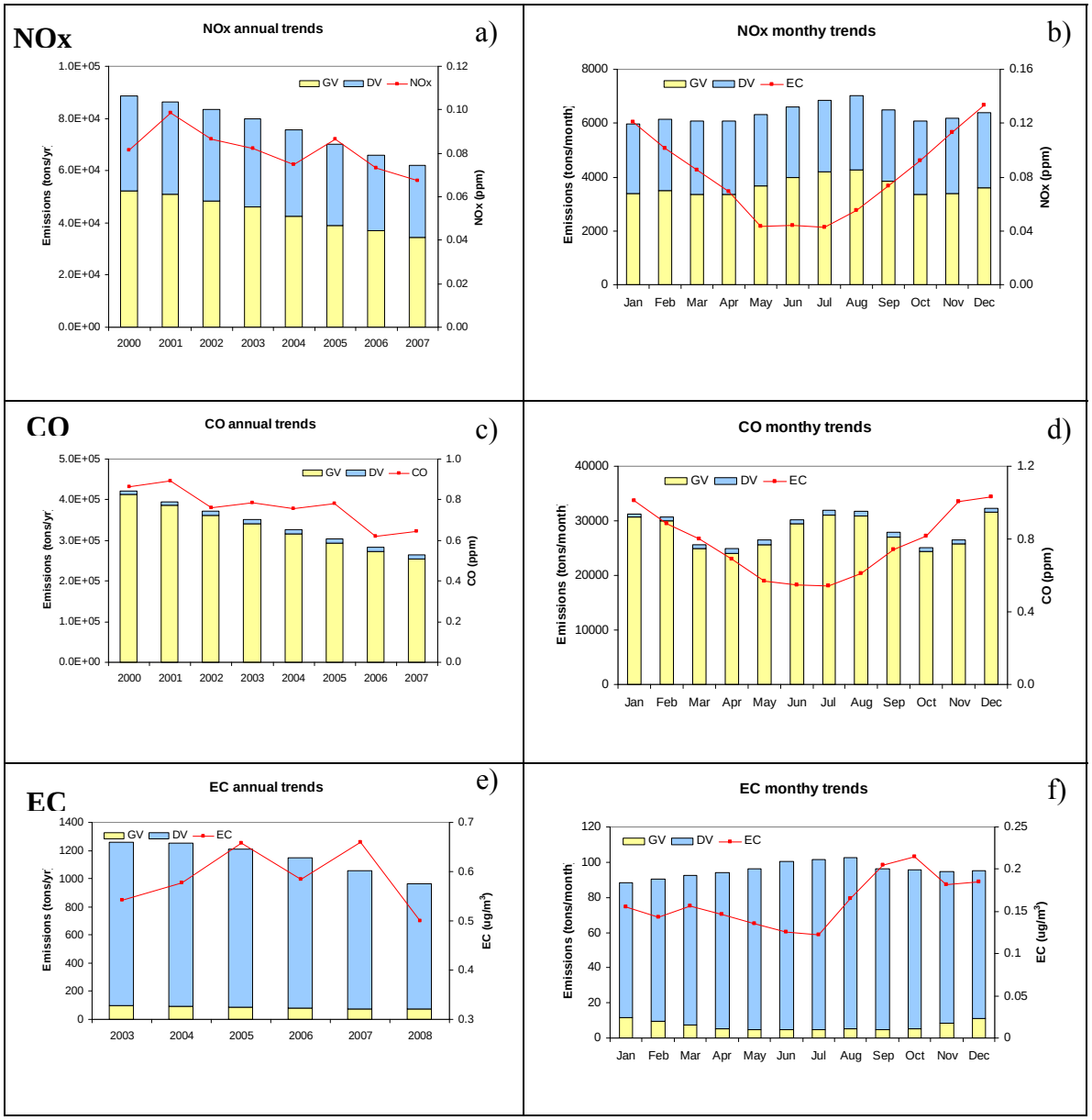

Figure B.2 Annual and monthly trends of NOx, CO and EC in Dallas.

In 2000, only 219 days recorded NOx concentrations at Hinton affecting the annual average for that year. Ambient NOx decreases from 98.5 ppb in 2001 to 67.4 ppb in 2007 representing a 32% decrease. However, the decrease has not been constant and average ambient NOx peaks in 2005 (86.6 ppb) which can be explained by meteorology, since this year was the driest in the period 2000-2007 (48 cm water versus an average of 90 cm water), and storms increase dispersion. On a monthly basis, ambient NOx decreases during summer months as a result of more rapid photochemical loss. The low concentrations in May and June are explained by larger precipitation during those months. On a weekly basis, NOx has higher concentrations during weekdays with respect to weekends (weekday/weekend ratio of 1.43) suggesting a similar trend to traffic.

CO mobile emissions decrease from 422,300 tons in 2000 to 264,000 tons in 2007, representing a 37% decrease (Fig B.2c). Of the total mobile CO emissions, 97% are estimated from GV and 3% from DV. On a monthly basis, CO emissions from GV increase in summer months due to the use of A/C and in winter months due to cold start emissions (Fig. B.2d).

Average ambient CO concentrations decrease from 0.86 ppm in 2000 to 0.64 ppm in 2007, representing a 25% decrease. Similar to NOx, CO decreases have not been constant throughout the years and ambient CO has a slight increase in 2001 (0.89 ppm) and 2005 (0.78 ppm). The peak in 2005 is explained by the dry meteorology for that year. On a monthly basis, ambient CO decreases during summer months as a result of an active photochemistry and greater dispersion. On a weekly basis, CO has higher concentrations during weekdays with respect to weekends (weekday/weekend ratio of 1.13) suggesting a similar trend to traffic.

EC ambient concentrations were available only during 2003-2008 at the Hinton site with a sampling period that vary from one filter collected every three days to one filter collected every six days, in contrast to CO and NOx which are measured every day. EC has an annual average of 0.59 μg/m^3 and a peak of concentration of 0.66 μg/m^3 during 2005 and 2007 (Fig. B.2e). The high values during those years are explained by lower precipitation (2005) and lower wind speeds (2007) with respect to other years. On a monthly basis, EC increases during September and October as a result of low precipitation and lower values are observed the rest of the months due to higher wind speeds. On a weekly basis, EC has higher concentrations during weekdays with respect to weekends (weekday/weekend ratio of 1.37). However, fewer samples were collected on Mondays (46) and Fridays (56) than the rest of the days (average 100 samples). While this bias is not expected to affect monthly or annual trends, it impacts weekly analysis of EC.

Estimated EC mobile emissions decrease from 1,260 tons in 2003 to 962 tons in 2008, representing a 24% decrease (Fig. B.2e). From the total mobile emissions, 93% are estimated from DV and 7% from GV. On a monthly basis, EC emissions from DV increase in summer months due to the increase in miles traveled by heavy-duty traffic (Fig B.2f).

B.2 Estimation of EB-IMSI uncertainties from propagation of errors

Uncertainties in multipollutant indicators were estimated propagating uncertainties from individual species and taking into account that CO, NOx and EC are correlated between each other and therefore, covariance terms need to be included, as in Equation 1.

$$\sigma_c^2(f) = \sum_{i=1}^{N}\left(\frac{\delta f}{\delta x_i}\right)^2 \sigma^2(x_i) + 2\sum_{i=1}^{N-1}\sum_{j=i+1}^{N}\frac{\delta f}{\delta x_i}\frac{\delta f}{\delta x_j}\mathrm{cov}(x_i, x_j) \qquad \text{(A.1)}$$

The expression for EB-IMSI can be expressed as: EB-IMSI= e*EC + c*CO + n*NOx, where $e=r_e/(R*s_{EC})$, $c=r_c/(R*s_{CO})$, $n=r_n/(R*s_{NOx})$, $r_e=(EC_{mob}/EC_{tot})$, $r_c=(CO_{mob}/CO_{tot})$, $r_n=(NOx_{mob}/NOx_{tot})$, $R=r_e+r_c+r_n$ and s are standard deviations of EC, CO and NOx respectively.

The uncertainty in EB-IMSI is expressed as follows:

$$\sigma^2_{EBIMSI} = \sigma^2_e EC^2 + \sigma^2_{EC} e^2 + \sigma^2_c CO^2 + \sigma^2_{CO} c^2 + \sigma^2_n NOx^2 + \sigma^2_{NOx} n^2 + 2cn\,\mathrm{cov}(CO, NOx) + 2ce\,\mathrm{cov}(CO, EC) + 2ne\,\mathrm{cov}(NOx, EC) \quad \text{(A.2)}$$

where

$$\sigma^2_e = \sigma^2_{r_e}\left(\frac{1}{R*s_{EC}}\right)^2 + \sigma^2_R\left(-\frac{r_e}{R^2*s_{EC}}\right)^2$$

$$\sigma^2_c = \sigma^2_{r_c}\left(\frac{1}{R*s_{CO}}\right)^2 + \sigma^2_R\left(-\frac{r_c}{R^2*s_{CO}}\right)^2$$

$$\sigma^2_n = \sigma^2_{r_n}\left(\frac{1}{R*s_{NOx}}\right)^2 + \sigma^2_R\left(-\frac{r_n}{R^2*s_{NOx}}\right)^2$$

Similarly, the expression for EB-IMSIGV can be expressed as: EB-IMSIGV= cg*CO + ng*NOx, where $cg=r_{cg}/(R_g*s_{CO})$, $ng=r_{ng}/(R_g*s_{NOx})$, $r_{cg}=(CO_{GV}/CO_{tot})$, $r_{ng}=(NOx_{GV}/NOx_{tot})$, $R_g=r_{cg}+r_{ng}$ and s are standard deviations of CO and NOx respectively.

The uncertainty in EB-IMSIGV is expressed as:

$$\sigma^2_{EBIMSIGV} = \sigma^2_{cg} CO^2 + \sigma^2_{CO} cg^2 + \sigma^2_{ng} NOx^2 + \sigma^2_{NOx} ng^2 + 2(cg)(ng)\,\mathrm{cov}(CO, NOx) \quad \text{(A.3)}$$

Where

$$\sigma_{cg}^2 = \sigma_{r_{cg}}^2 \left(\frac{1}{R_g * s_{CO}} \right)^2 + \sigma_{R_g}^2 \left(-\frac{r_{cg}}{R_g^2 * s_{CO}} \right)^2$$

$$\sigma_{ng}^2 = \sigma_{r_{ng}}^2 \left(\frac{1}{R_g * s_{NOx}} \right)^2 + \sigma_{R_g}^2 \left(-\frac{r_{ng}}{R_g^2 * s_{NOx}} \right)^2$$

In the same way, the expression for EB-IMSIDV can be expressed as: EB-IMSIDV= ed*EC + nd*NOx, where ed=$r_{ed}/(R_d*s_{EC})$, nd=$r_{nd}/(R_d*s_{NOx})$, $r_{ed}=(EC_{DV}/EC_{tot})$, $r_{nd}=(NOx_{DV}/NOx_{tot})$, $R_d=r_{ed}+r_{nd}$ and s are standard deviations of EC and NOx respectively.

The uncertainty in EB-IMSIDV is expressed as:

$$\sigma_{EBIMSIDV}^2 = \sigma_{ed}^2 EC^2 + \sigma_{EC}^2 ed^2 + \sigma_{nd}^2 NOx^2 + \sigma_{NOx}^2 nd^2 + 2(nd)(ed)\,\mathrm{cov}(NOx, EC) \qquad \text{(A.4)}$$

Where

$$\sigma_{ed}^2 = \sigma_{r_{ed}}^2 \left(\frac{1}{R_d * s_{EC}} \right)^2 + \sigma_{R_d}^2 \left(-\frac{r_{ed}}{R_d^2 * s_{EC}} \right)^2$$

$$\sigma_{nd}^2 = \sigma_{r_{nd}}^2 \left(\frac{1}{R_d * s_{NOx}} \right)^2 + \sigma_{R_d}^2 \left(-\frac{r_{nd}}{R_d^2 * s_{NOx}} \right)^2$$

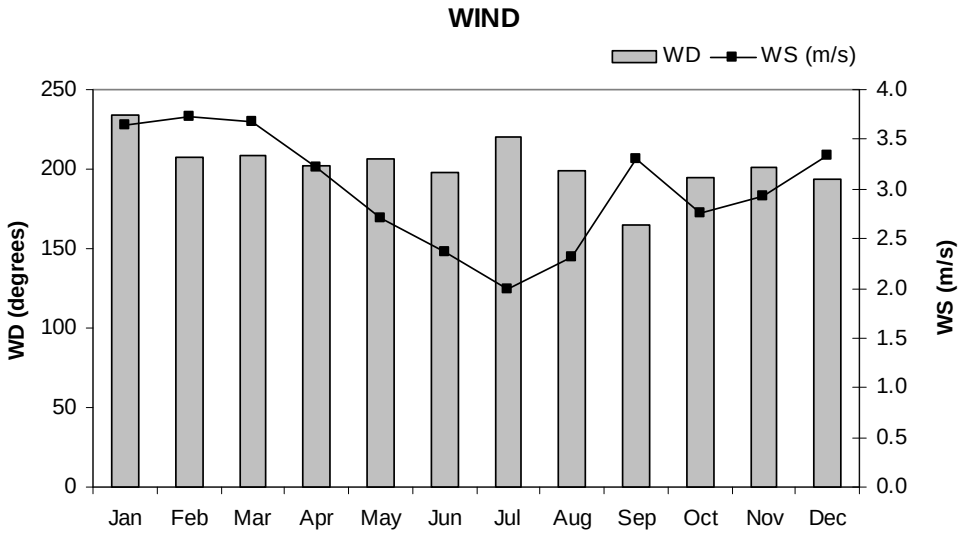

Figure B.3 Monthly average wind direction (degrees) and speed (m s^{-1}) at the JST station in Atlanta

Table B.1 Source impacts from CMB and PMF in μg/m^3 in Atlanta from 1999-2004

Source	PMF[£]	CMB[§]
Secondary Sulfate	8.10 ± 0.34	6.59 ± 6.37
Secondary Nitrate	1.38 ± 0.16	1.25 ± 0.99
Light duty GV	1.37 ± 0.27	1.35 ± 1.99
Heavy duty DV	1.57 ± 0.73	1.27 ± 1.60
Industrial source	0.04 ± 0.11	0.14 ± 0.30
Biomass burning	2.76 ± 0.26	1.65 ± 1.88
Soil dust	0.63 ± 0.16	0.34 ± 0.35
Other sources*	0.61 ± 0.92	2.47 ± 3.30

* Other sources not included in the balance for PMF and Secondary Organic Carbon for CMB. [§]The performance of CMB was: predicted vs. observed $PM_{2.5}$ R^2=0.94, χ^2=2.4, predicted $PM_{2.5}$ mass=93.2%. [£]All 20 runs in PMF converged, predicted vs. observed $PM_{2.5}$ R^2=0.88 and residuals of species were normally distributed.

VITA

JORGE EDUARDO PACHON QUINCHE

Jorge E. Pachon Quinche was born and raised in Bogota, Colombia. He pursued a B.S. in Chemical Engineering and a Master in Environmental Engineering at the National University of Colombia in 2000 and 2004 respectively. As part of his master degree, he participated in a semester-abroad program in the National University of Mexico with a fellowship to work at the Atmospheric Sciences Center. He joined the faculty at Environmental Engineering at Universidad de La Salle in Bogota in 2004, and after working two years as full time professor and researcher he received a scholarship from the Colombian Institute for the Development of Science and Technology (COLCIENCIAS) to pursue doctoral studies abroad. Jorge came to Georgia Tech in the Fall of 2006 and got a second Master in Environmental Engineering in 2008 and finished his PhD studies in August of 2011. As a grad student, he was the recipient of the 'Amina Ghosh Fellowship' in Environmental Engineering in 2007, he was an active member of the Association of Environmental Engineers and Scientists (AEES) and participated in several seminars and conferences with platform and poster presentations. As part of his enthusiasm for the outdoors, Jorge joined the Outdoor Recreation at Georgia Tech (ORGT) program since Fall of 2006 where later he became instructor of backpacking and mountain biking. At ORGT, he took part in two unforgettable expeditions to the Grand Canyon in 2009 and Yellowstone in 2010. Jorge married Cristina Vasquez in 2008 and they are parents of Sarah Isabel who was born in October 2010.